

# **STARCH INCORPORATED POLYMERIZATION OF THERMOPLASTIC POLYURETHANE**

zur Erlangung des Grades eines  
Doktors der Naturwissenschaften  
- Dr. rer. nat. -  
des Fachbereiches Chemie und Chemietechnik  
an der Universität Paderborn

vorgelegte

**Dissertation**

von

Master of Science

**Seung-kyu Ha**

aus Korea

Paderborn 2002

1. Gutachter: Prof. Dr. H. C. Broecker

2. Gutachter: Prof. Dr. H. Potente

Tag der Abgabe: 04.09.2002

Tag der Prüfung: 23.10.2002

Die vorliegende Arbeit entstand in der Zeit von August 1999 bis Juli 2002 an der Universität Paderborn im Fachgebiet Technische Chemie des Fachbereichs Chemie und Chemietechnik.

## **ACKNOWLEDGEMENT**

The author acknowledges indebtedness and expresses his deepest appreciation to Professor Hans- Christoph Broecker for his continuous guidance and inspiration during this research.

Sincere appreciation is also extended to Professors H. Potente, K. Huber, and H. Marsmann for their helpful comments.

The author also thanks all of the faculty members and students of Department of Chemie und Chemietechnik, Physikalische Chemie, and Kunststofftechnik for their help and discussions.

Finally, the author dedicates this dissertation to his parents, parents-in-law and wife Hyerim, son Myounghoon and daughter Youjin, without whose love this work would never have been achieved.

## **Danksagung**

Der Autor bedankt sich außerordentlich bei Prof. Hans-Christoph Broecker und drückt seine tiefe Wertschätzung für sein fortwährendes Interesse und seine Betreuung der vorliegenden Arbeit aus.

Für zahlreiche anregende Diskussionen möchte ich mich bei den Professoren K. Huber, H. Marsmann und H. Potente bedanken, letzterem insbesondere für die Übernahme des Korreferates.

Der Autor bedankt sich weiter bei allen Mitgliedern und Studenten des Fachbereichs Chemie und Chemietechnik, der Physikalischen Chemie und der Kunststofftechnik für ihre Unterstützung.

Die Dissertation widme ich meinen Eltern, meinen Schwiegereltern, meiner Frau Hyerim, unserem Sohn Myounghoon und Tochter Youjin. Ohne deren Zuneigung hätte die Arbeit nicht durchgeführt werden können.

# TABLE OF CONTENTS

LIST OF TABLES

LIST OF FIGURES

CHAPTER

page

<b>1</b>	<b>INTRODUCTION</b>	<b>1</b>
<b>2</b>	<b>LITERATURE SURVEY</b>	<b>3</b>
2.1	Reactions and Characteristics of Thermoplastic Polyurethane	3
2.1.1	Basic Reaction of the Thermoplastic Polyurethane	3
2.1.2	The Influences of Reaction Temperature and Catalysts in Bulk Phase for the Urethane Reaction	4
2.1.3	Characteristics of the Thermoplastic Polyurethane	4
2.2	Starch	9
2.3	Starch and Synthetic Polymer Blends	11
2.3.1	Physical Blending of Starch with Synthetic Polymers	11
2.3.2	Starch Grafting and Physicochemical Adhesion of Synthetic Polymers on the Surface of Starch	12
2.3.3	Grafting of Prepolymer on the Starch prior to Synthesis	13
2.3.4	Grafting Reaction by Extruder Blending	16
<b>3</b>	<b>EXPERIMENTAL</b>	<b>19</b>
3.1	Materials	19
3.2	Determination of Moisture and OH-Value of the Starches	19
3.2.1	Karl-Fischer Titration for the Measurement of the Moisture in Starch	19
3.2.2	Hydroxyl (-OH) Number Determination of the Surface of the Starch Granules by Titration (International Standard, 4629-1078)	20
3.2.3	Equivalent Weight of Raw Materials	20
3.3	Characterizations	21
3.3.1	Scanning Electron Microscopy (SEM)	21
3.3.2	Differential Scanning Calorimetry (DSC)	21
3.3.3	Fourier Transformation Infrared Spectroscopy (FTIR)	21
3.3.4	Grafted Percentage of Polyurethane to Starch Granule	21
3.3.5	Gel Permeation Chromatography (GPC)	22
3.3.6	Thermogravimetric Analysis (TGA)	22
3.3.7	Polymer Mechanical Properties	22
3.3.8	Rheological Measurements	23

3.4	Synthesis of Polyurethane	23
3.4.1	One-Step Reaction (OSR)	23
3.4.2	Two-Step Reaction (TSR)	23
<b>4</b>	<b>RESULTS AND DISCUSSION</b>	<b>29</b>
4.1	Characterization	29
4.1.1	Studies by Scanning Electron Microscopy	29
4.1.1.1	Dispersion and Adhering of Polyurethane with Starch granules	29
4.1.1.2	Polyurethane-Extracted Starch	29
4.1.1.3	Phase Separation (Gapping Formation) Phenomena at High Starch Contents	32
4.1.2	Infra-Red (IR) and Nuclear Magnetic Resonance (NMR) Studies.	35
4.1.2.1	Conformation of Remaining Polyurethane on Starch by Infrared Spectroscopy after Homo-Polymer-Extraction	35
4.1.2.2	Conformation of Remaining Polyurethane on Starch by Nuclear Magnetic Resonance Spectroscopy after Homo-Polymer-Extraction	36
4.1.3	Differential Scanning Calorimetry (DSC) Studies of the Polyurethane Phase	40
4.1.3.1	DSC for Rapidly Cooled Samples	40
4.1.3.2	Samples Annealed at 180 °C for 15 minutes	44
4.1.3.3	Samples Annealed at 140 °C for 4 hours	48
4.1.3.4	The Effect of Different Concentration of the catalyst	52
4.1.3.5	Two Step Reaction vs. One Step Reaction	55
4.1.3.6	Effect of the Different Molecular Weight of the Polyethylene Glycol Prepolymer	55
4.1.4	Grafted Percentage of Polycaprolactone Diol and Polyethylene Glycol Polyurethanes under Various Starch Contents	60
4.1.4.1	One-Step Reaction	60
4.1.4.2	Two-Step Reaction	60
4.1.4.3	Effect of the Different Molecular Weight of the Polyethylene Glycol Prepolymer	62
4.1.5	Swelling Behavior	63
4.1.5.1	One-Step Reaction	63
4.1.5.2	Two-Step Reaction	63
4.1.5.3	Effect of the Different Molecular Weight of the Polyethylene Glycol Prepolymer	63
4.1.6	Average Molecular Weight of Polyurethane Homopolymer	68

4.1.6.1 One-Step Reaction	68
4.1.6.2 Two-Step Reaction	68
4.1.6.3 Effect of the Different Molecular Weight of the Polyethylene Glycol Prepolymer	68
4.1.7 Thermogravimetric Analysis	72
4.1.7.1 One-Step Reaction (rapidly cooled)	72
4.1.7.2 Two-Step Reaction (rapidly cooled)	75
4.1.7.3 Effect of the Different Molecular Weight of Polyethylene Glycol Prepolymer	75
4.1.8 Mechanical Properties	82
4.1.8.1 One-Step Reaction (rapidly cooled)	82
4.1.8.2 Two-Step Reaction (rapidly cooled)	83
4.1.8.3 Effect of the Different Molecular Weight of the Polyethylene Glycol Prepolymer	83
4.2 Rheological Properties	89
4.2.1 Viscosity $\zeta^*$	89
4.2.1.1 One-Step Reaction	89
4.2.1.2 Two-Step Reaction	89
4.2.1.3 Viscosities against Starch Contents at Low Frequency $\omega$	92
4.2.1.4 Effects of the Different Molecular Weight of Polyethylene Glycol Prepolymer	92
4.2.2 Plots of $\log G''$ against $G'$	96
4.2.2.1 One-Step Reaction	95
4.2.2.2 Two-Step Reaction	95
4.2.2.3 Effect of the Different Molecular Weight of Polyethylene Glycol Prepolymer	99
4.2.3 Effect of Catalyst Concentrations	99
<b>5 Conclusion</b>	<b>103</b>
General Comments on the Study	104
Closing Comments	106
<b>6 References</b>	<b>107</b>

## LIST OF TABLES

Table	page	
2.1	Characteristic features of thermoplastic polyurethane elastomers	8
2.2	Starch content of various seeds and the characteristics of the starch granules	9
3.1	Properties of potato starch	24
3.2	Chemicals used for the synthesis of polyurethane	25
3.3	Hydroxyl (-OH) value of surface of various starch granules determined by titration	25
3.4	(a) Molar ratios in polyurethane-synthesis in combination with starch (OH/NCO mole ratio=1)	26
3.4	(b) Molar ratios in the polyurethane synthesis using different molecular weights of prepolymer (polyethylene glycol) (OH/NCO mole ratio=1)	27
4.1	Frequencies and percentages of bonded and free bands of carbonyl group in two series of samples	38
4.2	Effects of starch content on the soft segment $T_g$ and hard segments $T_m$ in various starch contents for samples prepared by one-step reaction (OSR C0.01)	43
4.3	Annealing effects (180 °C / 15 min) on the soft segments ( $T_g$ ) and hard segment ( $T_m$ ) for samples prepared in a one-step reaction (OSR C0.01)	47
4.4	Annealing effects (140 °C / 4 hrs) on the soft segments ( $T_g$ ) and hard segment ( $T_m$ ) for samples prepared in a one-step reaction (OSR C0.01)	51
4.5	Effects of various starch contents on soft segment $T_g$ and hard segments $T_m$ for samples prepared in a two-step reaction (TSR C0.01)	58
4.6	$T_g$ of soft segments and $T_m$ of hard segments for the samples prepared with different molecular weights of polyethylene glycols (OSR C0.01)	59
4.7	Percentage of grafting (wt.%) as a function of the molecular weights of the polyethylene glycol prepolymer	62
4.8	Swelling behavior of polyurethane starch blends for two series of the samples, psb2m3 (OSR C0.01) and psb4m5 (OSR C0.01). Swelling solvent: THF for 3 weeks	66
4.9	Average molecular weight of polyurethane homo-polymer separated from polyurethane-starch-blends in psb2m3 (OSR) and psb4m5 (OSR) series	70

4.10	Average molecular weights of polyurethane homo-polymer separated from polyurethane-starch-blends in psb2m3 (TSR) and psb4m5 (TSR) series	71
4.11	Average molecular weights of polyurethane homo-polymers separated from samples of polyethylene-glycol based polyurethane-starch blends. Influence of the molecular weight of the prepolymer	71
4.12	Residual percentage weight loss in two series of samples	76



## LIST OF FIGURES

Figure	page	
2.1	Chemical structures of polycaprolactone-diol and 4,4-diphenylmethane diisocyanate	7
2.2	bc projection of the Me-M-Me (4,4' -dimethoxycarbonyl -4,4' -diamino-diphenylmethane) structure showing the packing and intermolecular hydrogen bonding	7
2.3	Characteristics of (a) Amylose and (b) Amylopectin	10
2.4	Chemical bonding of synthetic polymer chains on the surface of starch	14
3.1	Schematic flow diagram of the experimental apparatus for the synthesis of polyurethane-starch blends	27
3.2	Photo of experimental apparatus	28
4.1	Cryogenically fractured SEM-micrograph for p7s3b2m3 (25.7 wt.% of starch) (magnification: x 1000)	30
4.2	SEM-micrograph for pure potato starch	30
4.3	SEM-micrograph for homo-polymer-extracted starch (p5s5b2m3)	31
4.4	SEM-micrograph (a) of the broken surfaces of p7s3b4m5 at liquid nitrogen temperature (b) and sketch of the texture	33
4.5	SEM-micrograph of p7s3b2m3 (TSR C0.01) for the broken surface at liquid nitrogen temperature	34
4.6	Phase separations between starch-granules and polyurethane phase for the fractured surface of a tensile bar of p5s5b4m5 (OSR, C0.01) at ambient temperature after tensile test	34
4.7	IR spectra of (a) p9s1b2m3 PU-extracted (b) p7s3b2m3 PU-extracted	37
4.8	IR spectra of (a) p9s1b4m5 PU-extracted (b) p7s3b4m5 PU-extracted	37
4.9	Peak separation of the IR carbonyl band by peak separation software	38
4.10	<sup>13</sup> C Solution state spectrum of p7s3b2m3 for the identification of grafted polyurethane. Solvent:DMSO-d <sub>6</sub> , Temperature: 60 °C	39
4.11	<sup>1</sup> H Solution state spectrum of p7s3b2m3 for the identification of grafted polyurethane. Solvent:DMSO-d <sub>6</sub> , Temperature: 60 °C	39

4.12	DSC thermograms of rapidly cooled compression-molded psb2m3 series prepared by one-step reaction (OSR C0.01) Heating rate: 10 °C / min.	41
4.13	DSC thermograms of rapidly cooled compression-molded psb4m5 series prepared by one-step reaction (OSR C0.01 ) Heating rate: 10 °C / min.	42
4.14	DSC thermograms of psb2m3 series annealed at 180 °C / 15 min. The samples were prepared in a one-step reaction (OSR C0.01) Heating rate: 10 °C / min.	45
4.15	DSC thermograms of psb4m5 series annealed at 180 °C / 15 min. The samples were prepared in a one-step reaction (OSR C0.01) Heating rate: 10 °C / min.	46
4.16	DSC thermograms of psb2m3 series annealed at 140 °C / 4 hours. The samples were prepared in a one-step reaction (OSR C0.01) Heating rate: 10 °C / min.	49
4.17	DSC thermograms of psb4m5 series annealed at 140 °C / 4 hours. The samples were prepared in a one-step reaction (OSR C0.01) Heating rate: 10 °C / min.	50
4.18	Effect of catalyst concentration on the system p7s3b2m3 prepared in a one-step reaction (OSR)	53
4.19	Effect of catalyst concentration on the system p7s3b4m5 prepared in a one-step reaction (OSR)	54
4.20	DSC thermograms of rapidly cooled compression-molded psb2m3 series prepared in a two-step reaction (TSR C0.01) Heating rate: 10 °C / min.	56
4.21	DSC thermograms of rapidly cooled compression-molded psb4m5 series prepared in a two-step reaction (TSR C0.01) Heating rate: 10 °C / min.	57
4.22	DSC thermograms of the samples prepared from prepolymers of polyethylene glycol with different molecular weights.	59
4.23	Percentage [%] of grafted starch contents for two series of the samples prepared by DMF and THF solvents for five days. (OSR C0.01)	61
4.24	Percentage [%] of grafted starch contents for the samples prepared by TSR. Swelled in DMF and THF solvents for five days. (TSR C0.01)	61
4.25	Swelling behavior of polyurethane-starch-blends for two series of the samples, psb2m3 (OSR C0.01) and psb4m5 (OSR C0.01) Swelling solvent: THF for 3 weeks.	64

4.26	Swelling of solvent uptake against the starch contents for the samples prepared by TSR. Swelling solvent: THF for 3 weeks.	65
4.27	Solvent swelling uptake against different molecular weight of polyethylene glycol prepolymer. Swelling solvent: THF for 3 weeks	67
4.28	Molecular weights, $M_w$ of polyurethane homo-polymer extracted from starch-polyurethane-blends, psb2m3 (OSR) and psb4m5 (OSR) samples	69
4.29	Molecular weights, $M_w$ of polyurethane homo-polymer extracted from starch-polyurethane-blends, psb2m3 (TSR) and psb4m5 (TSR) samples	69
4.30	Thermogravimetric Analysis (TGA); (a) integral and (b) differential weight loss for psb2m3 series (OSR C0.01)	73
4.31	Thermogravimetric Analysis (TGA); (a) integral and (b) differential weight loss for psb4m5 series (OSR C0.01)	74
4.32	Thermogravimetric Analysis (TGA); (a) integral and (b) differential weight loss for p7s3b2m3 series (OSR C0.01 ) at different catalyst concentration.	77
4.33	Thermogravimetric Analysis (TGA); (a) integral and (b) differentiatl weight loss for p7s3b4m5 series (OSR C0.01 ) at different catalyst concentration.	78
4.34	Thermogravimetric Analysis (TGA); (a) integral and (b) differential weight loss for the psb2m3 series (TSR C0.01 )	79
4.35	Thermogravimetric Analysis (TGA); (a) integral and (b) differential weight loss for the psb4m5 series (TSR C0.01)	80
4.36	Thermogravimetric Analysis (TGA); (a) integral and (b) differential weight loss for p7s3b2m3 series (OSR C0.01) prepared with different molecular weight of polyethylene glycol prepolymer	81
4.37	Tensile strength as a function of starch contents for psb2m3 and psb4m5 series (OSR C0.01)	84
4.38	Elongation at break as a function of starch contents for psb2m3 and psb4m5 series (OSR C0.01)	84
4.39	Elongation at break as a function of solvent uptake (crosslinking parameter) for two series of samples. Swelling solvent: THF for 3 weeks	85
4.40	Tensile strength as a function of solvent uptake for two series of samples. Swelling solvent: THF for 3 weeks	85

4.41	Tensile strength as a function of average molecular weight of homo-polymer extracted from polyurethane-starch-blends.	86
4.42	Elongation at break as a function of average molecular weight of homo-polymer extracted from polyurethane-starch-blends.	86
4.43	Tensile strength as a function of starch content for psb2m3 and psb4m5 series (TSR C0.01)	87
4.44	Elongation at break as a function of starch content for psb2m3 and psb4m5 series (TSR C0.01)	87
4.45	Ultimate tensile strength against different molecular weight of polyethylene glycol prepolymer (OSR C0.01)	88
4.46	Elongation at break against different molecular weight of polyethylene glycol prepolymer (OSR C0.01)	88
4.47	Complex viscosities $\zeta^*$ as a function of frequency $\omega$ for psb2m3 (OSR C0.01) series of samples.	90
4.48	Complex viscosities $\zeta^*$ as a function of frequency $\omega$ for psb4m5 (OSR C0.01) series of samples	90
4.49	Complex viscosities $\zeta^*$ as a function of frequency $\omega$ for psb2m3 (TSR C0.01) series of samples prepared in the two-step reaction	91
4.50	Complex viscosities $\zeta^*$ as a function of frequency $\omega$ for psb4m5 (TSR C0.01) series of samples prepared in the two-step reaction	91
4.51	Melt viscosities as a function of the starch contents at frequency 0.2, the samples prepared by OSR and TSR for psb2m3 series.	93
4.52	Melt viscosities as a function of the starch contents at frequency 0.2, the samples prepared by OSR and TSR for psb4m5 series.	93
4.53	Complex viscosity $\zeta^*$ against frequency $\omega$ for the samples prepared by different molecular weight of polyethylene glycol prepolymer	94
4.54	Log $G'$ against Log $G''$ for psb2m3 series (OSR C0.01)	96
4.55	Log $G'$ against Log $G''$ for psb4m5 series (OSR C0.01)	96
4.56	Log $G'$ against Log $G''$ for the samples, psb2m3 prepared by TSR	97
4.57	Log $G'$ against Log $G''$ for the samples, psb4m5 prepared by TSR	97
4.58	Log $G'$ against Log $G''$ for the samples prepared by using different molecular weight of prepolymer of polyethylene glycol	98

4.59	Complex viscosity $\zeta^*$ against frequency $\omega$ for p7s3b2m3 at different catalyst concentration.	101
4.60	Complex viscosity $\zeta^*$ against of frequency $\omega$ for p7s3b4m5 at different catalyst concentration.	101
4.61	Log $G'$ against Log $G''$ for the samples, p7s3b2m3 prepared at different catalyst concentration.	102
4.62	Log $G'$ against Log $G''$ for the samples, p7s3b4m5 prepared at different catalyst concentration.	102

## 1. INTRODUCTION

World production of native starch is high and inexpensive; this leads to enormous interest in studying its uses. Studies concerning the use of starch have hitherto been related to the blending of synthetic polymers with starch. The blending of starch granules with synthetic polymers generally results in a filler effect on the polymer properties<sup>1-3)</sup>.

When the starch content in a polymer is increased, elongation to break and tensile strength decrease,<sup>4), 5)</sup> but the modulus increases<sup>6)</sup> due to the stiffening effect of the starch granule. The general reason for the lowering of the mechanical properties of the synthetic polymer incorporated with starch could be explained by the different properties of the hydrophilic starch and the hydrophobic synthetic polymers. Therefore, many researchers have tried to modify the surface of the starch granule<sup>7-10)</sup> and also used de-structured starch<sup>11-13)</sup> introducing the compatible component by grafting with starch. Polyurethane elastomer is a complicated polymer system consisting of polyphases such as soft segments and hard segments.<sup>1-3)</sup>

DSC indicates several endothermic peaks related to glass transition of soft segments, and morphological transitions of hard segments, dissociation of ordering in the hard micro-phase and melting transition of the hard segment crystal structure.<sup>1),4)</sup>

The polyurethane synthesized at a high temperature (>150°C) can also form a crosslinked network polymer system through allophanated and biureted bonding, which is more complicated<sup>3)</sup> than a linear polyurethane chain.

Incorporation of starch granules with polyurethane may increase this complication because starch has a polyol structure of the hydroxyl group, which could accelerate the three dimensional network structure with polyurethane chains by crosslinking.<sup>6)</sup>

The properties of these polymer systems can be determined by the level of grafting of the polyurethane chain with the hydroxyl group of the surface of the starch granules and by the level of crosslinking of polyurethane chains between the starch-granules. The average molecular weight of the homo-polyurethane extracted from the starch-synthetic polymer blend could also be another factor to explain the properties of the starch-synthetic polymer blend.

If the hydrophilic properties cause difficulties in the grafting of polyurethane on starch at high concentrations, phase separation can be achieved due to homo-polymerization tendencies.<sup>14)</sup>

The product can also produce a micro-heterogeneous polymer system depending on the levels of grafting and crosslinking. This could induce different rheological behaviour of viscosity and the moduli.

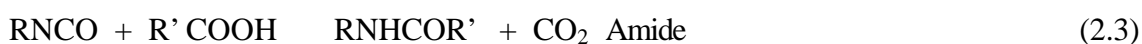
In this study, without any modification to increase the compatibility of the starch, we directly utilized the hydroxyl group of the starch granule surface for the urethane reaction in the polymerization process with the polyurethane as the prepolymer. Polycaprolactone diol ( $M_n=2000$ ), MDI and 1,4 butane diol as reactants could produce linear thermoplastic polymers, but as starch is a large sphere-like granule with polyol, three-dimensional network structure of the products could be anticipated. Furthermore, we adapted a high temperature bulk reaction at 175°C in an extruder bearing in mind reactive polymerization. The purpose of this study is to understand the structure and properties of such a polyurethane system incorporating starch granules and to observe the variation of rheological parameters in relation to the starch-granule content. We changed the catalyst concentration as well as the reaction scheme in order to obtain varied grafting and crosslinking.

## 2. LITERATURE SURVEY

### 2.1 Reactions and Characteristics of Thermoplastic Polyurethane

#### 2.1.1 Basic Reaction of the Thermoplastic Polyurethane<sup>3)</sup>

The NCO group can react generally with any compound containing active hydrogen atoms, i.e. according to the following:



Thus, if the reagents are di- or polyfunctional, 3D polymer formation can occur. While these reactions normally occur at different rates, equation 2.2 being the most rapid, they can be influenced appreciably and controlled by the use of catalysts. Reactions 2.3 and 2.4 also give rise to carbon dioxide, a feature of value when forming foamed products but introducing difficulty when bubble-free castings and continuous surface coatings are required. The reactions noted have the advantage that, unlike polycondensation, the processes normally give rise to no by-products that require removal as macromolecules are built up.

Linear products are obtained, if the reactants are bifunctional, but higher functionality leads to the formation of branched chains or crosslinked materials. Figure 2.1 shows the linear structures of polycaprolactone-diol and 4,4-diphenylmethane diisocyanate. Again, additional reaction of the isocyanate with the urea, urethane and amide groups introduced during initial polymer formation is also possible. Chain branching or crosslinking then occurs, due to the formation of acylurea, biuret and allophanate links onto the main chain. The initial studies on polyurethane synthesis were based on simple diisocyanates and diols, but the main importance of the reaction is now concerned with the use of intermediates which are often themselves polymeric in character and carry terminal groups (-OH or -NCO) capable of further reaction and thus of increasing the molecular size frequently during the actual fabrication processing by chain extension, branching or crosslinking according to the reactions indicated above. Some of the reactions are reversible at higher temperature, thus introducing the possibility of molecular rearrangement during processing.



### ***2.1.2 The Influences of Reaction Temperature and Catalysts in Bulk Phase for the Urethane Reaction***

In general, tertiary amine in catalyst favours NCO/OH and NCO/H<sub>2</sub>O combination, while organotin catalysts are most effective for NCO-OH reaction and for influencing urea and biuret linking, but do not promote isocyanurate formation. Basic conditions favour branching and crosslinking via allophanate, biuret and trimer formation. In practice, a mixture of tertiary amines and tin catalysts can be used to achieve the appropriate balance of chain extension and crosslinking.

Reaction temperature can also be important. Up to 50 °C the linear-chain formation reaction predominates, but at higher temperatures (up to 150 °C) biuret and isocyanurate formation become effective and branching occurs. Above 150°C some of the less stable links are affected and reversion or degradation can take place. It must be stressed that the isocyanate reactions are highly exothermic, and under conditions where heat transfer is slow, an appreciable temperature rise can be experienced; care is necessary to minimize this, otherwise deterioration in properties results.

### ***2.1.3 Characteristics of the Thermoplastic Polyurethane***

On the molecular basis, thermoplastic urethanes<sup>15-19)</sup> may be described as linear block copolymers of the (AB)<sub>n</sub> type. One block of the polymer chain consists of a relatively long, flexible polyester diol or polyether diol,<sup>4),20)</sup> in the typical number-average molecular weight of 1000 to 3000. These amorphous polyol blocks are usually termed the soft segment since they impart the elastomeric character to the polymer. The second block of the copolymer is commonly referred to as the hard segment and is formed by the reaction of aromatic diisocyanates with low molecular weight diol and triol chain extender. Due to the polar nature of the urethane groups in the hard segment and their ability to form hydrogen bonds, these hard segments are capable of intermolecular association and possible domain segregation.<sup>15)</sup> NH- and CO- groups in interurethane bonding can form hydrogen bonds, which can be a direct measure of phase segregation for the hard and soft segments.<sup>21)</sup>

The phase separation of the microphases in the urethane indicates the relation between structure and physical properties of the urethane elastomer. Hydrogen bonding between NH and C=O in the polyurethane phase has been the subject of numerous investigations using infrared spectroscopy to relate the physical property with hydrogen bond level. Schneider et al.<sup>21)</sup> studied the temperature dependence of the hydrogen bonding. The

onset temperature for dissociation of both hydrogen bonded NH and C=O in 2,6-TDI occurred at 65 °C, independent of urethane content and well below the melting temperature of the crystalline hard segment structure (130-170°C). Coleman et al.<sup>22)</sup> investigated the NH stretching region of the infrared spectrum of poly (1,4 butylene hexamethylenecarbamate). The infrared bands at 3440 and 3320 cm<sup>-1</sup> are associated with the NH stretching modes of the free and the hydrogen bonded NH group of the polyurethane, respectively. The frequencies of these two bands are remarkably similar to those observed for analogous aliphatic polyamides. The other two bands at about 3362 and 3260 cm<sup>-1</sup> are attributed to a two-proton-vibration involving the intense carbonyl vibrations in Fermi resonance with the HN stretching fundamental vibration. As the temperature rises, the hydrogen bonded NH absorption decreases while a free NH absorption shoulder develops which is centered at 3460 cm<sup>-1</sup>. Also, hydrogen bonded carbonyl absorption at 1700 cm<sup>-1</sup> decreased and free carbonyl absorption at 1740 cm<sup>-1</sup> increased. Recently, Yoon et al.<sup>1)</sup> determined the fraction of hydrogen-bonded C=O groups using Gaussian method for peak deconvolution in IR-spectra.

The FTIR spectra were obtained by varying the temperature from 50 to 230 °C. Results indicated that the C=O absorption bands of ester-based TPU consist of at least five peaks (three peaks from free, ordered, and disordered C=O groups from hard segments; two peaks from free and bonded C=O groups from soft segments). However, the second-derivative spectra of ester-based TPU gave three major spectral components, indicating that the absorption band could not be resolved to five contributing peaks. A schematic diagram of polyurethane and hydrogen bonding is shown in Figure 2.2.

The thermally reversible network structure of these copolymers provides for the elastomeric or apparent crosslinked nature of these polymers. Several studies have been performed with regard to the various relationships of molecular structure and physical properties for thermoplastic urethane elastomers.

In 1971, Huh et al.<sup>23)</sup> studied the hard and the soft segments in polyurethane to identify their influences on dynamic mechanical properties. Results indicated that the  $\delta$  peak observed in polyester (polyether) urethane can be assigned mostly to the micro-Brownian motion of the amorphous hard segments. Other molecular processes appear to be contributing to the relaxational behavior in this region as suggested by the breadth and asymmetry of the  $\delta$  relaxation. The  $\delta'$  relaxation is the mechanical dispersion caused by the melting of MDI-BD crystallites in the hard domains. In addition, the  $\delta$  and  $\delta'$  relaxations were found to depend on the size of the domain structure in

polyurethane block polymers, with longer block segments favouring more ordered structures. The lower temperature glass transition region for these elastomers appears to be influenced primarily by the degree of flexibility of the amorphous, soft segments and their interactions with the hard segments. The higher temperature relaxation region is controlled mainly by the extension of associated rigid and hard segments. In addition, the relative concentration of the hard and soft segments affects the level of the plateau modulus at temperatures between the major relaxation regions.

The polyurethane elastomer exhibited soft segment crystallization when a polycaprolactone diol with  $M_n > 3000$  was used. The glass transition temperature of these materials progressively shifted to lower temperatures as the chain length of the soft segment was increased.<sup>15)</sup> The urethane polymer based on a low molecular weight ( $M_n=830$ ) polycaprolactone diol exhibited a progressive increase in glass transition temperature as the level of hard segment increased.<sup>16)</sup> However, the polyurethane based on polycaprolactone diol with  $M_n = 2000$  as the soft segment maintained a relatively constant glass transition temperature. These differences have been attributed to the relative degree of phase separation between the constitutive blocks of copolymer.<sup>16)</sup>

In the polyether system, inversion or possibly mixing of continuous and dispersed phases appears to occur in the system at approximately 60 - 65 % of hard segment.<sup>20)</sup> For the different isocyanates, polymer glass transition temperatures increased for the TDI-based polyurethane, but remained relatively constant for the MDI.<sup>4)</sup> The glass transition temperature of the soft phase decreases largely if the annealing temperature is lowered. At high annealing temperatures, long sequences of hard segment are excluded from the soft phase in which short segment are still soluble. At low temperature, even short hard segments separate from the soft segments.<sup>20)</sup> Table 2.1 shows characteristic features of thermoplastic polyurethane elastomers.

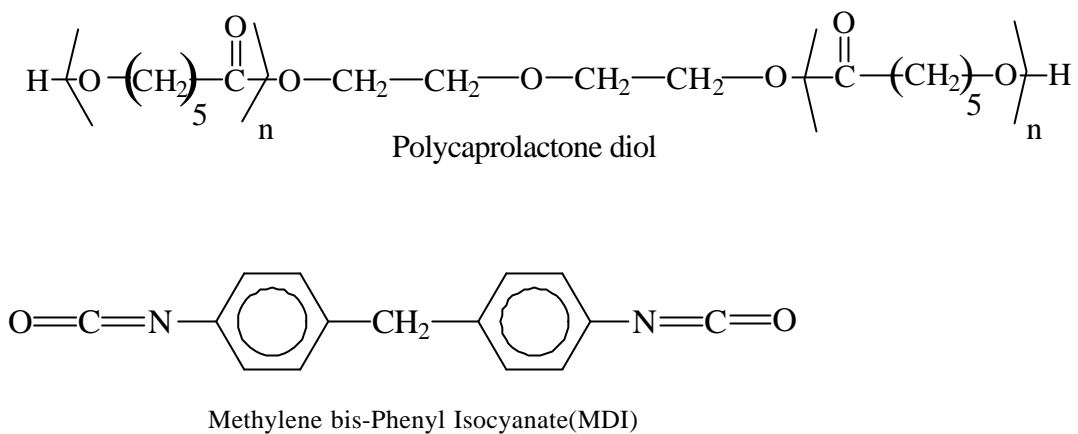


Figure 2.1 Chemical structures of polycaprolactone-diol and 4,4-diphenylmethane diisocyanate

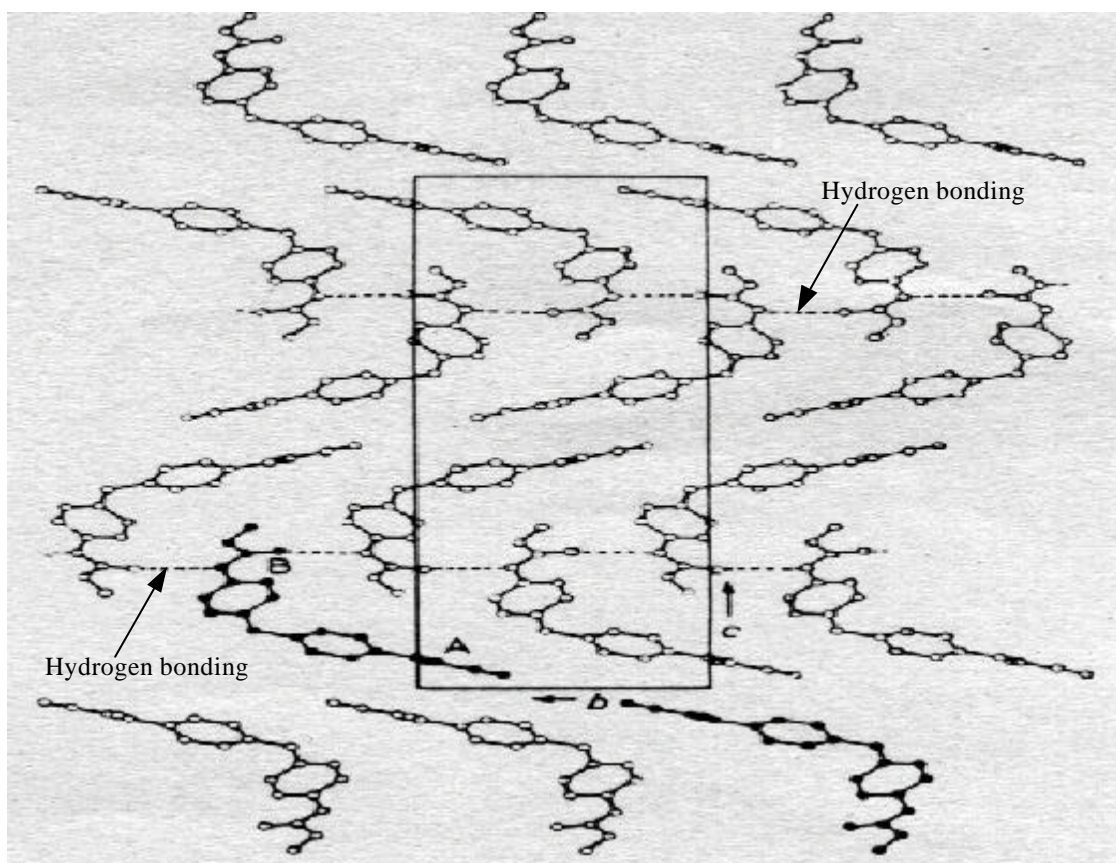


Figure 2.2 bc projection of the Me-M-Me (4,4'-dimethoxycarbonyl-4,4'-diamino-diphenylmethane) structure showing the packing and intermolecular hydrogen bonding<sup>24)</sup>

Table 2.1 Characteristic features of thermoplastic polyurethane elastomers<sup>25)</sup>

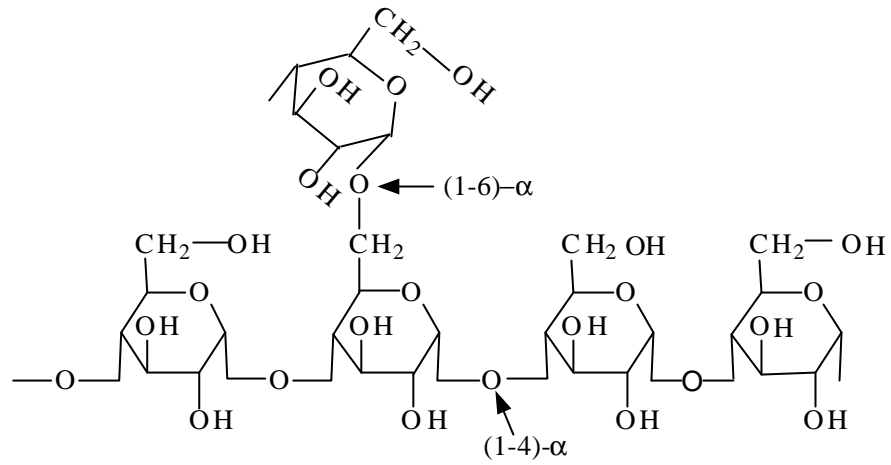
Properties	Units	Desmopan 385 (Bayer AG)	Desmopan 790 (Bayer AG)
	SI	SI	SI
Density	$\text{g/cm}^3$	1.20	1.21
Mechanical			
Ultimate tensile strength	$\text{N/mm}^2$	35 to 40	35 to 45
Elongation at break	%	400 to 450	450 to 500
Abrasion resistance	$\text{mm}^3$	20 to 30	20 to 30
Shore hardness A/D	-	85/33	92/42
Thermal			
Service temperature in air without mechanical loading			
short-term	$^{\circ}\text{C}$	110	120
long-term	$^{\circ}\text{C}$	80	80
Glass transition temperature	$^{\circ}\text{C}$	-40	-40
Coefficient of linear expansion	$\text{K}^{-1} \cdot 10^6$	150	180
Optical	-	translucent	opaque
Permeability to water vapor (2mm/0.0788 in specimen)	$\text{g/m}^2 \cdot \text{day}$	7.0	3.0
Water absorption	$\text{g}/(7 \text{ days})$	53	59

## 2.2 Starch

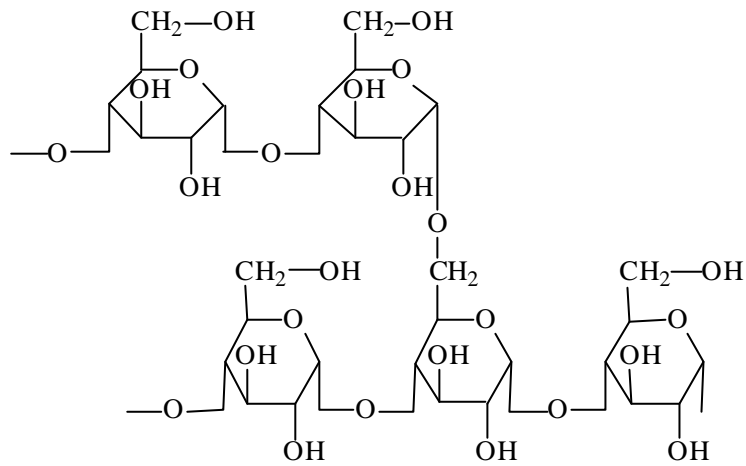
Starch is a combination of amylose, which is a linear polymer and has a molecular weight of 2 to 6 x 10<sup>5</sup> [g/mol], and amylopectin (molecular weight ~10<sup>6</sup> [g/mol]). Both are polysaccharides<sup>26</sup> composed of 1,4-alpha-D-glucopyranosyl units (C<sub>6</sub>H<sub>10</sub>O<sub>5</sub>)<sub>x</sub>. Native starch granules swell when they absorb water through hydrogen bonding with their free hydroxyl groups, but they still retain their order and crystallinity. However, when these swollen starch granules are heated, hydrogen bonding between adjacent glucose units is disrupted. The crystallinity is progressively destroyed. This process is called gelatinization. Processing with water in a heated extruder is an efficient way to obtain gelatinized starch. High shear can be generated in the extruder to disrupt the starch granules. The pressure generated raises the boiling point of water so that high temperature is attainable for rapid and complete disruption of the granular structure.

Table 2.2 Starch content of various seeds and the characteristics of the starch granules<sup>26)</sup>

Botanical origin	Starch (% dry basis)	Shape	Diameter (µm) (mean in parentheses)	Amylose (% dry starch)
Wheat	67.2-68.4	Lenticular, polyhedral	2-38	26-28
Maize	71.0-74.0	Polyhedral	5-25	28.0
Smooth pea	43.0-48.0	Reniform(simple)	5-10	33.2-35
Wrinkled pea	32.0-37.0	Rosette (compound)	30-40	62.8-75.4
Sweet potato	69.2-72.0	Polyhedral	10-25	-
Potato	65.0-85.0	Ellipsoidal	15-100	23



(a) Amylose



(b) Amylopectin

Figure 2.3 Characteristics of (a) Amylose and (b) Amylopectin

### ***2.3 Starch and Synthetic Polymer Blends***

#### ***2.3.1 Physical Blending of Starch with Synthetic Polymers***

Simple addition of starch granules onto synthetic polymers follows the general trend of filler effect on the polymer properties.<sup>5), 27-28)</sup> The structure and the property of the starch and the synthetic polymer blends varies with the granule size (normally two sizes of 7-30 and 20-35  $\mu$ m in wheat starch) and the source of the native starch (differing in the granule sizes and the ratio of amylose and amylopectin).<sup>26), 29)</sup> The modulus increases due to the stiffening effect of the granules and the elongation decreases as the starch content increases.

As was shown recently, materials from gelatinized starch and synthetic polymer blends<sup>30-32)</sup> have properties different from those of composites incorporating native starch granules. Studies of the behaviour of starch and polyethylene blends<sup>33-35)</sup> were first performed by Lim et al.<sup>5)</sup> Small particle corn starch (2- $\mu$ m average diameter) films showed the highest elongation rate and tensile strength with lowest light transmission. In contrast, the large granule size of potato starches (35- $\mu$ m average diameter) showed lowest mechanical properties and highest light transmission and film thickness. Also, Lim et al. point out that starch octenyl succinate (SOS) / LLDPE cast films showed higher tensile strength and elongation values than did corresponding native corn starch / LLDPE cast films.

Simmons et al.<sup>36)</sup> investigated the extrusion blending of corn starch (Waxy Maize (WM); Native Corn (NC); High Amylose Corn Starch (HY)) and poly (ethylene-vinyl alcohol) (EVOH) using glycerol and water as plasticizers. Results indicated that all granules were destructured during the extrusion process, and all of blends showed evidence of phase separation between starch and EVOH. The NC and HY blends appeared to be partially miscible as evident from EVOH melting point depression due to the plasticizers and smaller domain size. The starch-rich domain size decreased as the amylose content of the starch components was increased (i.e.,  $d_{WM50} > d_{NC50} > d_{HY50}$ ) and the contrast between phases decreased, indicating increased miscibility between the polymer components. The authors found also that the phase separation of the amylose and amylopectin components in amorphous starch is probably due to branching and molecular weight differences. A similar study of miscible blends between natural starch and synthetic polymers was made by Cascone et al.<sup>37)</sup> using dextran and poly (acrylic acid).



Dextran is miscible with poly (acrylic acid), and the miscibility is ascertained on the basis of the occurrence of a single, composition dependent glass transition temperature in each blend and also on the basis of the transparency and homogeneity of the films.

Studies of polycaprolacton (PCL), and corn starch, wheat thermoplastic starch (TPS) blends were reported by Koenig et al.<sup>38-40)</sup> using glycerol as a plasticizer. Generally, the blends showed a fairly low compatibility with phase separation and were too brittle for mechanical testing. However, a small size of the starch granules and good dispersion in the PCL matrix increased the mechanical properties, and the disadvantages of pure TPS, namely low resilience, high moisture sensitivity and high shrinkage, could be reduced. Depending on the plasticizer content, the elongation at break increased and then decreased for the highest glycerol concentrations. When the starch matrix has a glassy behavior, blending with PCL results in a decrease of the material modulus but the impact resistance is improved. On the other hand, when the starch has a rubbery behavior, PCL increases the modulus of the materials. Also, the dimensional stability was improved significantly, whatever the starch formulation, and with a level of PCL incorporation as high as 10 wt %.

In 1999, Bikiaris et al.<sup>41)</sup> produced low-density polyethylene (LDPE) blends with different amounts of fatty esters of amylose and starch using a Haake-Buchler Rheomixer. They point out that even after esterification of the polysaccharides, their blends with LDPE have unsatisfactory mechanical properties at higher ester concentrations due to the incompatible system. A DMTA study showed some transitions in pure esters and specially in octadecanoated esters, which indicates that the amount of ester in the blend plays an important role in the viscoelastic behavior of the materials.

### ***2.3.2 Starch Grafting and Physicochemical Adhesion of Synthetic Polymers on the Surface of Starch***

Starch and plastics are hard to blend. In general, products made from mixtures of incompatible polymers show reduced physical properties. Most polymers are thermodynamically immiscible,<sup>42)</sup> precluding generation of a truly homogeneous product because of high interfacial tension and poor adhesion between two materials. High interfacial tension and high viscosities contribute to the inherent difficulty of achieving desired dispersion to random mixtures. This leads to their lack of stability and the gross separation during melt processing or use. Poor adhesion is responsible, in part,

for extremely weak and brittle mechanical behavior. But, addition of small amounts of a synthetic polymer with functionalized groups can lead to significant phase stability<sup>37)</sup> between starch and synthetic polymer blends. The presence of functionalized groups on the polymer can promote compatibilities as a result of graft reaction or interaction that generates bonding between polymers. A large number of functional groups attached to synthetic polymers or starches can react. In reactive blending,<sup>43)</sup> one polymer phase contains reactive groups, which find their counterpart functional groups such as a hydroxyl group in starch, amine and carboxyl group in protein. In some cases, reactive groups that are not inherent in the polymer can be introduced into the second phase. Common functional groups capable of reacting with starch include carboxyl, epoxy, anhydride, oxazoline, isocyanate<sup>13)</sup> and urethane. For the improvement of compatibility by reaction between starch and synthetic polymers, there are two approaches. The first is to graft the external surface of the starch granules with prepolymers prior to the blending. The second is grafting in the processing step through the two functional groups on starch and the synthetic polymers. Most graft copolymerization reactions have been carried out with unswollen starch, and granules of grafted starch often remain intact, even after the incorporation of large amounts of synthetic polymer.

### ***2.3.3 Grafting of Prepolymers on the Starch prior to Synthesis***

Various efforts<sup>31), 44-46)</sup> have been made to increase grafting by using functional groups. In 1965, Otey et al.<sup>47-49)</sup> investigated a series of six glycoside mixtures that were polymerized using a propoxylating acid-catalyzed reaction, which was etherified with propylene oxide on anhydroglucose unit. The preparation and properties of the glycoside-based polyethers are within the limits of commercial acceptability for use in rigid urethane foam production. Pfannemüller et al.<sup>10)</sup> also reported an improvement of the compatibility of starch and synthetic polymers. They modified the surface of starch granules, which allowed a dense layering of synthetic chains via urethane linkage without loss of its structure. The properties of products coated with poly (oxyethylene) of different chain lengths and starch being part of a covalent network were studied as to their suitability for being part of a thermoreversible network.

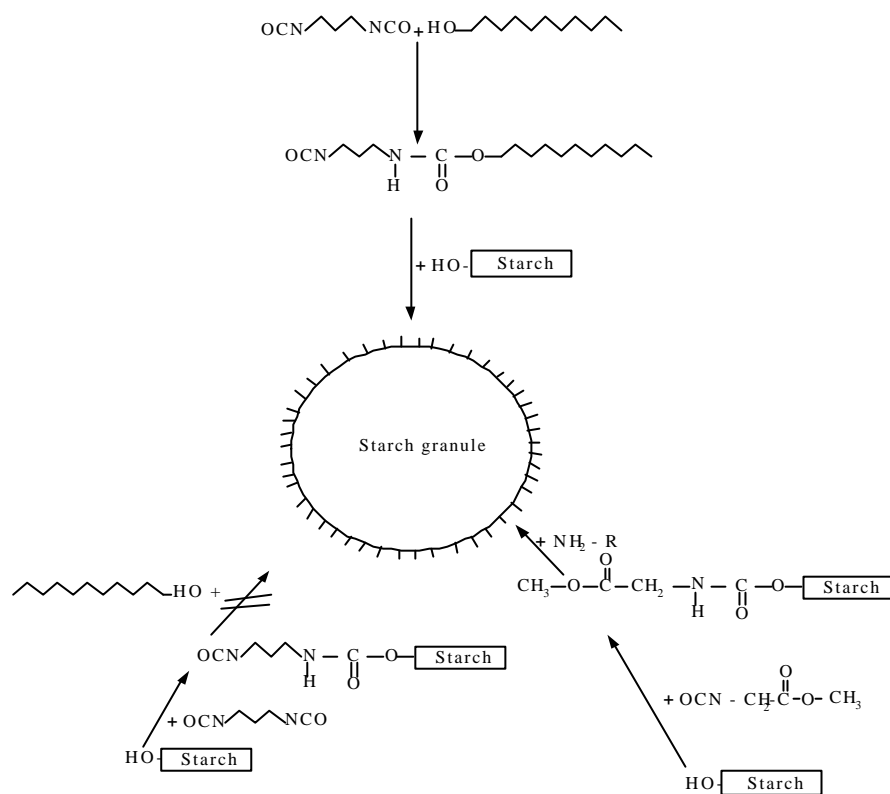


Figure 2.4 Chemical bonding of synthetic polymer chains on the surface of starch<sup>10)</sup>

In 1964, grafting of methyl methacrylate and starch was reported by Brockway.<sup>44)</sup> Hydrogen peroxide (HOOH-) and iron ( $\text{Fe}^{+2}$ ) initiation in aqueous slurry were applied to granular corn starch. Results were focused on finding appropriate solvents for the starch and PMMA system. Chloroform ( $\text{CCl}_4$ ) and dichloroethane ( $\text{Cl-CH}_2\text{-CH}_2\text{-Cl}$ ) are approximately equally efficient.

In 1968, Gugliemelli et al.<sup>50)</sup> found that vinyl grafting on starch in hot acid can alter sensitive functional groups of some vinyl polymers. The vinyl polymer components of starch-polyacrylonitrile (starch-PAN), starch-poly (methyl acrylate) (starch-PMA) and starch-poly (methylmethacrylate) (starch-PMMA) graft copolymers can be isolated readily after depolymerization of the starch by periodate and methanolic alkali treatments.

In 1983, Fanta et al.<sup>45)</sup> achieved starch-g-polystyrene grafting in a solution of potassium persulfate ( $\text{K}_2\text{S}_2\text{O}_8$ ) in water at  $80^\circ\text{C}$  under nitrogen. Fracturing some of the eroded-appearing polystyrene granules that remained after removal of the starch component gave only small fragments and did not reveal the hollow centers that one might expect if polystyrene were located primarily near the granule surface and if the granule centers were thus composed largely of un-grafted starch. They concluded as an interesting point that polymerization takes place not only on the surface but throughout the starch granule matrix as well. Furthermore, the maintenance of birefringence after graft polymerization suggests that grafting takes place in amorphous regions of the granules.

Several researchers<sup>7), 12-13)</sup> reported polyurethane formation on the external surface of destructured starch. In 1992, rigid polyurethane foams were prepared by Cunningham et al.<sup>12)</sup> using unmodified and modified cornstarches. The cornstarches were modified by breeding or conversion methods and included waxy, acid-modified waxy, malto-dextrin, and canary dextrin starches. The foams containing canary dextrin exhibited a higher compressive strength value than any foams filled with unmodified, waxy, acid-modified waxy, or malto-dextrin starch. Foams containing malto-dextrin and canary dextrin (20 %, based on weight of polyol) responded to compressive stress in the same way as the control foam, exhibiting yield points before 10 % deformation. Upon application of additional amounts of canary dextrin, foams containing 40 % (based on weight of polyol) gave compressive strength values of  $134 \text{ kN/m}^2$ . Additionally, application of canary dextrin in rigid polyurethane foam formulations provided foams with similar or improved thermal stability, open-cell content, and thermal conductivity.

In 1997, Athawale et al.<sup>7)</sup> performed graft polymerization of methacrylic acid (MA) onto starch using  $Ce^{4+}$  initiator in aqueous medium. They point out that methacrylic acid can be easily graft polymerized onto starch. The thermal properties of starch were less affected due to grafting which affects the solubility and gelatinization properties of starch.

Recently, in 2000, Desai et al.<sup>13)</sup> studied starch as a crosslinker in polyurethane elastomers. The polyurethane elastomers were synthesized using polypropylene glycol (PPG 2000) as the polyol, starch and 1,1,1-trimethylol propane (TMP) as the crosslinker in varying concentrations. The starch / polyurethanes were found to show better mechanical properties than TMP / polyurethanes. With increasing the NCO:OH equivalent ratio, the stress-strain properties were observed to increase. DSC thermograms of TMP / polyurethanes showed the appearance of only one glass transition, whereas thermograms of starch / polyurethane showed two, indicating phase separation. The solubility parameter from the swelling data of starch and polyurethane blends was discussed about a correlation with thermo-mechanical properties, and the potential for biodegradation.

#### ***2.3.4 Grafting Reaction by Extruder Blending***

In the last 10 years, various researchers<sup>51-55)</sup> focused on reactive blending of starch and synthetic polymers in twin screw extruders and injection molded samples. The blending of corn starch and ethylene-propylene-g-maleic anhydride (EPMA) and modified polystyrene with maleic anhydride (SMA) was studied by Vaidya et al.<sup>52)</sup> They found that the torque generated during the blending was higher for the blends of the anhydride functional polymers than for the blends of corresponding nonfunctional polymers. Blends containing 80 % or more of starch could not be made in the extruder, due to higher viscosity and pressure. Water absorption of the blends increased with an increase in the starch content and in SMA blends compared to the EPMA. In starch/EPMA blends, the starch in the blend formed a cocontinuous phase with the rubbery phase. The starch phase became finer as the amylopectin content in the starch increased. In starch/SMA blends, the starch granules were still intact, presumably because the torque generated was lower than that used for corresponding starch/EPMA blends.

In 1991, Carr<sup>43)</sup> reported the reaction of starch with ethylene glycol and glycerol in the presence of sulfuric acid catalyst using a corotating, intermeshing, twin screw extruder

with a barrel length / screw diameter (L / D) ratio of 43 : 1. Results showed that starch can be continuously and rapidly converted to glucosides in 90 % yield at high production rates, and that short reaction periods of 45-60 sec can be achieved in a continuous twin-screw extruder.

In 1992, Yoon et al.<sup>56)</sup> performed graft polymerization of acrylonitrile (AN) onto unmodified cornstarch by continuous reactive extrusion. The effects of AN / starch weight ratios, level of ceric ammonium nitrate (CAN) initiator, starch in water concentration, reaction temperature, reaction time, and screw speed were studied. Processing times in the twin-screw extruder (ZSK) were 2-3 minutes, and total reaction time was about 7 min before reaction of the extruded material was terminated, compared to a reaction time of 2 hours used in the typical batch procedure. The reactive extrusion process was found to be a rapid and efficient means of preparing starch-g-PAN with high add on (% PAN of the grafted product). For example, 42 % add-on was achieved within the 7 minute reaction period using AN / starch weight ratio of 1.0 (3.5 % CAN, starch weight basis), as compared to 38-49 % for the 2 hours batch process (0.75-1.5 AN / starch ratio). Grafting ratios were substantially higher while molecular weight (MW) was significantly lower for grafts from the extrusion process.

In 1998, Seidenstücker et al.<sup>57)</sup> reported hydrolysis of different thermoplastic poly(ester-urethane) samples such as adipic acid (ADPA) and dodecyldi-acid (DDDA), poly( $\alpha$ -caprolacton), short chain alcohols (monoethylenglycol (MEG), diethyleneglycol (DEG), butanediol (BD), poly(ethylene)-glycol (PEG). Additionally, diphenylmethan-4,4' -diisocyanate or its hydrogenated version (HMDI) were used. The compounding of materials with TPU as matrix and starch as a filler of thermoplastic starch (TPS) is achieved by using co-rotating intermeshing twin screw extruders. A vacuum devolatilization at the end of the barrel was used to reduce the remaining water content of the compound. Native corn starch (CS) influences the mechanical properties of the compound when the starch content is varied between 30 and 70 % (w/w). The higher the starch content the lower the mechanical strength and the higher the stiffness. The authors point out that the use of TPS can lead to materials whose initial stress/strain-curves are not very much altered to that of the native corn starch matrix. The morphology of a 50/50 (w/w) blend, for instance, can be shown in a way that the dispersed phase i. e. the thermoplastic starch, is finely distributed within the matrix, the drop size being in the range of  $0.3 < d < 1.2 \text{ } \mu\text{m}$  with the average drop size  $d$  of approximately  $0.5 \text{ } \mu\text{m}$ . Recently, Seidenstücker et al.<sup>58)</sup> investigated the blending of

thermoplastic poly (ester-urethanes) and destructure starch using glycerol, poly (ethylene glycol) or epoxidized linseed oil as a destructure agent. Short residence time of the blend components in the extruder was used to reduce or prevent significant polymer degradation. The extrusion methods, so-called two-step process (TSP) and single step process (SSP) were studied to improve the morphology and quality of the product. The two step process can be run at much higher throughput, reducing drastically the residence time of the TPU in the twin screw extruder. On the other hand, the single step process may be more economical and is suited for many different types of TPS which can be produced by adding polyfunctional alcohols.

### 3. EXPERIMENTAL

#### 3.1 Materials

The basic materials used in this research were 1,4-butanediol and polycaprolacton-diol ( $M_n \cong 2000$ ) and 4,4-diphenylmethane diisocyanate (MDI, 98 %) from Aldrich Chemical Company. The dibutyltin dilaurate (DBTDL) used as a catalyst was supplied by Merck. All the chemicals were used as such, without further purification. Potato starch was kindly supplied by the Institute for Cereal, Potato and Starch Technology (in Detmold, Germany). Tables 3.1 and 3.2 show the specifications of the potato starch and chemicals used.

#### 3.2 Determination of Moisture and OH-Value of the Starches

##### 3.2.1 Karl-Fischer Titration for the Measurement of the Moisture in Starch

The moisture content of the potato starch was determined by Karl-Fischer titration methods. The potato samples were dried in a vacuum oven at 100 °C for two days. KF solvent was placed in the titration glass bottle up to the mark; then the bottle was plugged with a polyethylene stopper. The KF titrant bottle with cannula was pierced by the stopper and the bottle was turned upside down to fill the syringe to the mark "0 ml". The solution was shaken while the titrant was added drop by drop. The colour of the solution changed from colourless to yellow. Exactly 0.136g of potato starch was added. The water content G in percentage by weight was calculated from consumption a in ml of titrant, titer b of the titrant and weight m in mg.

$$G = a \times b \times 100 / m \quad (3.1)$$



### ***3.2.2 Hydroxyl (-OH) Number Determination of the Surface of the Starch Granule by Titration (International Standard, 4629-1078)***

Potato starch is dried for two days in a vacuum oven at 110 °C. First, 5ml of the ethyl acetate is added to the contents of the conical flask and shaken, if necessary with gentle warming, until the test portion is dissolved. After cooling to ambient temperature, 5.00 ± 0.02 ml of the acetylating reagent is added by means of a microburette or pipette, and the reflux condenser is fitted onto the conical flask. The flask is heated and maintained at 50 ± 1 °C for 20 minutes, and shaken every 5 minutes. After cooling the contents of the flask to ambient temperature, the condenser is removed and 2ml of water added, then the condenser is replaced and the flask is vigorously shaken. 10 ml of a pyridine/water mixture is added from the top of the condenser to rinse the condenser tube. The contents of the flask are mixed and allowed to stand for 5 minutes at ambient temperature. After adding 30 ml of the toluene/butanol mixture from the top of the condenser, the condenser is removed and a further 30 ml of the toluene/butanol mixture is used to rinse the condenser/flask glass joint. The potassium hydroxide (KOH-) solution is titrated in the presence of a colour indicator: 5 drops of the phenolphthalein solution. The hydroxyl value is given in milligrams of potassium hydroxide per gram of sample by the formula.

$$(V_0 - V_1) \times T \times 56.1 / m = \text{-OH.} \quad (3.2)$$

where  $V_0$  is the volume[ml] of the potassium hydroxide (KOH-) solution (Blank Test),  $V_1$  is the volume[ml] of the potassium hydroxide (KOH-) solution with sample.  $T$  is the exact normality of the potassium hydroxide (KOH-) solution.  $m$  is the mass [g] of the test portion. Secondly, a blank test is carried out, following the same procedure and using 5.00 ± 0.02 ml of the acetylating reagent, but omitting the test portion.

OH-values for three kinds of the starch are presented in Table 3.3.

### ***3.2.3 Equivalent Weight of Raw Materials***

Polycaprolactone diol prepolymer (2000 ( $M_n$ )/2) = 1000

1.4 Butane diol = 90 ( $M_n$ )/2 = 45

Potato starch = 1344 Using equation 3.2

$$\text{OH-value} = (61.355 - 58.35) \times 0.5 \times 56.1 / 2.02 = 41.74$$

$$\text{Equivalent weight} = 56100 / 41.74 = 1344$$

$$\text{MDI} = 250 (M_n)/2 = 125$$

### **3.3 Characterizations**

#### **3.3.1 Scanning Electron Microscopy (SEM)**

The specimens were mounted on aluminum stubs using double-sided carbon tape and were coated with gold-palladium to a thickness of about 2  $\mu\text{m}$  in a sputter coater. The coated specimens were observed in a SEM (Hitachi H301U). An accelerating potential of 10 kV was used for the analysis of samples. The micrographs of representative areas of the samples were taken at various magnifications.

#### **3.3.2 Differential Scanning Calorimetry (DSC)**

The transition behavior of the polyurethane incorporating starch was characterized using differential scanning calorimetry (Mettler TC 10A / TC 15, TA controller). The samples were quenched using liquid  $\text{N}_2$  to the required temperature and then scanned at a rate of 10  $^\circ\text{C}/\text{min}$  in a dynamic nitrogen atmosphere with a flow rate of 6  $\text{cm}^3/\text{min}$ . The sample size was  $30 \pm 1$  mg. The temperature scale was calibrated with an indium standard before the experiments. Indium has a melting temperature of 156.6  $^\circ\text{C}$  and a heat of fusion of 28.45 J/g. The glass transition temperature ( $T_g$ ) was measured at the point of intersection between tangents drawn at the point of inflection of transition and at the flat part of the curve before transition.

#### **3.3.3 Fourier Transformation Infrared Spectroscopy (FTIR)**

The sample was fully dissolved in dimethylsulfoxide and dropped onto a NaCl salt plate. The dried extracted polyurethane was recorded in the transmittance mode. FTIR spectra were obtained using a Nicolet 510 P FT-IR spectrometer at a range of 4000-400  $\text{cm}^{-1}$  and resolution was maintained at 2  $\text{cm}^{-1}$ .

#### **3.3.4 Grafted Percentage of Polyurethane to Starch Granule**

Polyurethane incorporating starch was extracted with a mixed solvent (DMF (95 %) + THF (5 %)) to remove the homo-polymer of polyurethane in the sample. 1g of the blended sample was thinly sliced and stored in 25 ml of solvent for 24 hours at room temperature; it was then washed by decanting four times in 25 ml of fresh solvent. The washed blends were dried at 100  $^\circ\text{C}$  in a vacuum oven for three days. In this study, we defined the polyurethane grafted to starch as follows:

$$\text{Grafted (\%)} = \frac{\text{weight of PU remaining after extraction}}{\text{weight of PU before extraction}} \times 100$$

### 3.3.5 Gel Permeation Chromatography (GPC)

Molecular weight and molecular weight distribution were measured using a GPC equipped with a Waters 515 HPLC pump/ 717 auto-sampler/410 differential Refractometer and Styragel HR 4 (MW 5000-600000) column at Hanyang University in Seoul, Korea. The mobile phase was tetrahydrofuran (THF) at a rate of 1.0 ml/min and the column temperature was maintained at 35 °C. All samples were prepared in DMF and THF at a concentration of 0.01 (w/v). Average molecular weights of polyurethane separated from the blends were determined by relative calibration method. Standard polystyrenes (Shodex Standard, SM-105) were used with 6 different molecular weights (range of molecular weight: 103~106) of polydispersity of 1.02~1.06. We calibrated the curve (cubic was fitted) using the standard polystyrene and determined relative molecular weights of the polyurethane by comparing the retention volume. Number-average ( $M_n$ ), weight average ( $M_w$ ), and polydispersity ( $M_w/M_n$ ) were calculated using Waters Chromatography Millennium software.

### 3.3.6 Thermogravimetric Analysis (TGA)

The thermal stability of thermoplastic polyurethane and starch blends was determined using the Thermogravimetric Analysis (T.G.A, Mettler TG 50). The rate of the TGA scans was 10 °C /min under nitrogen atmosphere at a flow rate of 5 cm<sup>3</sup> / min. The initial weight of the samples was about 20 mg and the temperature range 30-550 °C.

### 3.3.7 Polymer Mechanical Properties

Specimens for tensile testing were compression molded in a Lauffer und Butscher compression molder at 200 kg/cm<sup>2</sup>. The detailed dimension of test specimen bars was in the form of dumbbells according to DIN (EN ISO 527-2). Tensile specimens were dried in a vacuum oven at 10 mmHg and 100 °C for 5 hrs. The tensile mechanical properties of the polyurethanes incorporating starch were measured using a Zwick (Material prüfung 1446) machine. The specimens were fixed using a grip with a tensiometer. A crosshead speed of 50 mm/min with a 0.1 N/mm<sup>2</sup> load cell was used at room temperature.

### **3.3.8 Rheological Measurements**

The temperature dependence of the dynamic mechanical properties and melt viscosity were measured using a Rheometric Dynamic Spectrometer (RDS-2) with a parallel plate fixture (25 mm diameter). The test specimen was placed in a compression molding press for 15 minutes at 30 bar at a temperature of 10 °C above the melting temperature of the sample. The compression-molded specimens were immediately quenched at room temperature and then stored inside a desiccator before using. We determined the storage- and loss-modulus ( $G'$  and  $G''$ ), and the complex viscosity( $\eta^*$ ) at 200 °C for the frequency range of  $10^{-1}$  to  $10^2$  .

## **3.4 Synthesis of Polyurethane**

### **3.4.1 One-Step Reaction(OSR)**

Polycaprolactone diol and 1,4-butane diol were added to a 2 l reaction flask equipped with a heating mantel, stirrer, thermometer, and vacuum inlet. Each diol was heated to 100°C and degassed for 1 hr to remove moisture and dissolved gases. The temperature of the diol was then increased to 175 °C while degassing was continued under vacuum. The pre-measured hydroxyl (-OH) value of potato starch was poured into the reactor in order to have longer pre-mixing with polycaprolactone diols and dried again under vacuum at 175°C. After this pre-blending of the diols, the dibutyltin dilaurate (DBTDL) catalyst and 4,4-diphenylmethane diisocyanate (MDI) were added. The mixture was stirred vigorously for about 1 minute, degassed for 30 minutes and transferred to an aluminium tray that had previously been treated at 100°C with a silicon release agent. It was then placed in an oven and cured at 120 °C for 4 hrs. After removal from the oven, the samples were removed from the mold and post-cured at room temperature for one week before further characterization.

The molar ratios in polyurethane-synthesis of polycaprolactone-diol incorporated with starch and different molecular weight of prepolymer (polyethylene glycol) for p7s3b2m3 series in the one-step reaction are shown in Tables 3.4 (a) and (b).

The schematic diagram and the photo of the experimental apparatus for the polymerization of the polyurethane-starch blends are presented in Fig. 3.1 and 3.2, respectively.

### 3.4.2 Two-Step Reaction (TSR)

In the first step, Polycaprolactone diol ( $M_n=2000$ ) was heated to 100 °C and degassed for 1hr to remove water and dissolved gases. The temperature of the diol was then increased to 175 °C while degassing was continued. The excess of pre-dried MDI was dropped into the reactor in order to terminate the –OH of the PCD diol. After four minutes, potato starch was poured into the reactor. Degassing was continued for 10 minutes. Next, the polyurethane chain was extended with 1,4-Butane-diol. The reaction ended when the –NCO group was completely consumed. The remaining –NCO was confirmed by the disappearance of FT-IR absorption at 2280  $\text{cm}^{-1}$ .

Table 3.1 Properties of potato starch

Protein Content	< 0.13 %
Starch Total	
Polarimetric Ewers Procedure	> 98 %
Megazyme Procedure	> 98 %
Amylose Content	appr. 30-34 %
Particle Size	appr. 37 $\mu\text{m}$
Lipid Content	No Lipid
Ash Content	< 0.63 %

Table 3.2 Chemicals used for the synthesis of polyurethane

Materials	Description	Sources
Polycaprolacton-diol ( $M_n$ 2000)	Hydroxyl value: 56.1 mg KOH/gm Molecular weight: 2000 Softening temperature, 50°C	Aldrich
Polyethylene glycol ( $M_n$ 2000, 4000, 6000, 10000)	Hydroxyl number: (51-63, 25-32, 16-23, 9-12)	Merck
4,4-Diphenylmethane Diisocyanate (MDI, 98 %)	$F_p = 42-44^\circ\text{C}$	Aldrich
1.4-Butane diol	$B_p = 230^\circ\text{C}$	Aldrich
Starch	Hydroxyl number: 41.7	Detmold
Dibutyl tin dilaurate(DBTDL, 98 %)	-	Merck

Table 3.3 Hydroxyl (-OH) value of surface of various starch granules determined by titration

	-OH value	Amylose content (%)	Equivalent weight
Potato starch	41.7	App. 30-34 %	1344
Pea starch	7.1	App. 68 %	7920
Maize starch	24.7	App. 35 %	2266

Table 3.4 (a) Molar ratios in polyurethane-synthesis in combination with starch (OH/NCO mole ratio=1)

Samples	Starch-OH	PCL-OH	1.4 BDO-OH	MDI	Cata. Con./wt.%	Hard segment (wt. %) in polyurethane phase	Starch wt %
p1b2m3(OSR)	0.0	1.0	2	3	0.01	31.74	0.0
p9s1b2m3(OSR)	0.1	0.9	2	3	0.01	34.07	8.96
p8s2b2m3(OSR)	0.2	0.8	2	3	0.01	36.76	17.53
p7s3b2m3(OSR)	0.3	0.7	2	3	0.01	39.91	25.71
p6s4b2m3(OSR)	0.4	0.6	2	3	0.01	43.66	33.55
p5s5b2m3(OSR)	0.5	0.5	2	3	0.01	48.19	41.05
p7s3b2m3(OSR C0.05)	0.3	0.7	2	3	0.05	39.91	25.71
p7s3b2m3(OSR C0.1)	0.3	0.7	2	3	0.1	39.91	25.71
p7s3b2m3(TSR)	0.3	0.7	2	3	0.01	39.91	25.71
p1b4m5(OSR)	0.0	1.0	4	5	0.01	44.60	0.0
p9s1b4m5(OSR)	0.1	0.9	4	5	0.01	47.21	7.31
p8s2b4m5(OSR)	0.2	0.8	4	5	0.01	50.16	14.35
p7s3b4m5(OSR)	0.3	0.7	4	5	0.01	53.49	21.13
p6s4b4m5(OSR)	0.4	0.6	4	5	0.01	57.30	27.67
p5s5b4m5(OSR)	0.5	0.5	4	5	0.01	61.69	33.96
p7s3b4m5(OSR C0.05)	0.3	0.7	4	5	0.05	53.49	21.13
p7s3b4m5(OSR C0.1)	0.3	0.7	4	5	0.1	53.49	21.13
p7s3b4m5(TSR)	0.3	0.7	4	5	0.01	53.49	21.13

Table 3.4 (b) Molar ratios in the polyurethane synthesis using different molecular weights of prepolymer (polyethylene glycol) (OH/NCO mole ratio=1)

Samples	Starch-OH	PCL-OH	1,4 Butane diol	MDI	Hard segment / wt.% in polyurethane phase	Starch / wt.%
p7s3b2m3-peg2000(OSR)	0.3	0.7	2	3	29.86	25.90
p7s3b4m5-peg2000(OSR)	0.3	0.7	2	3	30.74	21.25
p7s3b2m3-peg4000(OSR)	0.3	0.7	2	3	20.71	17.95
p7s3b2m3-peg6000(OSR)	0.3	0.7	2	3	16.13	13.99
p7s3b2m3-peg10000(OSR)	0.3	0.7	2	3	10.08	8.75

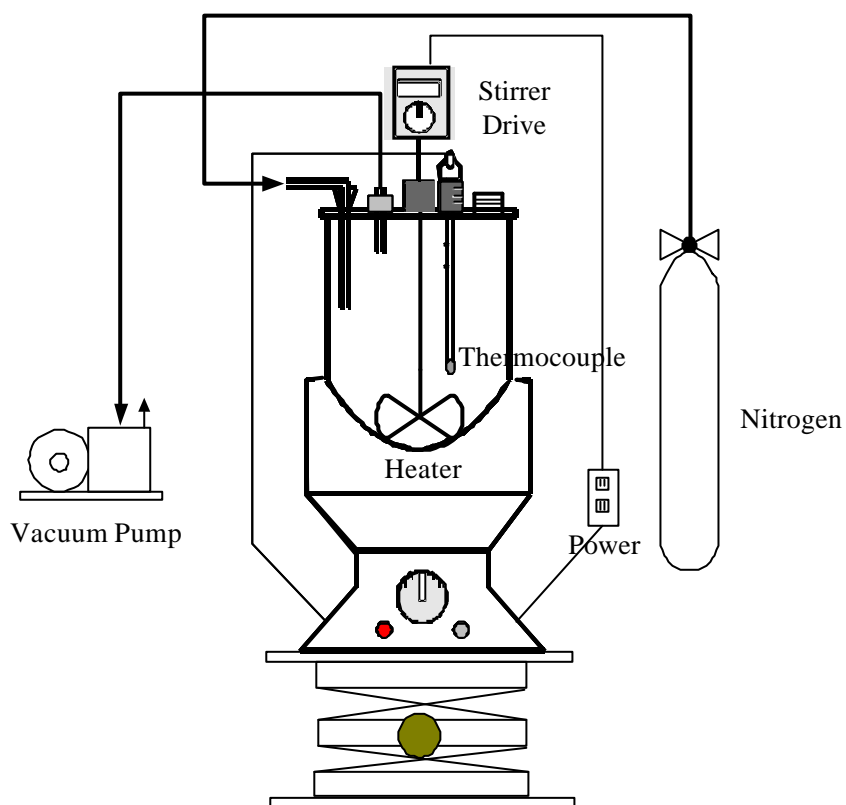


Figure 3.1 Schematic flow diagram of the experimental apparatus for the synthesis of polyurethane-starch blends.





Figure 3.2 Photo of experimental apparatus

## 4. RESULTS AND DISCUSSION

### 4.1 Characterization

#### 4.1.1 Studies by Scanning Electron Microscopy

##### 4.1.1.1 Dispersion and Adhesion of Polyurethane on Starch Granules

The dispersion of the starch in the continuous polyurethane phase and the adhesion between them were confirmed by SEM. Figure 4.1 shows the SEM-micrographs of p7s3b2m3(starch, 17.5 wt.%). The surface of the sample for the SEM was prepared by breaking the samples at liquid nitrogen temperature. As shown in Figure 4.1, the starch granules are well dispersed in the polyurethane phase without any aggregation. The scanned surface reveals that some starch granules were broken into two parts and others were completely coated by a tightly adhering polyurethane layer. Some gaps were found between the starch and polyurethane phases in which stretched polyurethane threads connect the two phases. This also confirms the strong adhesion between the polyurethane and the surface of the starch granules. This phenomenon as evidence of grafting between the starch and polyurethane, as shown in Figure 4.1, is supported in previous reports (e.g. Suh et al.<sup>59</sup>). The SEM micrographs show that the potato starch granule has a relatively large granule size that is not de-structured during the reactions.

##### 4.1.1.2 Polyurethane-Extracted Starch

The evidence of starch grafted with a polyurethane phase was also confirmed directly by comparing SEM-micrographs of homo-polymer-extracted starch with pure starch granules. Extraction was carried out with a mixed solvent, DMF(95%)+THF(5%), at ambient temperature for 5 days. The surface of pure starch is clean and has its original shape (Figure 4.2). The sample after extraction with the mixed solvent (Figure 4.3) shows a layered polyurethane phase on the surface of the starch granule.

Chain alignments of polyurethane between the surfaces of the starch granule of the blends were observed. The observed surface was obtained by breaking the sample at liquid nitrogen temperature. Breaking may have occurred along the texture of the polymer chains. Figure 4.4(a) shows SEM-micrographs of the broken surfaces of the p7s3b4m5 sample. The broken surface indicates that the polyurethane chain texture was connected vertically between the starch-granular-surfaces.

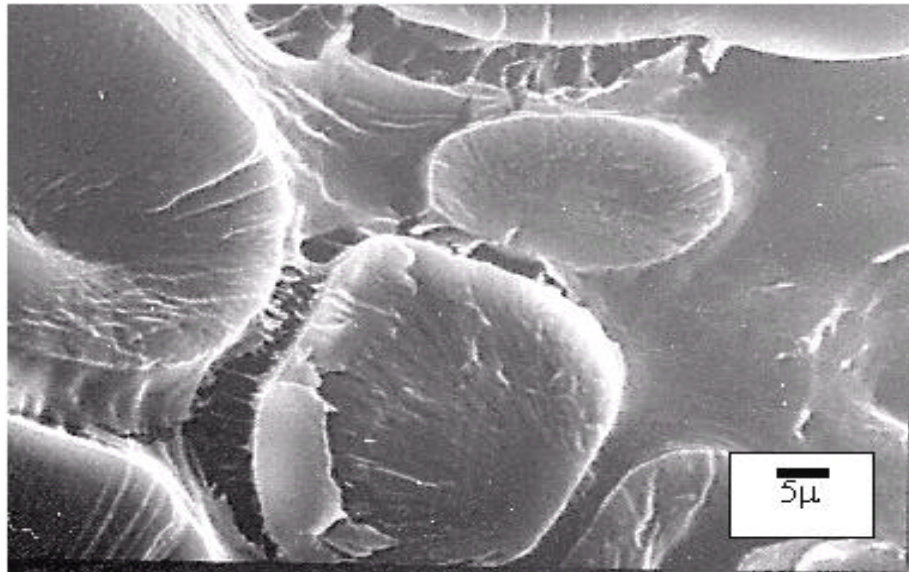


Figure 4.1 Cryogenically fractured SEM-micrograph for p7s3b2m3 (25.7wt % of starch) (magnification: x1000)

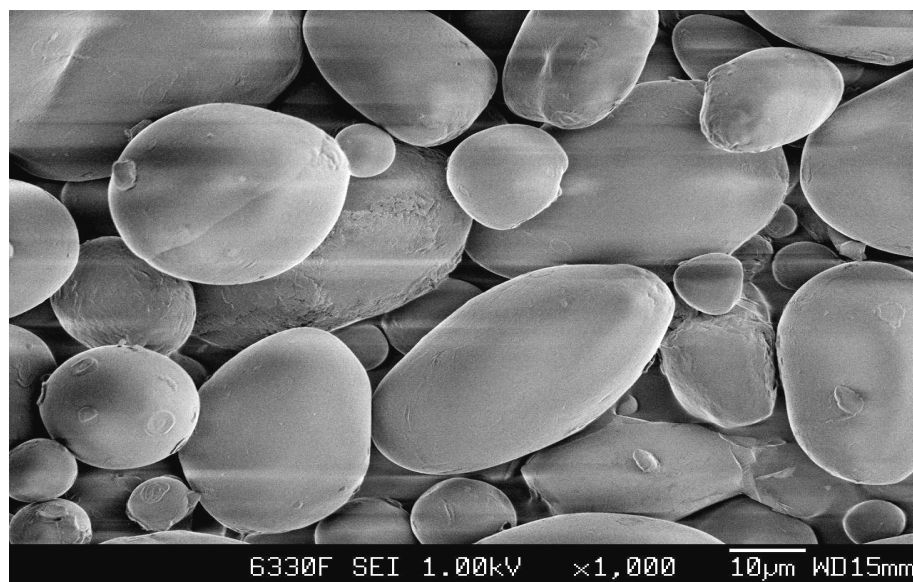


Figure 4.2 SEM-micrograph for pure potato starch

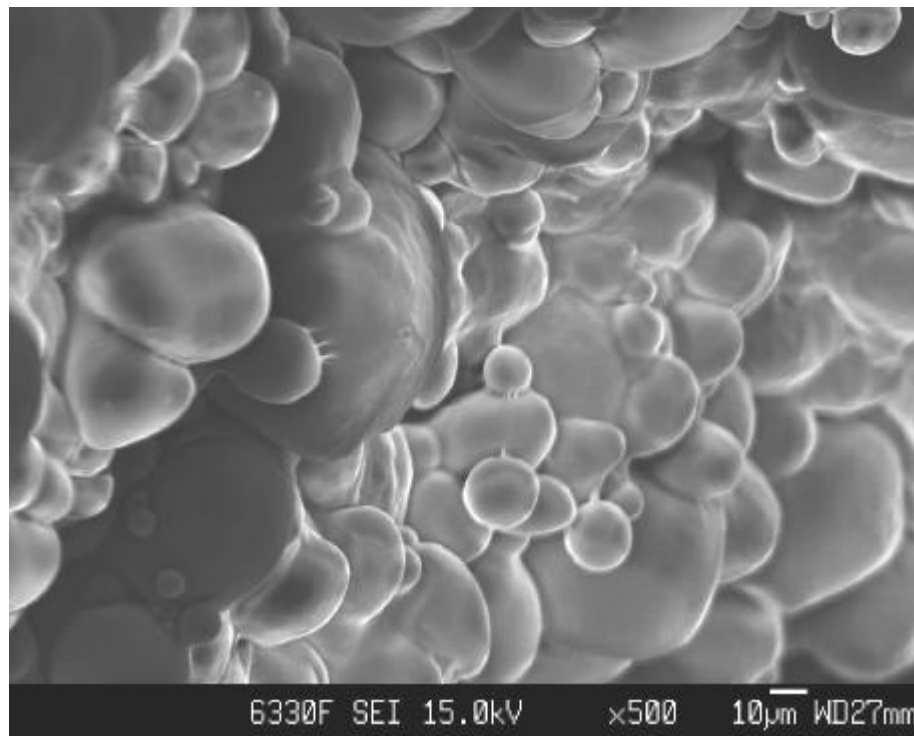
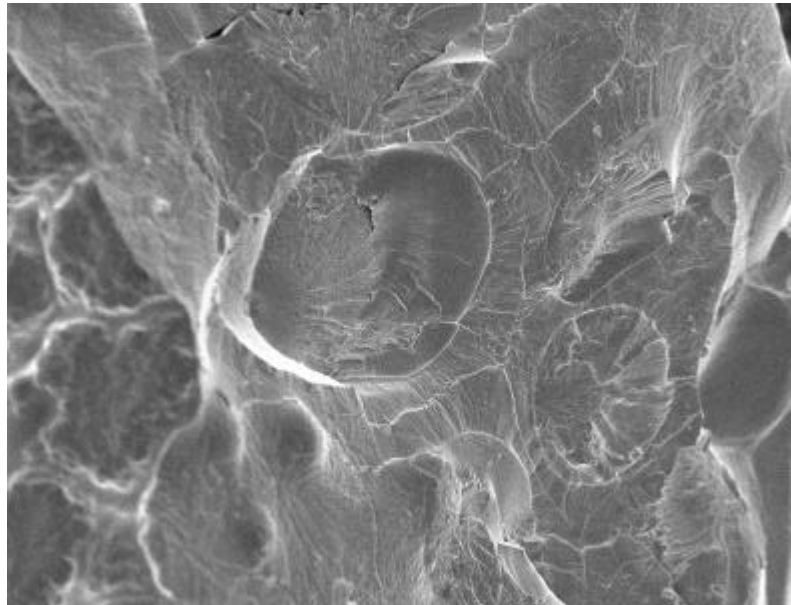


Figure 4.3 SEM-micrograph for homo-polymer-extracted starch (p5s5b2m3)

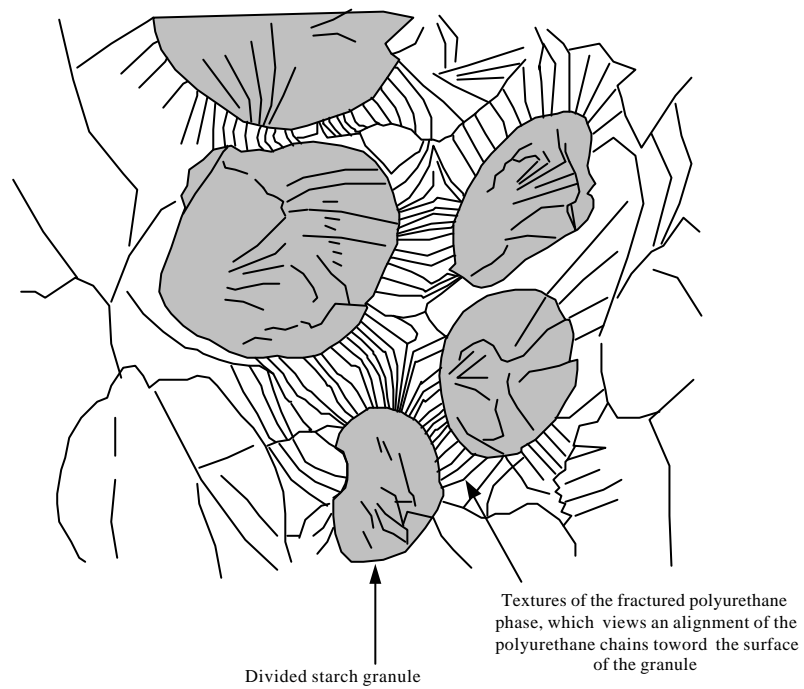
This is most clear in sample, p7s3b4m5. Such developed texture reveals that polyurethane chains are fairly crosslinked between starch-granules. The possible alignment of the polymer chains vertically to the surface of the starch granules was sketched in Figure 4.4(b). This phenomenon indicates that the urethane reaction between  $-NCO$  and  $-OH$  was started from the surface of the granule and/or the polymerization of the polyurethane was terminated on the surface of the granules. Additionally, parallel chain alignment of the polyurethane was supposed to be more developed than in the pure polyurethane system due to the crosslinking of the polyurethane between granules. The structure of the over-all three-dimensional networking of the polymer system is shown in Figure 4.5.

#### ***4.1.1.3 Phase Separation (Gapping Formation) Phenomena at High Starch Contents***

Polyurethane is hydrophobic whereas starch is a hydrophilic material, which indicates that the attachment of the two phases cannot be possible by simple physical blending. At low starch contents, it was difficult to find many gaps between two phases, but at higher starch contents, many gaps were found as shown in Figure 4.6. As shown in Figure 4.6, mechanical properties, in this range, are much decreased. Such a phenomenon could be explained by a tendency to homo-polyurethane due to the high starch content.<sup>14)</sup>



(a)



(b)

Figure 4.4 SEM-micrograph (a) of the broken surfaces of p7s3b4m5 at liquid nitrogen temperature (b) and sketch of the texture.

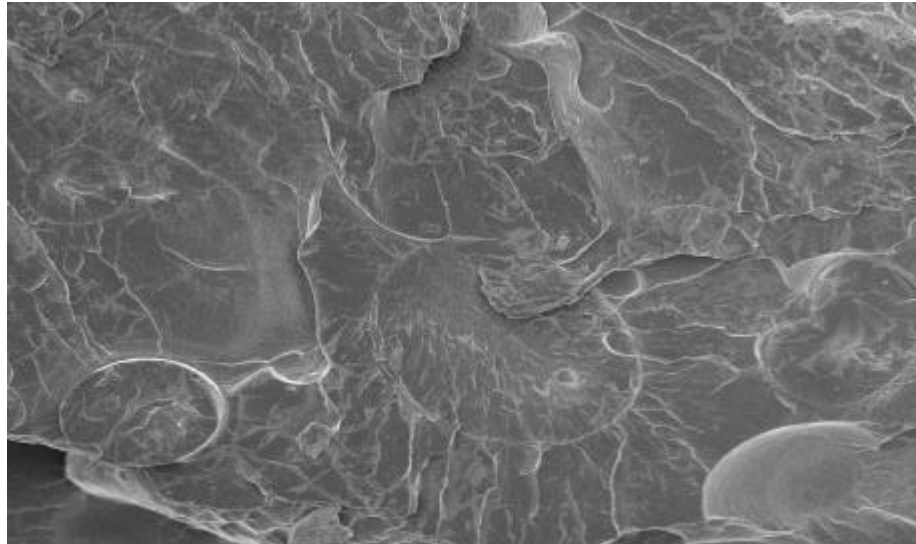


Figure 4.5 SEM-micrograph of p7s3b2m3 (TSR C0.01) for the broken surface at liquid nitrogen temperature

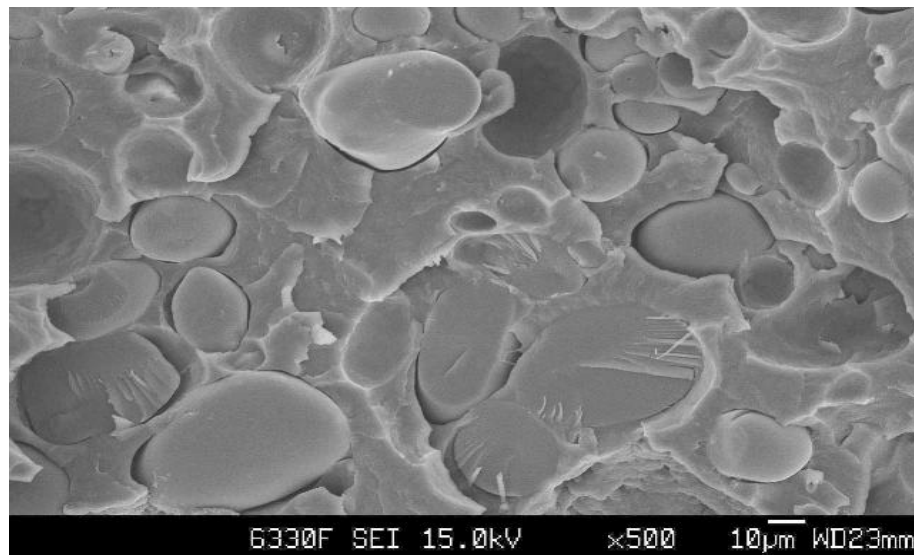


Figure 4.6 Phase separations between starch-granule and polyurethane phase for the fractured surface of a tensile bar of p5s5b4m5 (OSR C0.01) at ambient temperature after tensile test.

### ***4.1.2 Infra-Red (IR) and Nuclear Magnetic Resonance (NMR) Studies.***

#### ***4.1.2.1 Confirmation of Remaining Polyurethane on Starch by Infrared Spectroscopy after Homo-Polymer-Extraction***

The polyurethane-starch blend can be totally dissolved in dimethyl sulfoxide(DMSO). The solution containing the dissolved sample was poured and spread on a KBr window, with which infrared measurement was carried out. The infrared bands at 3440 and 3320  $\text{cm}^{-1}$  are associated with the NH stretching modes of the free and the hydrogen bonded NH groups of the polyurethane, respectively. Hydrogen bonded carbonyl absorption for polyurethane at  $\sim 1700 \text{ cm}^{-1}$  and free carbonyl absorption at  $\sim 1740 \text{ cm}^{-1}$  can also be observed.

IR spectrograms for the polyurethane-starch blends (p9s1b4m5 (7.31wt% starch) and p7s3b4m5 (21.1wt% starch)) are shown in Figures 4.7 and 4.8. Figure 4.7 shows the overlapping band of broad OH and NH bands due to un-reacted  $-\text{OH}$  because the total polymer system was dissolved in DMSO, which allows the OH group inside of the starch granule to be seen. There is a band at  $\sim 3440 \text{ cm}^{-1}$  that can be attributed to the bonded NH band of the polyurethane inside overlapped with the broad OH band. At  $\sim 1703$  and  $1732 \text{ cm}^{-1}$ , the bands resulting from hydrogen bonded and free carbonyl bands can also be observed. These two bands also confirm the grafting between the starch and polyurethane phase.

Hydrogen bonding in polyurethane has been the subject of numerous investigations using infrared spectroscopy.<sup>68-69)</sup> It is manifested by shifts in the N-H and C=O stretching frequency to lower values compared to groups that are not hydrogen bonded.

In the presence of starch, the separation of hard segments can be interfered by starch granules. Therefore, the carbonyl band in the IR spectra, which shows free and hydrogen bonded bands as an overlapped state, can give information of the bonding level of hard segments. Figure 4.9 shows the carbonyl band at around  $1700 \sim 1735 \text{ cm}^{-1}$  which reveals an overlapped state, in which the peaks are separated by peak separation software.

Table 4.1 shows the percentage fractions of the frequencies of bonded and free carbonyl bands. The bonded carbonyl fraction increases with the starch contents whereas the free band decreases. This can be explained by the starch inducing the hydrogen bonding of the hard segment through chain vertical alignment of polyurethane on the surface of the starch granule as indicated in Figure 4.1 and Figure 4.4 (b).



#### ***4.1.2.2 Confirmation of Remaining Polyurethane on Starch by Nuclear Magnetic Resonance Spectroscopy after Homo-Polymer-Extraction***

The NMR technique is the best tool to identify the specific chemical structures. As shown in previous results such as SEM and IR, we could detect the attached insoluble polyurethane grafted to the outer surface of starch granule by SEM (Figure 4.1) and also polyurethane such as  $\text{-C=O}$  band in IR spectra (Figures 4.7 and 4.8) of polyurethane-extracted samples. Polyurethane identification in the extracted phase of the blends was also carried out by  $^1\text{H-NMR}$  and  $^{13}\text{C-NMR}$  technique. The starch-polyurethane samples were dissolved in  $\text{DMSO-d}_6$  at  $60^\circ\text{C}$  (solution concentration 5 w/v %). Figures 4.10 and 4.11 show the  $^1\text{H-NMR}$  and  $^{13}\text{C-NMR}$  spectra of the polyurethane-extracted p7s3b2m3. It can be observed that in  $^{13}\text{C-NMR}$  spectra as indicated in Figure 4.10 several peaks appear at about 24-29 ppm, indicating the presence of the hydrocarbon chains of PCL, at 152-173 ppm from the carbonyl peak, and around 120-140 ppm from the benzene rings. The  $^{13}\text{C-NMR}$  spectrum also shows glucose unit carbons with peaks around 70-110 ppm. In the  $^1\text{H-NMR}$  spectra in Figure 4.11 the protons of D-glucose units absorb in the range of 3-6 ppm. On the other hand, the protons of the aromatic groups and amine occur in the range of 7.0-9.2 ppm.

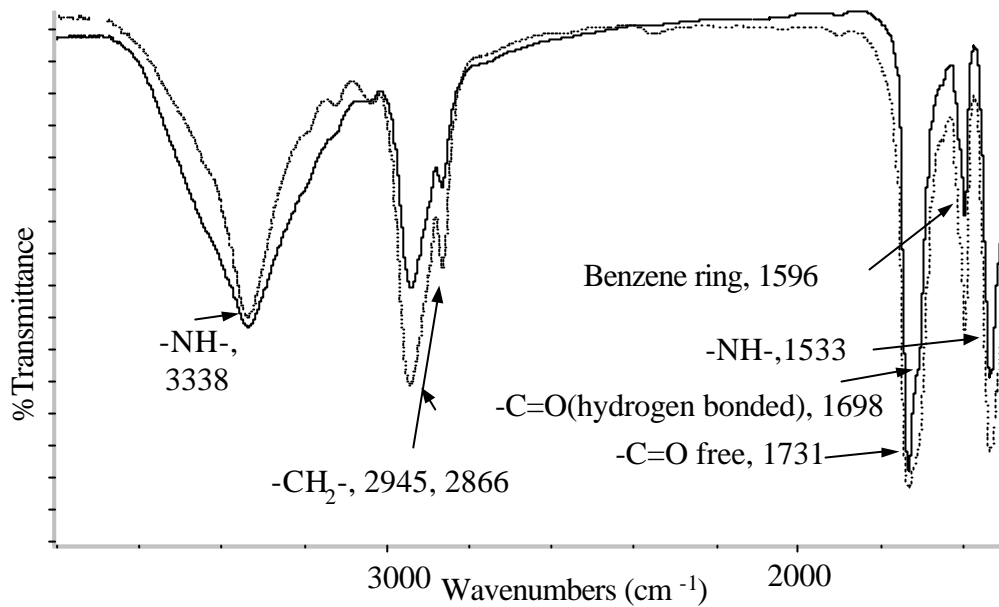


Figure 4.7 IR spectra of (a)  $\cdots$  p9s1b2m3 PU-extracted (b)  $\text{—}$  p7s3b2m3 PU-extracted

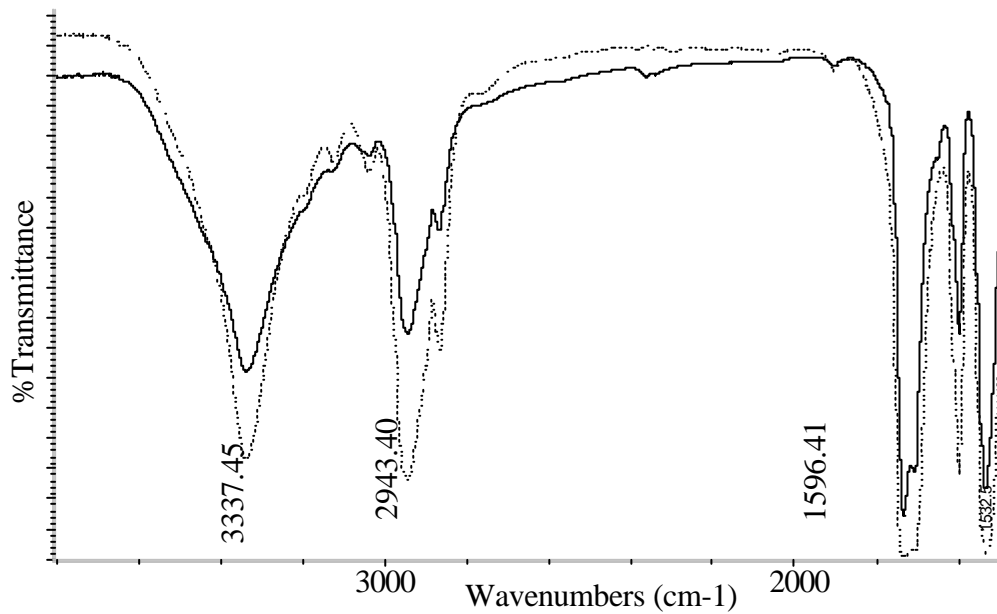


Figure 4.8 IR spectra of (a)  $\cdots$  p9s1b4m5 PU-extracted (b)  $\text{—}$  p7s3b4m5 PU-extracted

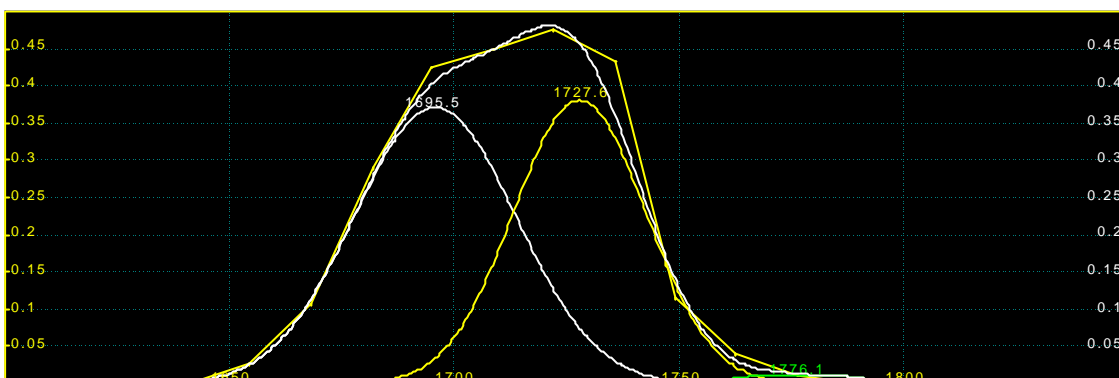


Figure 4.9 Peak separation of the IR carbonyl band by peak separation software

Table 4.1 Frequencies and percentages of bonded and free bands of carbonyl group in two series of samples\*

Samples	Frequency bonded	Frequency free	% of bonded C=O	% of free C=O
p1b2m3	1698	1730	61	39
p9s1b2m3	1695	1731	60	40
p8s2b2m3	1695	1732	65	35
p7s3b2m3	1698	1730	67	34
p6s4b2m3	-	-	-	-
p5s5b2m3	-	-	-	-
p1b4m5	1694	1730	62	38
p9s1b4m5	1691	1733	78	33
p8s2b4m5	1693	1730	68	32
p7s3b4m5	-	-	-	-
p6s4b4m5	-	-	-	-
p5s5b4m5	-	-	-	-

\*For the samples containing higher starch contents, it was impossible to measure the data due to the low transmittance.

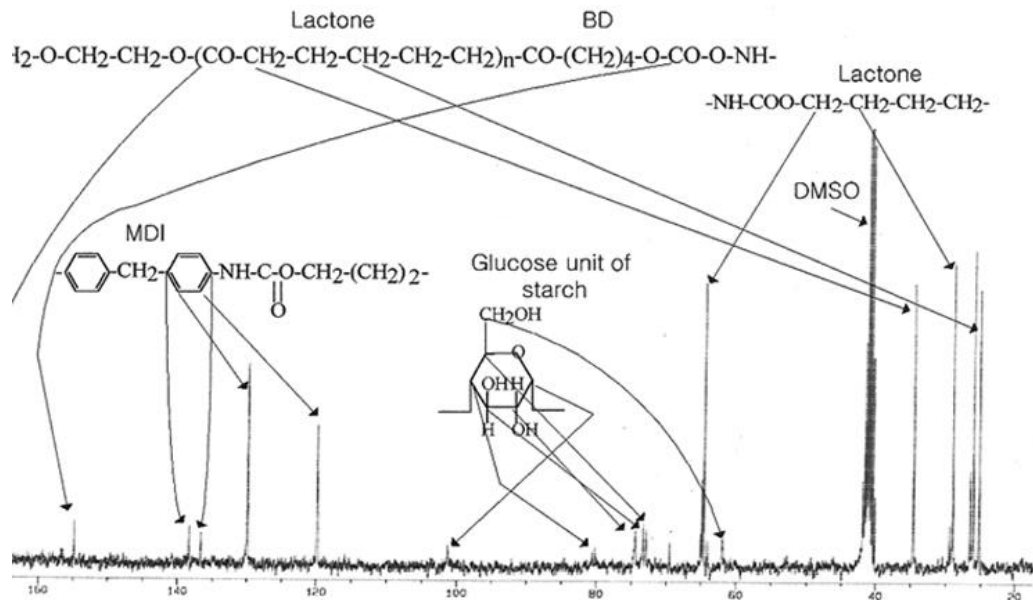


Figure 4.10  $^{13}\text{C}$  solution state spectrum of p7s3b2m3 for the identification of grafted polyurethane. Solvent:  $\text{DMSO-d}_6$ , Temperature :  $60^\circ\text{C}$

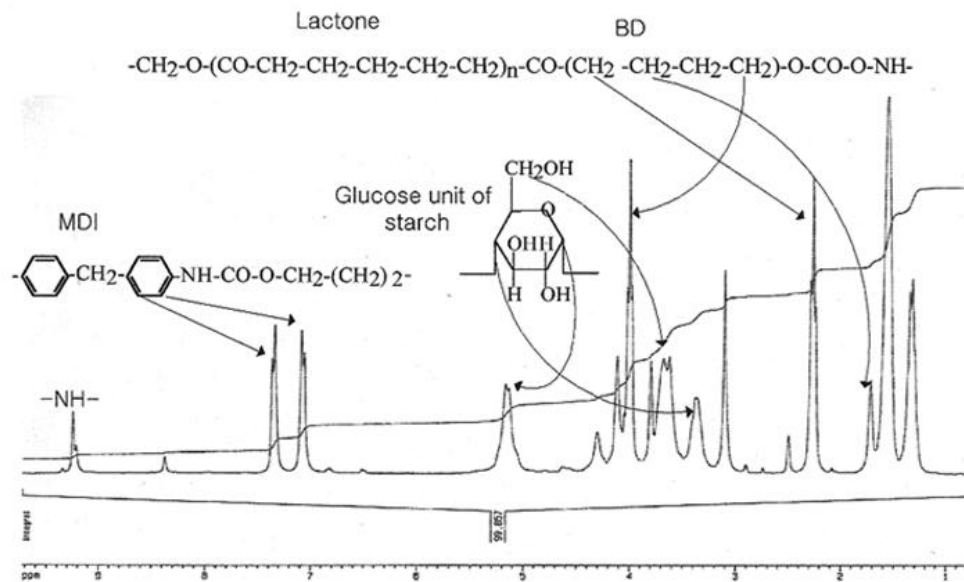


Figure 4.11  $^1\text{H}$  solution state spectrum of p7s3b2m3 for the identification of grafted polyurethane. Solvent:  $\text{DMSO-d}_6$ , Temperature :  $60^\circ\text{C}$

### ***4.1.3 Differential Scanning Calorimetry(DSC) Studies of the Polyurethane Phase***

#### ***4.1.3.1 DSC for Rapidly Cooled Samples***

In this study, one glass transition  $T_g$  and three endothermic transitions associated with the hard segments of the polyurethane phase were observed at 40-70 °C (endotherm I), 120 - 190°C (endotherm II) and above 200 °C (endotherm III) as shown in Figures 4.12 and 4.13. The three endothermic peaks were associated with different morphologies of the hard segments of the polyurethane phase. Yoon et al.<sup>1)</sup> indicated that these endotherms are quite sensitive concerning the thermal processing history and annealing conditions. Therefore, it might be expected that the phase transitions of polyurethane in our samples were also changed by starch addition because of crosslinking between the starch and polyurethane. Furthermore, starch is a polyol that can produce a complicated and crosslinked network of the polyurethanes.

The glass transition temperature  $T_g$  increased with the starch content due to an increase in hard segment concentration for the psb2m3 series. However, for the psb4m5 series that has a higher hard segment concentration than the psb2m3 series,  $T_g$  transition did not clearly appear and also disappeared completely at a high starch content level. Transition I can be attributed to the morphology of short-range hard segments.<sup>60), 61)</sup> These are randomly distributed and decrease with starch content without a temperature change for the transition in both series of samples. Transition II can be attributed to dissociation of long-range ordering in the hard micro-phase and increases with the starch content up to 25.71 wt % (p7s3b2m3) for the psb2m3 series. At even higher starch contents, transition III appeared and this transition temperature increased with starch content despite decreased molecular weight, as shown in figure 4.25 and Table 4.7, and decreased space of the polyurethane phase. Therefore, due to the starch content, the increase of crystalline melting transition temperature III could be explained by the polyurethane grafted on the starch and by crosslinking between starch granules, which enhanced the hard segment arrangement due to the stretching behaviour between two starch granules as shown in Figure 4.4(b). The changes of  $T_g$ ,  $T_m$  and  $\Delta H_f$  for the psb2m3 and psb4m5 series are shown in Table 4.2.

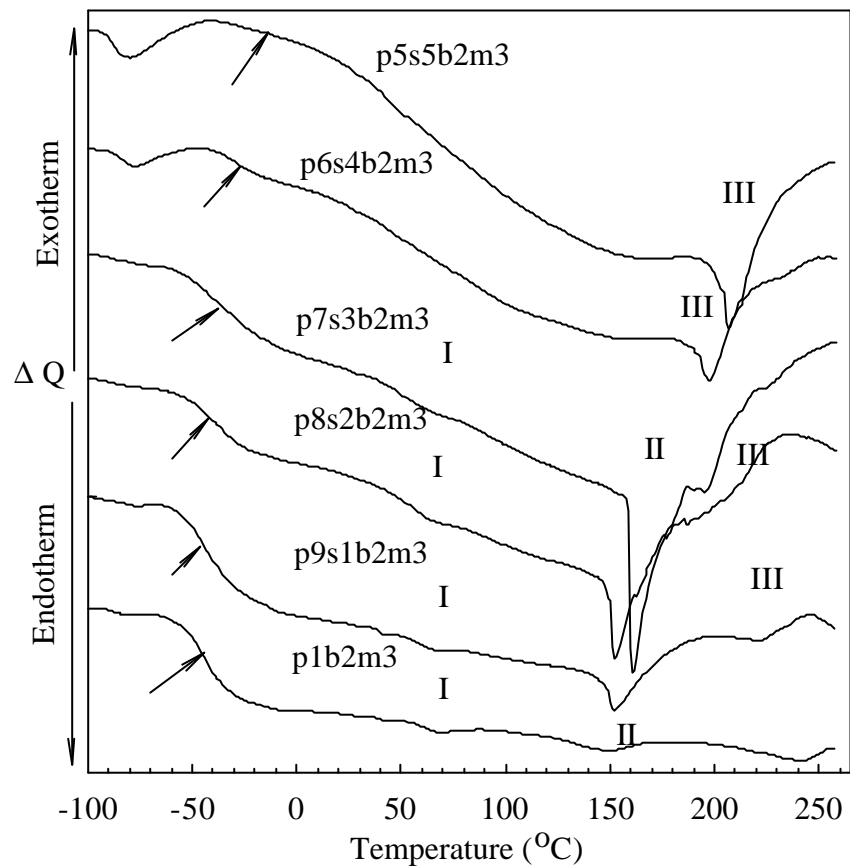


Figure 4.12 DSC thermograms of rapidly cooled compression-molded psb2m3 series prepared by one-step reaction (OSR C0.01). Heating rate: 10  $^{\circ}\text{C}$  / min.

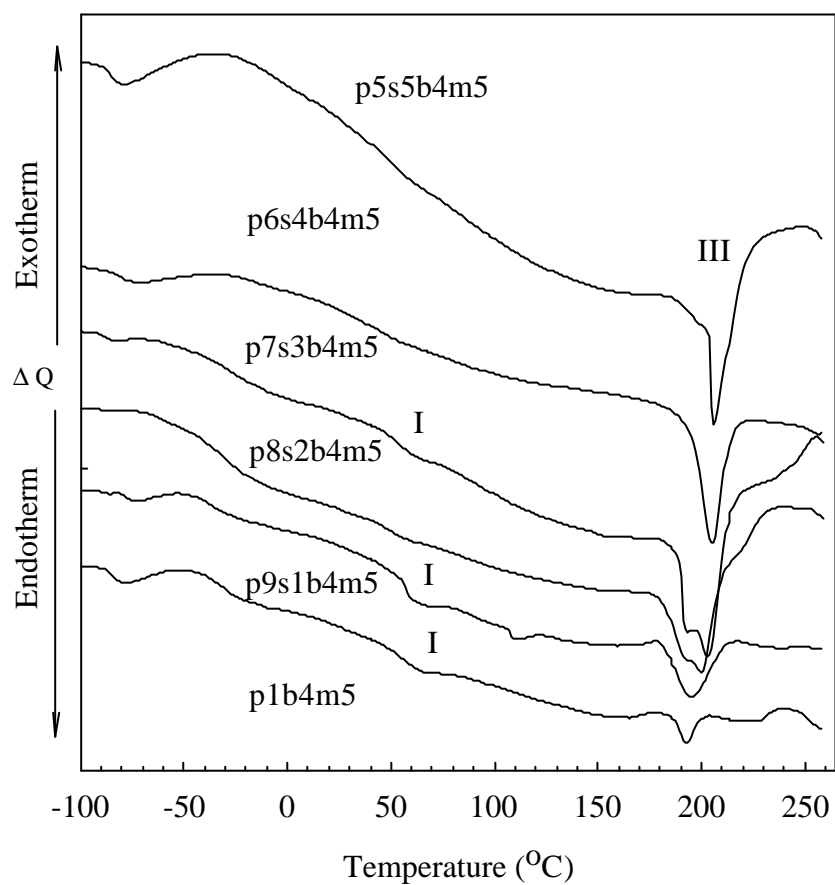


Figure 4.13 DSC thermograms of rapidly cooled compression-molded psb4m5 series prepared by one-step reaction (OSR C0.01). Heating rate: 10 °C / min.

Table 4.2 Effects of starch content on the soft segment  $T_g$  and hard segments  $T_m$  in various starch contents for samples prepared by one-step reaction (OSR C0.01).

Samples	Starch contents wt. %	$T_g$ ( $^{\circ}\text{C}$ )	$T_m$ ( $^{\circ}\text{C}$ )			$\Delta H_f$ (J/g)			$\Delta H_f$ , Total (J/g)
			I	II	III	I	II	III	
1b2m3	0.0	-45.09	67.86	147.36	242.42	0.98	2.81	3.27	7.06
p9s1b2m3	8.96	-45	65.54	152.36	222.75	0.88	7.4	2.07	10.35
p8s2b2m3	17.53	-42.43	64.30	152.44	206.53	1.13	8.6	3.38	13.11
p7s3b2m3	25.71	-42.75		161.52, 196.39			17.02, 2.15		19.17
p6s4b2m3	33.55	-30.19		198.32			9.48		9.48
p5s5b2m3	41.05	-8.32			207.14			11.74	11.74
p1b4m5	0.0	-35.26	64.19	192.48	228.29	1.55	1.97	1.35	4.87
p9s1b4m5	7.31	-38.11	63.36	109.74, 194.86		1.11	0.46, 7.95		9.52
p8s2b4m5	14.35	-41.70	56.91		200.13	0.64		16.28	16.92
p7s3b4m5	21.13	-22.18			205.56			13.80	13.80
p6s4b4m5	27.67	-38.59			208.85			9.88	9.88
p5s5b4m5	33.96	-48.18			211.39			11.47	11.47



In the case of the psb4m5 series, an endothermic peak III clearly appeared because the hard segment concentrations in the polyurethane phase increased with the starch content as indicated in Table 3.4 (31.7  $\rightarrow$  48.19 wt.% for psb2m3, 44.6  $\rightarrow$  61.69 wt.% for psb4m5). The total heat of fusion related to transition I, II and III increased with the starch content up to 20~25wt.%. This trend agrees with change of mechanical properties as shown in Figures 4.37 and 4.38. As shown in Figure 4.4, it is supposed that the grafted polyurethane phase aligned from the starch granule surface to polyurethane phase in a stretched form, which should have increased the transition temperature.

#### ***4.1.3.2 Samples Annealed at 180 °C for 15 minutes***

The high temperature annealing near melting point may increase the inter-mixing of the polyurethane chain, which can change the endotherms II and III. Therefore, this annealing at high temperature was performed to determine which state of polyurethane phase formed between the starch granules. The effects of high temperature annealing on the thermal transition in polyurethane-starch blends were obtained in two series of samples. The annealing temperature was 180 °C for 15 minutes, and the samples were slowly crystallized at a temperature rate of 5 °C / min down to -120 °C. The polyurethane hard segments could be freely mobilized at 180 °C which is sufficiently high for hard segment rearrangement. Figures 4.14 and 4.15 show  $T_g$  and endotherms II and III without endotherm I that is related to the ordering of short-range hard segments. Table 4.3 shows the high temperature annealing effects on enthalpy change in both series.  $T_g$  shows clear phase separation of soft segments at low starch contents for the sample psb2m3 series. Decreased total amounts of endothermic peaks of the psb2m3 series in comparison to the rapidly cooled sample (Figure 4.12) could be explained by the effect of the increased crosslinking of freely mobilized polyurethane hard segments. However, for the psb4m5 series, the phase separation of the soft segments is less pronounced than in the psb2m3 series. This means that high concentration of a segment controlled the phase separation to be rich for its own phase. At higher starch contents, the  $T_g$  transition almost disappeared because long and short range soft segments ordering were inter-mixed by annealing at high temperature. Furthermore, the average molecular weights of polyurethane are lower<sup>63)</sup> in the range of high starch content, which reduced the separation of the soft segments as well as the endotherm I.

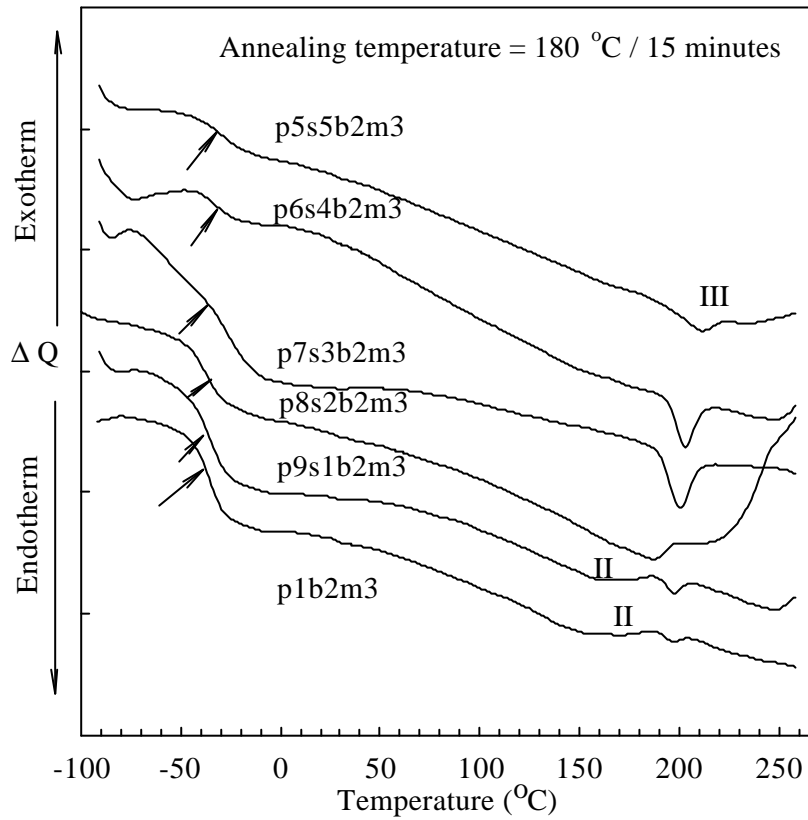


Figure 4.14 DSC thermograms of psb2m3 series annealed at 180 °C / 15 min. The samples were prepared in a one-step reaction(OSR C0.01). Heating rate: 10 °C / min.

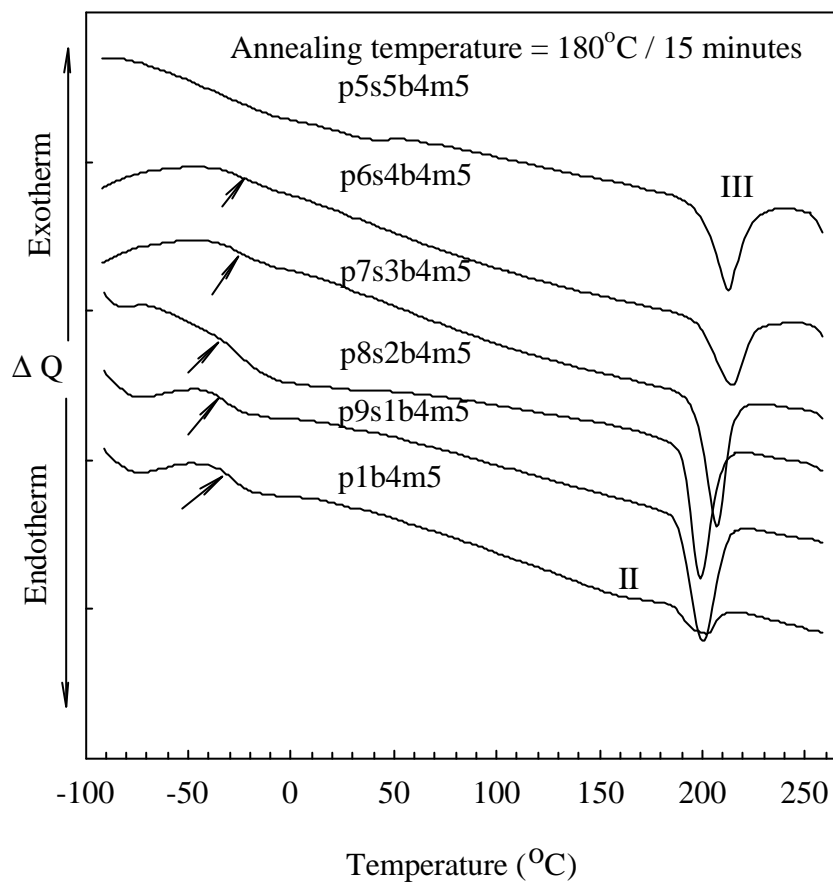


Figure 4.15 DSC thermograms of p5b4m5 series annealed at 180 °C / 15 min.

The samples were prepared in a one-step reaction(OSR C0.01).

Heating rate: 10 °C / min.

Table 4.3 Annealing effects (180 °C / 15 min) on the soft segments ( $T_g$ ) and hard segments ( $T_m$ ) for samples prepared in a one step reaction (OSR C0.01).

Samples	Starch contents wt. %	$T_g$ (°C)	$T_m$ (°C)			$\Delta H_f$ (J/g)			$\Delta H_f$ , Total (J/g)
			I	II	III	I	II	III	
p1b2m3	0.0	-37.26		152.7, 196.96			3.2, 0.21		3.41
p9s1b2m3	8.96	-39.31		156.7, 197.76			4.37, 0.48		4.85
p8s2b2m3	17.53	-35.82		176.68	211.08		3.73	0.35	4.08
p7s3b2m3	25.71	-41.36			200.49			3.6	3.6
p6s4b2m3	33.55	-32.91			202.85			2.53	2.53
p5s5b2m3	41.05	-36.89			210.50			3.22	1.78
p1b4m5	0.0	-28.38		152.91	202.10		1.99	3.27	5.26
p9s1b4m5	7.31	-31.29			200.42			15.14	15.14
p8s2b4m5	14.35	-37.42			199.02			13.88	13.88
p7s3b4m5	21.13	-28.20			207.28			13.05	13.05
p6s4b4m5	27.67	-28.22			213.91			9.98	9.98
p5s5b4m5	33.96	-47.62			212.83			12.08	12.08

In fact, for psb4m5 at the higher hard segment concentration, the annealing temperature is adequate for crystallization.

However, for psb2m3 at the low level of the hard segment, inter-mixing was believed to be easier than phase separation. Hesketh et al.<sup>60)</sup> indicated that the soft segment  $T_g$  is also influenced by the restricted movement imposed by the hard segment-soft segment junction and by phase boundaries where the hard domain acts as a filler particle. The fraction of hard segments dissolved in the soft phase increased with increasing annealing temperature, based on the elevation of the soft segment  $T_g$ . A detailed study of high temperature annealing (150 – 250 °C) was performed by Jacque.<sup>62)</sup> By annealing the samples for short times (2 min) at a given temperature, he obtained disruption of hard segment domains characterized by disordering endotherms below the annealing temperature. During the annealing period, the mobile hard segments appear to reassociate with the more stable hard domains after annealing. The endotherms exhibit larger peak areas and are shifted towards higher temperatures. These annealing effects increased domain size due to improved ordering. For the two series of our samples, the increased melting transitions III of the hard segments, despite the low molecular weight,<sup>63)</sup> could be ascribed to easy alignment of the polyurethane grafted on starch granules.

#### ***4.1.3.3 Samples Annealed at 140 °C for 4 hours***

The annealing temperature 140 °C is just below the transition temperature II, and the annealing time is long enough for the polyurethane chains to be rearranged. But, this temperature range, which is too low for the hard segment molecules to be easily mobilized, may induce rearrangements of the soft segments and, maybe, of the short-range hard segments. As shown in Figures 4.16 and 4.17, for the lower concentration range of starch,  $T_g$  and all endotherms I, II and III for polyurethane appeared. For both series of the samples, at this temperature, two-phase separations were well developed despite the low annealing temperature, compared to the annealing temperature of 180 °C for 15 min. The figures also indicate that as the starch contents increased, I and II transitions diminished, and the temperature of transition III increased for both series of samples. Increased  $T_m$  was also observed as the starch contents increased. Table 4.4 shows the annealing effects of enthalpy changes in both series. The total amounts of enthalpy are relatively low for the low hard segment concentration (psb2m3) whereas the specimens with higher hard segment concentration (psb4m5) show an increase.

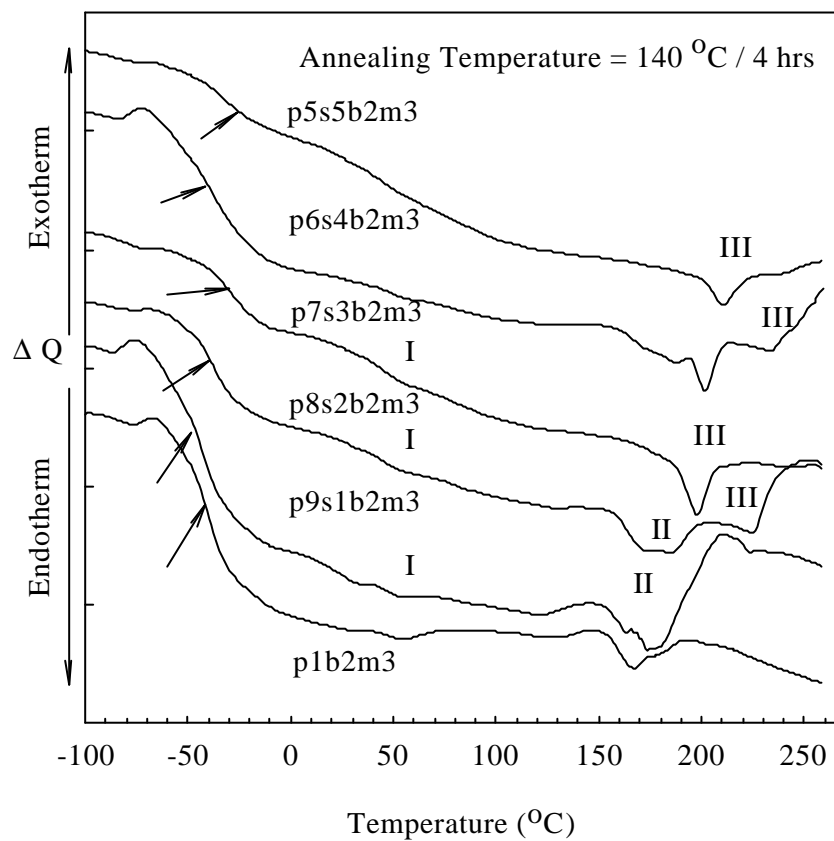


Figure 4.16 DSC thermograms of p5s5b2m3 series annealed at 140  $^{\circ}\text{C}$  for 4 hours. The samples were prepared in a one-step reaction(OSR C0.01). Heating rate: 10  $^{\circ}\text{C}$  / min.

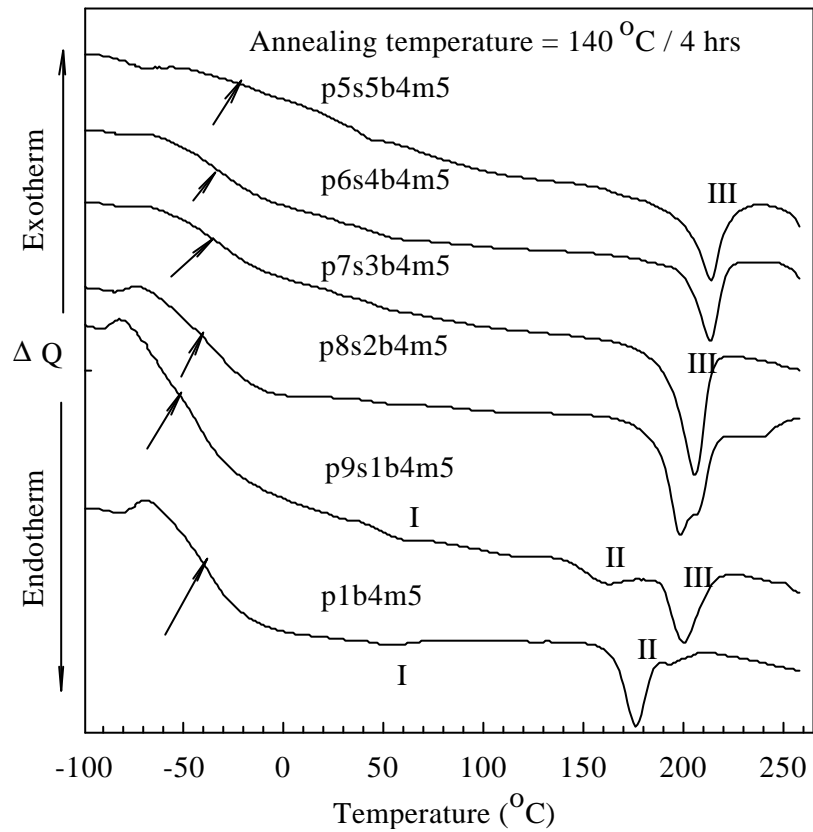


Figure 4.17 DSC thermograms of p5s5b4m5 series annealed at 140  $^{\circ}\text{C}$  for 4 hours. The samples were prepared in a one-step reaction(OSR C0.01). Heating rate: 10  $^{\circ}\text{C}$  / min.

Table 4.4 Annealing effects (140 °C / 4hrs) on the soft segment ( $T_g$ ) and hard segments ( $T_m$ ) for samples prepared in a one-step reaction(OSR C0.01).

Samples	Starch contents wt. %	$T_g$ (°C)	$T_m$ (°C)			$\Delta H_f$ (J/g)			$\Delta H_f$ , Total (J/g)
			I	II	III	I	II	III	
p1b2m3	0.0	-54.16	54.94	130.89, 166.98		0.74	0.85, 3.23		4.82
p9s1b2m3	8.96	-47.17	53.73	119.13, 179.40		0.5	2.43, 12.44		15.37
p8s2b2m3	17.53	-45.31	52.59	172.48	225.59	0.32	5.05	3.42	8.79
p7s3b2m3	25.71	-35.12	53.01	197.76		0.31	4.73		5.04
p6s4b2m3	33.55	-41.40	54.60	185.05	201.8, 234.81	0.2	1.05	1.63, 3.91	6.79
p5s5b2m3	41.05	-38.53			210.54			3.22	3.22
p1b4m5	0.0	-45.2	53.11	176.21		0.77	10.31		11.08
p9s1b4m5	7.31	-55.21	58.24	160.35	200.64	0.95	1.96	8.21	11.12
p8s2b4m5	14.35	-38.67	56.91		198.29			17.63	17.63
p7s3b4m5	21.13	-40.12			205.74			16.25	16.25
p6s4b4m5	27.67	-32.09			213.35			10.05	10.05
p5s5b4m5	33.96	-36.78	44.28		213.97	0.6		13.94	14.54



At low hard segment concentration (psb2m3), the thermal expansion of soft segments may impose stress on the formation of hard segments, whereas at higher hard segment concentrations (psb4m5) the short and long range order of hard segments add to the strong hard segment formation.<sup>60)</sup> There is no significant change of the crystalline melting transition in samples, p6s4b2m3, p5s5b2m3, p6s4b4m5, and p5s5b4m5 because soft and hard domain mobility may be fixed by starch grafting and the original size of hard domain and perfection could not be changed by higher starch contents. During annealing, the hard segment formation may increase the degree of entanglement at this annealing temperature between hard segment domains, and increase crystalline hard segment order and its stability at low starch content. Previously, Hesketh et al.<sup>60)</sup> studied a series of polyurethanes which were annealed at various temperatures between 120 to 190 °C. They indicated that the reformation of the disrupted hard segments occurred slowly in such a way as to produce more crystallites rather than better ordered long range domains. Subsequent quenching produced a long range of crystalline domains of fully melted hard segments with no thermal history in the formation of hard segments.

#### ***4.1.3.4 The Effect of Different Concentration of the Catalyst***

The catalyst generally accelerates the reaction rate. Therefore, increasing the catalyst concentration promotes the main urethane reaction as well as all other bonding such as formation of allophanate, urea, biuret, etc. As shown in Figures 4.18 and 4.19, an increased catalyst concentration diminished the peak of the melting transition III of the hard segments, which indicates crosslinking between polyurethane-chains. This crosslinking hindered the formation of the arrangement of the hard segments. However, the sample p7s3b2m3 that has more soft-segments than that of the p7s3p4m5 shows more developed soft segment shape in Figure 4.18. A change in the catalyst concentration from 0.01 to 0.1% removed the most of them. Table 4.5 shows the results of  $T_g$ ,  $T_m$  and  $\Delta H_f$ .

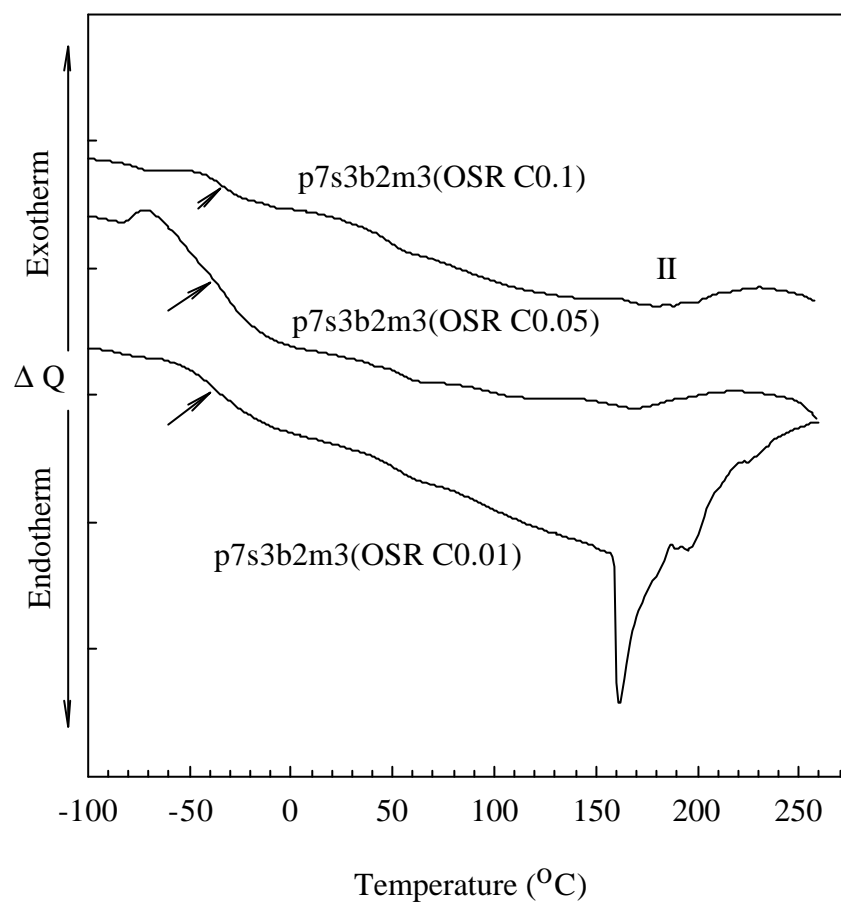


Figure 4.18 Effect of catalyst concentration on the system p7s3b2m3 prepared in a one-step reaction (OSR).

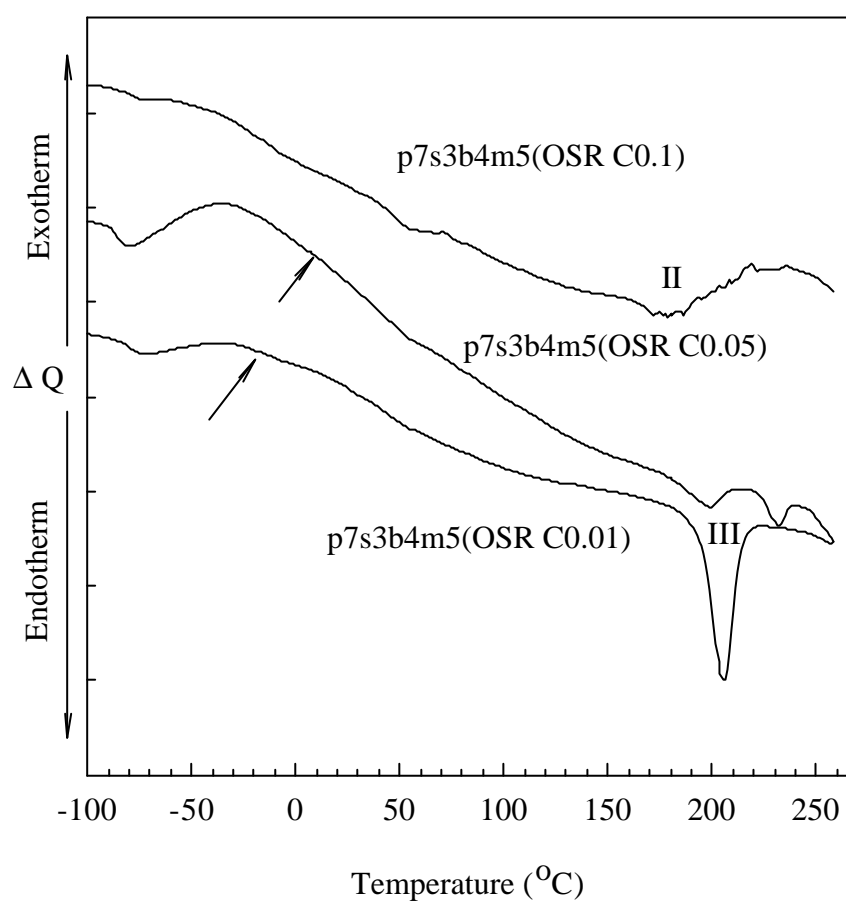


Figure 4.19 Effect of catalyst concentration on the system p7s3b4m5 prepared in a one-step reaction (OSR).

#### ***4.1.3.5 Two Step Reaction vs. One Step Reaction***

DSC-analysis for two-step reaction is shown in Figures 4.20 and 4.21 for psb2m3 and psb4m5 series. High crosslinking may be occurred because the melting transition of the hard segment is greatly reduced. However, as shown in Figure 4.25 and 4.26, the solvent uptake of the samples prepared by TSR is larger than that of the OSR. The viscosity of psb2m3(TSR C0.01) is also lower than that of psb2m3(OSR C0.01) as shown in Figure 4.47 and 4.49. This reduced melting transition is supposed to be caused by two step reaction, in other words, the addition of starch in the second step hindered the developing of the hard segment. However, the samples p6s4b4m5 (TSR C0.01) and p7s3b4m5 (TSR C0.01) in the series of psb4m5 contain a higher hard-segment concentration than that of the psb2m3 series, which show large transition III of hard segment melting. Therefore, the large melting transition peaks of the samples may be related to the increased grafting, as shown in Figures 4.24, in which graftings of p7s3b4m5 and p6s4b4m5 are higher than those of psb2m3. Table 4.5 shows the results of  $T_g$ ,  $T_m$  and  $\Delta H_f$ , which can be compared to the decreased total amounts of enthalpy from the Table 4.2 in psb2m3 series of one step reaction (OSR).

#### ***4.1.3.6 Effect of the Different Molecular Weight of the Polyethylene Glycol Prepolymer***

The phase transitions of starch granules at various molecular weights of polyethylene glycol polyurethane are shown in Figure 4.22. There is a  $T_g$ , and three endothermic peaks I, II and III can be observed. The  $T_g$  of the soft segments is not changed by the molecular weight of the prepolymer. However, endothermic peak I (approximately 50 °C) can clearly be attributed to the melting point of soft segment crystal<sup>67)</sup>.

These transition temperatures and the peak size are increased with the molecular weight of prepolymer. In the case of the samples prepared with PEG-2000 prepolymer, this endothermic peak I did not appear. The crystal formation of the soft segments at low molecular weight is reduced, which indicates that the crystals of the soft segments may be formed by soft segments of the long prepolymer. As shown in Table 4.6,  $H_f$  also increased with the molecular weight of the prepolymer, indicating increased crystal size in the homopolymer phase, which may point to strong crosslinking in this polymer system.

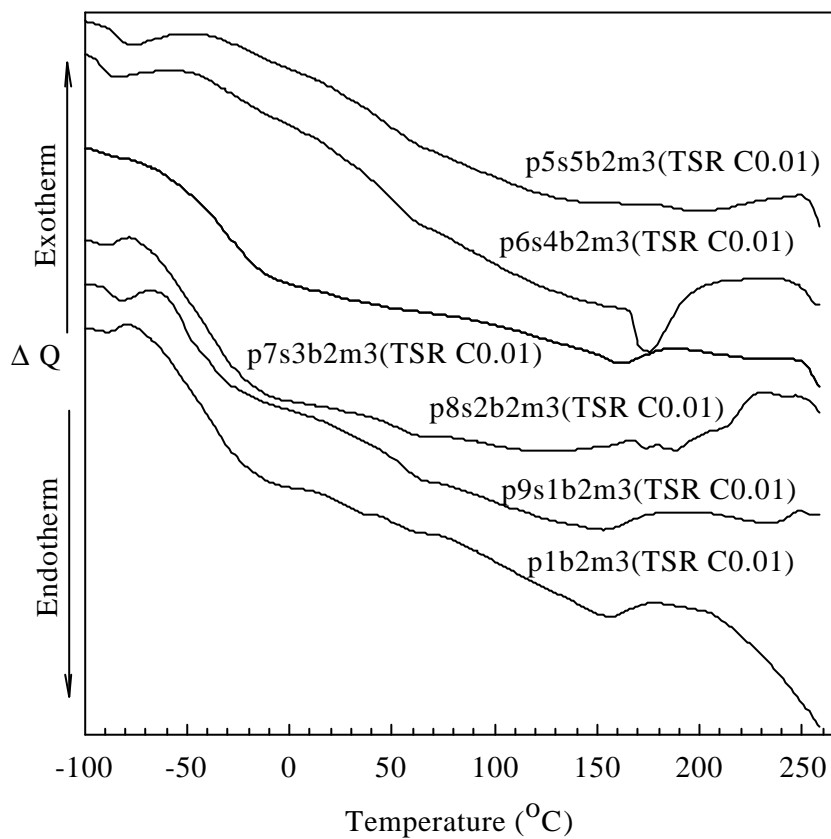


Figure 4.20 DSC thermograms of rapidly cooled compression-molded psb2m3 series prepared in a two-step reaction (TSR C 0.01). Heating rate: 10 $^{\circ}\text{C}/\text{min}$ .

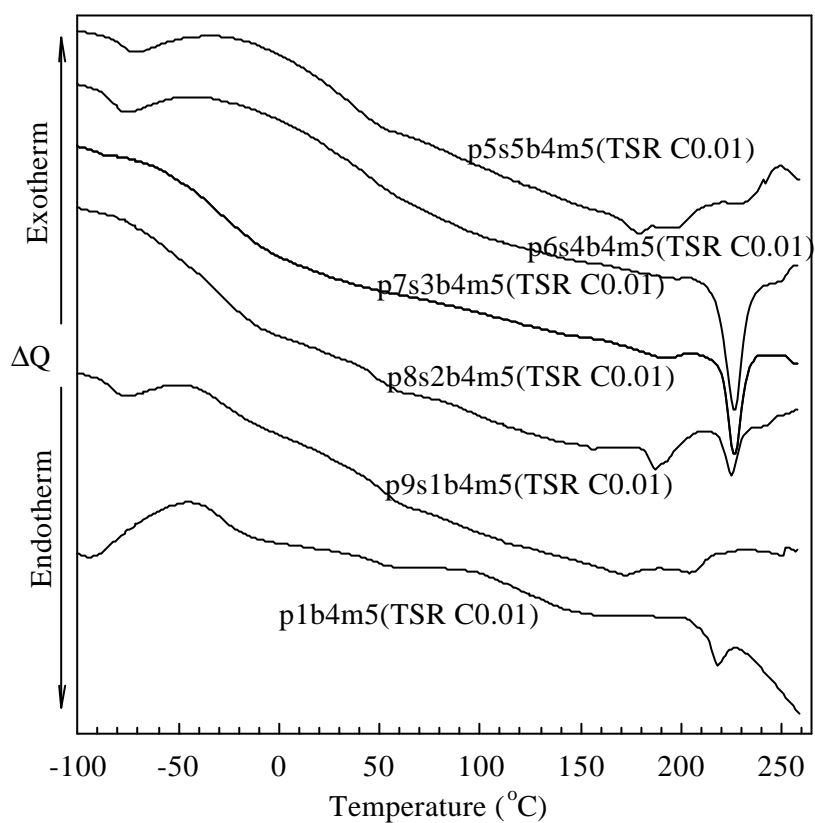


Figure 4.21 DSC thermograms of rapidly cooled compression-moulded psb4m5 series prepared in a two-step reaction (TSR C0.01). Heating rate: 10°C/min.

Table 4.5 Effects of various starch contents on soft segment  $T_g$  and hard segments  $T_m$  for samples prepared in a two-step reaction (TSR C0.01).

Samples	Starch contents wt. %	$T_g$ ( $^{\circ}\text{C}$ )	$T_m$ ( $^{\circ}\text{C}$ )			$\Delta H_f$ (J/g)			$\Delta H_f$ , Total (J/g)
			I	II	III	I	II	III	
p1b2m3-2	0.0	-46.83	35.49, 58.42	150.94		0.22, 0.48	9.23		9.93
p9s1b2m3-2	8.96	-57.53	63.25	153.30	237.42	1.28	3.93	2.00	7.21
p8s2b2m3-2	17.53	-45.21	61.30	188.70		1.03	6.09	-	7.12
p7s3b2m3-2	25.71	-41.40	55.89	160.73	246.52	1.20	4.03	1.77	7.00
p6s4b2m3-2	33.55	-39.16	61.05	175.14		1.74	5.64	-	7.38
p5s5b2m3-2	41.05	-17.92	59.69		200.19	1.02	-	2.30	3.32
p1b4m5-2	0.0	-27.69	56.18	145.53	218.02	1.04	6.37	1.46	8.87
p9s1b4m5-2	7.31	-33.15	60.12	172.09	204.79, 250.9	0.82	0.83	1.01, 0.43	3.09
p8s2b4m5-2	14.35	-46.33	59.32	186.97	225.16	1.29	2.10	2.22	5.61
p7s3b4m5-2	21.13	-41.69		191.02	226.53		1.26	5.68	6.94
p6s4b4m5-2	27.67	-30.60			226.51			9.45	9.45
p5s5b4m5-2	33.96	-	49.46	178.95, 198.49	232.62	1.94	0.69, 0.82	1.72	5.17

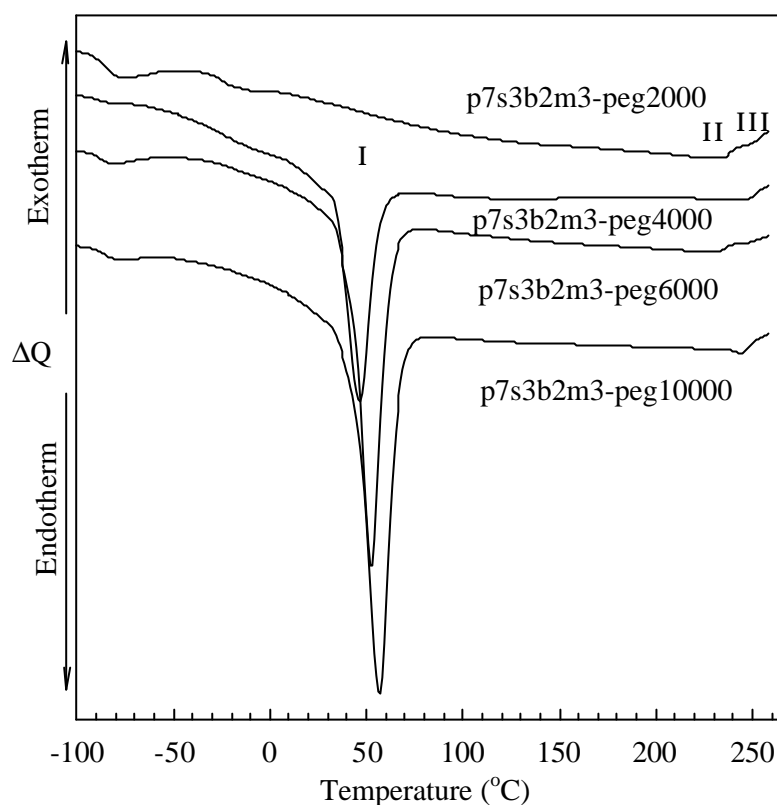


Figure 4.22 DSC thermograms of the samples prepared from prepolymer of polyethylene glycol with different molecular weights.

Table 4.6  $T_g$  of soft segments and  $T_m$  of hard segments for the samples prepared with different molecular weights of polyethylene glycols(OSR C0.01).

Samples	Starch contents wt. %	$T_g$ ( $^{\circ}\text{C}$ )	$T_m$ ( $^{\circ}\text{C}$ )			$\Delta H_f$ (J/g)			$\Delta H_{f,T_0}$ tal(J/g)
			I	II	III	I	II	III	
p7s3b2m3(OSR), PEG-2000	25.90	-25.9	-	-	227.7, 249.0	-	-	5.81, 0.32	6.13
p7s3b2m3(OSR), PEG-4000	17.95	-41.5	46.8	106.1	247.9	43.90	0.96	2.58	47.44
p7s3b2m3(OSR), PEG-6000	13.99	-	52.5	-	225.0	66.59	-	3.90	70.49
p7s3b2m3(OSR), PEG-10000	8.75	-	56.6	-	244.8	78.67	-	1.36	80.03



#### ***4.1.4 Grafted Percentage of Polycaprolactone Diol and Polyethylene Glycol Polyurethanes under Various Starch Contents***

##### ***4.1.4.1 One-Step Reaction***

The percent of grafting was defined as the weight of the polyurethane remaining on the starch after solvent extraction in relation to the weight of polyurethane with starch before extraction.<sup>70)</sup> Therefore, if there is crosslinking between polyurethane chains, this grafted percentage could be slightly increased in comparison to the non-crosslinked fraction. The grafted weight percent was measured at various starch contents. As shown in Figure 4.23, the grafted percentage for psb2m3(OSR C0.01) is higher than that of the psb4m5 and increased up to ~25% of starch and then decreased. The decrease in the percentage of grafting at higher starch contents may be ascribed to the separation between the polyurethane phase and starch granule probably due to the homopolymerization tendency of the polyurethane phase as indicated in the grafting of polypropylene.<sup>14)</sup> The apparent gaps between the two phases in SEM-micrographs at high starch contents confirm this, as already shown in Figure 4.6.

##### ***4.1.4.2 Two-Step Reaction***

As can be seen in Figure 4.24, the percentage of grafting for the samples prepared by TSR shows a similar change of grafting as that of OSR. The amount of the grafting between maximum (84%) and minimum (~70%) is smaller than that of OSR. However, there is a maximum point of grafting with starch content. The maximum point for two series of samples is different, and also the minimum point of grafting could be observed at lower range of starch content. The grafting on psb2m3 is lower than that of psb4m5 in the middle range of the starch content. It is interesting that in contrast to the OSR-samples the percentage of grafting for psb2m3 series is lower than that of the psb4m5 in the middle range of the starch content, which is contrary to the results on the samples prepared by OSR. Currently, we cannot understand this inverse result for the middle range, but it may depend on the reaction scheme. In TSR scheme, initial concentration of the isocyanate was consumed at the first step just before the starch addition and in this lowered isocyanate concentration starch was added. As the psb2m3 series have lower isocyanate concentration than that of psb4m5, it is assumed that this lowered isocyanate concentration of psb2m3 influenced much on the grafting of starch.

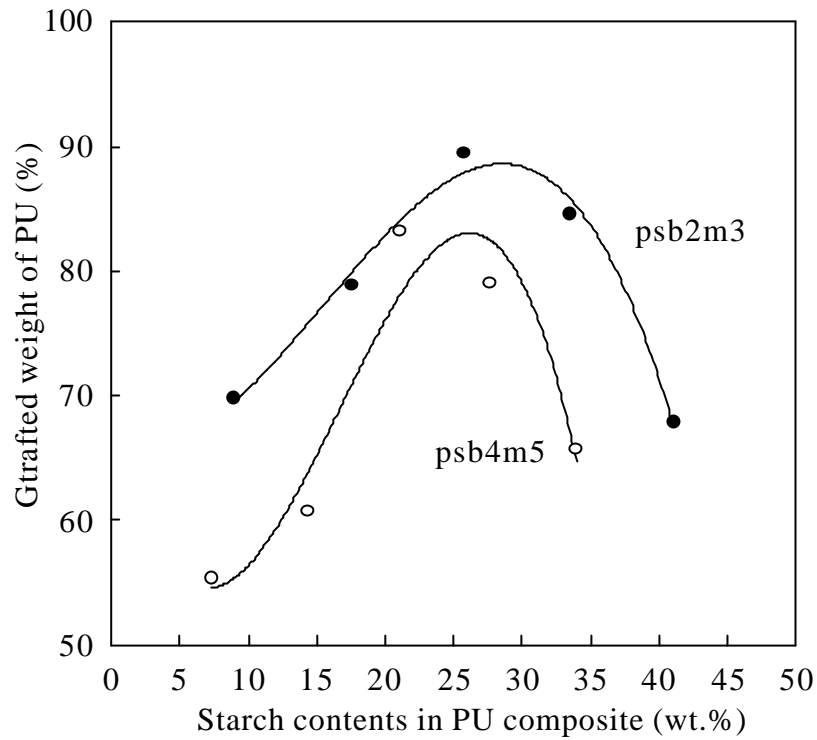


Figure 4.23 Percentage [%] of grafted starch contents for two series of the samples prepared by DMF and THF solvents for five days. (OSR C0.01)

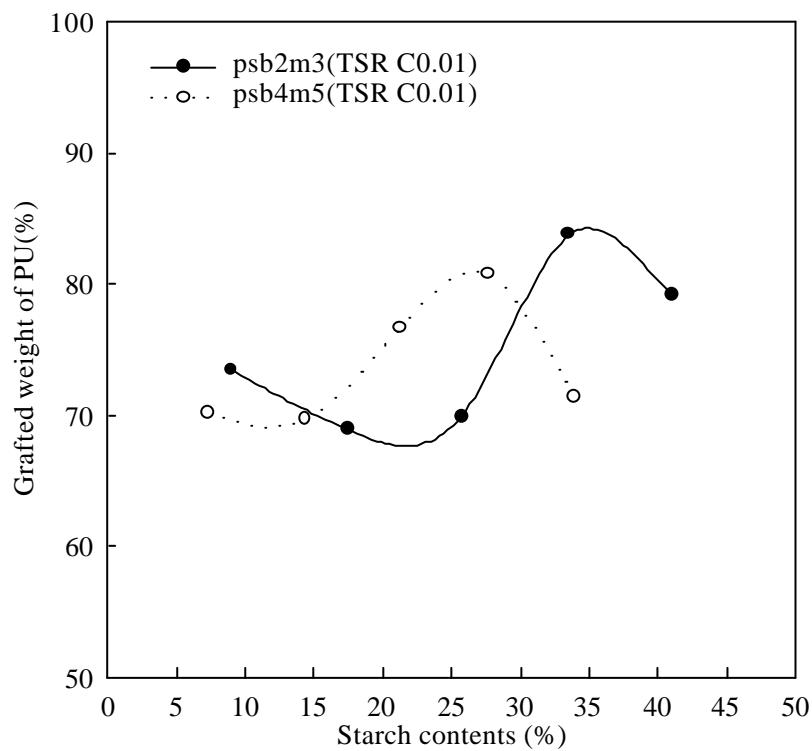


Figure 4.24 Percentage [%] of grafted starch contents for the samples prepared by TSR. Swelled in DMF and THF solvents for five days. (TSR C0.01)

#### ***4.1.4.3 Effect of the Different Molecular Weight of the Polyethylene Glycol Prepolymer***

The percentage of grafting decreased slightly with the molecular weight of the prepolymer as shown in Table 4.7. The starch content decreased on increasing the molecular weight of polyethylene glycol at the fixed molar ratio (p7s3b2m3(OSR C0.01)). Therefore, the large molecular size of soft segment and crystals of hard segments probably cause strong hindrance of hard segment formation. However, the degree of the grafted percentage is similar to the results obtained with a polycaprolactone prepolymer.

Table 4.7 Percentage of grafting (wt.%) as a function of the different molecular weights of the polyethylene glycol prepolymer

Samples	Starch wt.%	Grafted %
p7s3b2m3(OSR), PEG-2000	25.90	72.20
p7s3b2m3(OSR), PEG-4000	17.95	78.13
p7s3b2m3(OSR), PEG-6000	14.00	71.52
p7s3b2m3(OSR), PEG-10000	8.75	69.40

### ***4.1.5 Swelling Behavior***

#### ***4.1.5.1 One-Step Reaction***

To identify the crosslink-density of the polymers, a swelling test was carried out with THF solvent for two series of the samples. As expected, Figure 4.25 and Table 4.8 show that swelling (solvent uptake) decreases with the starch content due to the increased crosslinking of the polymers. The crosslinked density of psb4m5 is higher than that of psb2m3 due to higher concentration of isocyanate in the psb4m5 series. Even in the samples p1b2m3 and p1b4m5 that contain no starch, solvent uptake could be measured without dissolving of the polyurethane due to biuret and allophanate branching.

#### ***4.1.5.2 Two-Step Reaction***

The solvent uptake against starch content is presented in Figure 4.26. For both series (OSR, TSR), the progress of the curves has the same tendency. However, the solvent uptake of both series of TSR is higher than that of both series of OSR, which indicates that TSR produces materials that are (in comparison to OSR) less crosslinked between the starch-granules as well as polyurethane chains. In the case of p1b2m3 (without starch) uptake measurement was impossible because of dissolving the sample. These results can be explained by the reaction scheme. In the first step, a constant amount of polycaprolactone diol (the same as in OSR) was mixed with excess of MDI. In this step, almost all isocyanates were terminated with –OH of polycaprolactone-diol, and then the starch was added in a second step. Therefore, relatively few isocyanates reacted with –OH of the starch surface, which decreases the crosslinking. As the shown in Figures 4.49 and 4.50 (rheological part), the viscosity was much decreased for the samples prepared by TSR.

#### ***4.1.5.3 Effect of the Different Molecular Weight of the Polyethylene Glycol Prepolymer***

The solvent uptake against molecular weight of prepolymer of polyethylene glycol is presented in Figure 4.27. The swelling increased with increasing molecular weight of prepolymer. It is assumed that the increasing range of the curve contributes to the increase of the soft-segment concentration whereas lowering the range of high molecular weight of prepolymer is due to the increased crosslinking by the increased crystal content of soft segment.

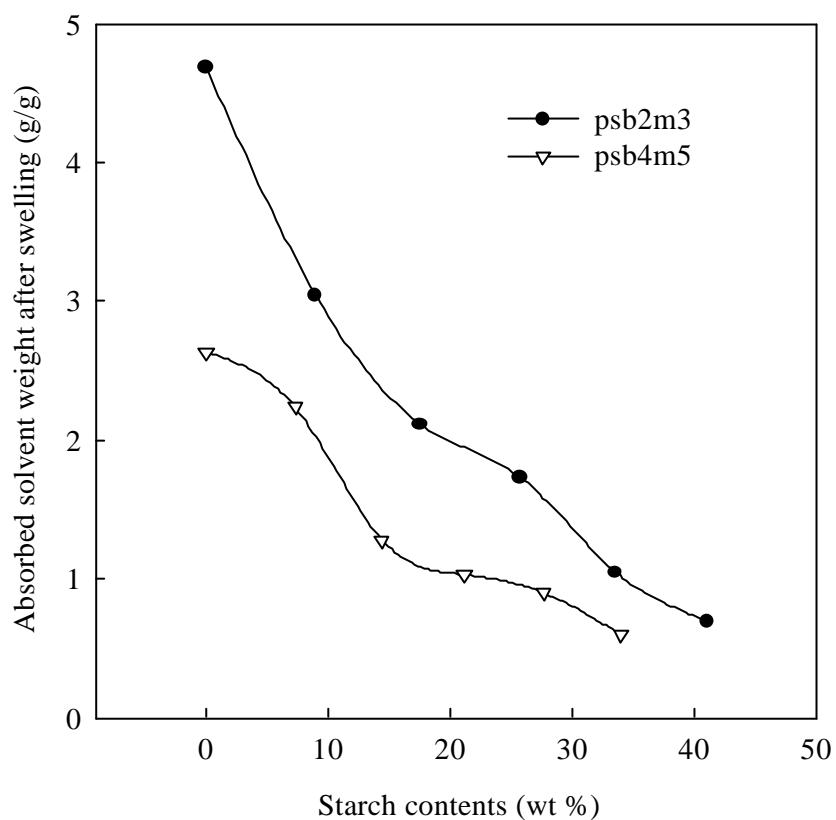


Figure 4.25 Swelling behavior of polyurethane-starch-blends for two series of the samples, psb2m3 (OSR C0.01) and psb4m5 (OSR C0.01). Swelling solvent: THF for 3 weeks.

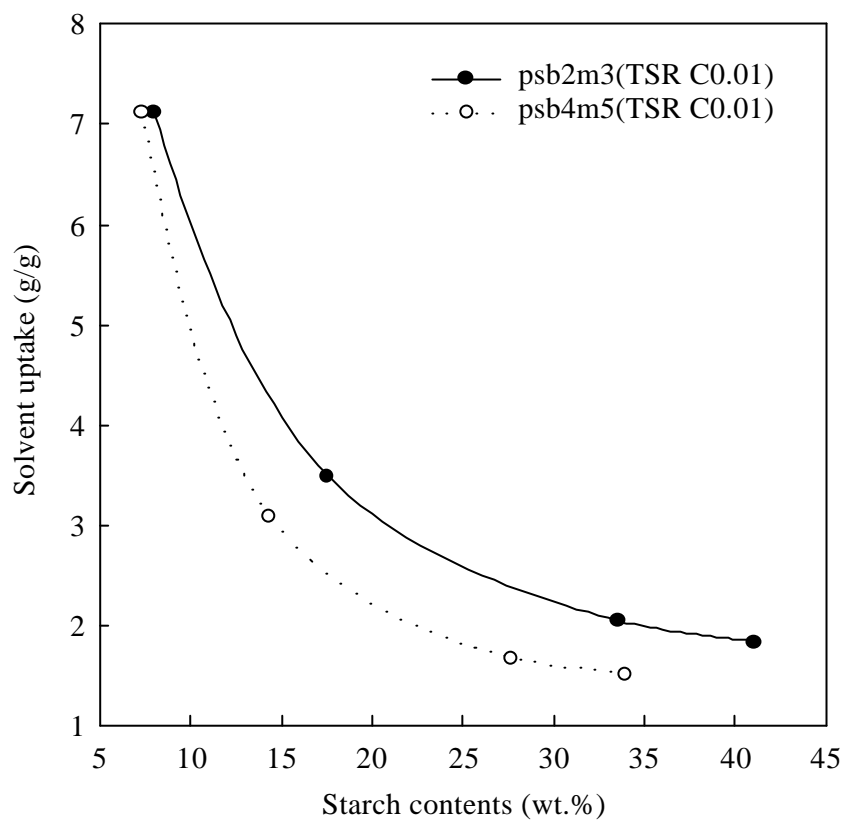


Figure 4.26 Swelling of solvent uptake against the starch contents for the samples prepared by TSR. Swelling solvent: THF for 3 weeks

Table 4.8 Swelling behavior of polyurethane starch blends for two series of the samples, psb2m3 (OSR C0.01) and psb4m5 (OSR C0.01). Swelling solvent: THF for 3 weeks

Samples	Starch wt.%	Original weight (a)	After swelling (b)	After drying (b)	b/a
p1b2m3	0.0	0.54	4.686	0.413	8.6777
p9s1b2m3	8.96	0.457	3.048	0.429	6.6695
p8s2b2m3	17.53	0.556	2.112	0.565	3.7985
p7s3b2m3	25.71	0.59	1.731	0.612	2.9338
p6s4b2m3	33.55	0.474	1.045	0.475	2.2046
p5s5b2m3	41.05	0.431	0.691	0.431	1.6032
p1b4m5	0.0	0.435	2.637	0.402	6.0620
p9s1b4m5	7.31	0.321	2.238	0.291	6.9719
p8s2b4m5	14.35	0.456	1.282	0.474	2.8114
p7s3b4m5	21.13	0.544	1.032	0.569	1.8970
p6s4b4m5	27.67	0.568	0.898	0.586	1.5809
p5s5b4m5	33.96	0.416	0.598	0.437	1.4375

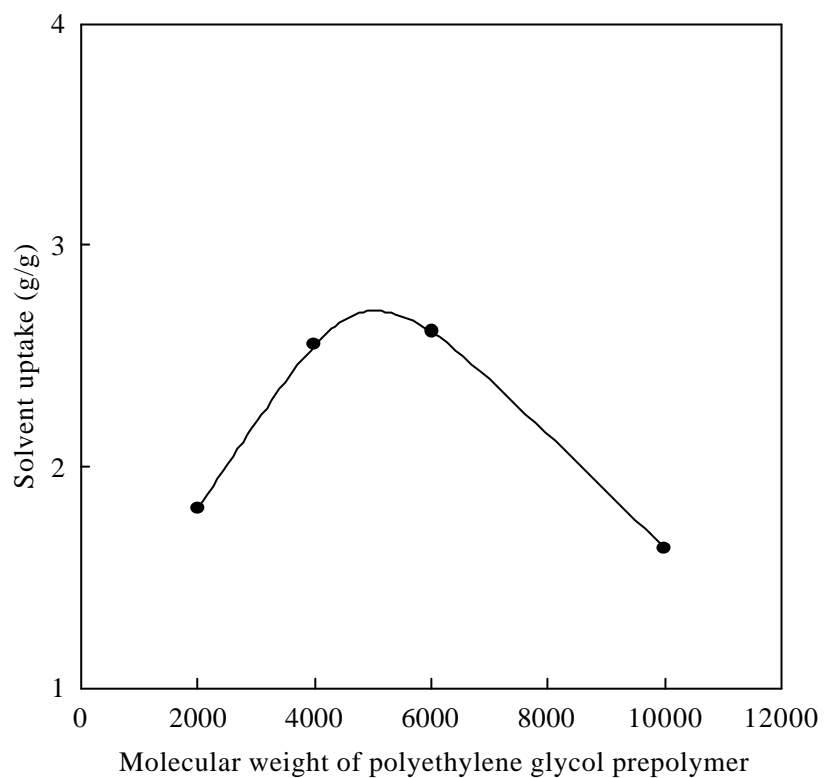


Figure 4.27 Solvent swelling uptake against different molecular weight of polyethylene glycol prepolymer. Swelling solvent: THF for 3 weeks



### ***4.1.6 Average Molecular Weight of Polyurethane Homopolymer***

#### ***4.1.6.1 One-Step Reaction***

The entire polyurethane phase was separated from the starch granules by using a strong mixed solvent (DMF (95 %) + THF (5 %)), long agitation (12 ~ 48 hours) and a high temperature (70 ~ 80 °C). Table 4.9 and Figure 4.28 show the results for two series of the samples psb2m3 and psb4m5. As expected, the average molecular weight of homopolyurethane decreased with the starch content. This decrease can be explained by the decrease of pre-polymer content in the reactant as well as a decrease in the space of the polyurethane phase between starch-granules. It can be shown that the average molecular weights were high, possibly due to the crosslinking between polyurethane-chains, which may have increased the molecular weight.

#### ***4.1.6.2 Two-Step Reaction***

The molecular weights of the samples prepared by TSR show a similar tendency to the samples prepared by OSR, as shown in Figure 4.29 and Table 4.10. The average molecular weight at the low range of starch content for psb2m3 (TSR) is similar to those of psb2m3 (OSR). Despite the different reaction scheme, this similar decreasing tendency of molecular weight for TSR scheme against the OSR indicates that the average molecular weight of polyurethane-homo-polymer can be determined by reactant formulation rather than by the polymerization scheme.

#### ***4.1.6.3 Effect of the Different Molecular Weight of the Polyethylene Glycol Prepolymer***

The average molecular weight of the homopolymer separated from the blends was determined, as shown in Table 4.11. Despite different molecular weights of the prepolymers of polyethylene glycol, the average molecular weight of the homo-polymer did not change. The sample prepared with the PEG-10000 prepolymer was not soluble in a DMF+THF mixed solvent, even at 70~90°C in spite of long and strong agitation. This is probably because of strong crosslinks that were formed by crystal formation of the soft segments as well as by the biuret and allophanate bonding. The average molecular weights of the homo-polymers were too small to allow comparison with the data of the polycaprolactone prepolymer. This point remains for further study.

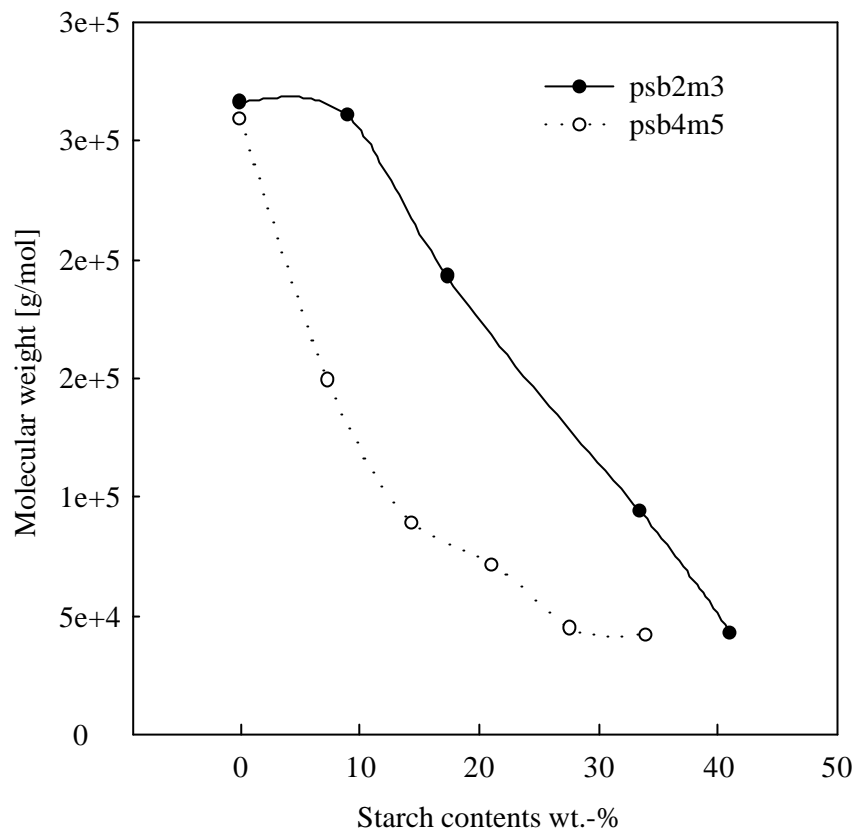


Figure 4.28 Molecular weights,  $M_w$  of polyurethane homo-polymer extracted from starch-polyurethane-blends, psb2m3 (OSR C0.01) and psb4m5 (OSR C0.01) samples

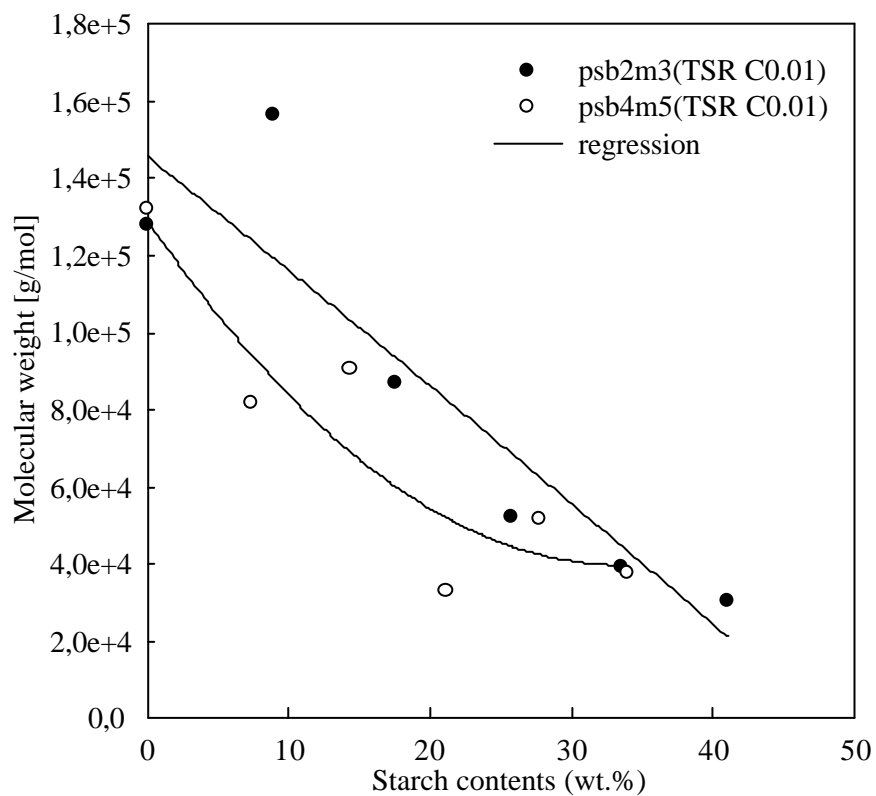


Figure 4.29 Molecular weights,  $M_w$  of polyurethane homo-polymer extracted from starch-polyurethane-blends, psb2m3 (TSR C0.01) and psb4m5 (TSR C0.01) samples

Table 4.9 Average molecular weights of polyurethane homo-polymer separated from polyurethane-starch-blends in psb2m3 and psb4m5 series

Samples	$M_n$	$M_w$	$M_p$	$M_z$	$M_w/M_n$
p1b2m3(OSR C0.01)	116,900	266,110	268,436	478,105	2.276
p9s1b2m3(OSR C0.01)	136,878	260,584	233,500	429,772	1.903
p8s2b2m3(OSR C0.01)	102,439	192,829	182,745	333,137	1.882
p7s3b2m3(OSR C0.01)	49,979	75,613	65,466	109,693	1.512
p6s5b2m3(OSR C0.01)	55,751	93,753	73,276	167,007	1.681
p5s5b2m3(OSR C0.01)	32,254	42,795	34,176	55,552	1.326
p7s3b2m3(OSR C0.05)	21,600	48,910	30,759	145,369	2.264
p7s3b2m3(OSR C0.1)	29,574	84,458	46,808	298,477	2.855
p7s3b2m3(TSR C0.01)	52,328	102,203	59,687	184,474	1.953
p1b4m5(OSR C0.01)	127,680	258,641	238,795	459,118	2.025
p9s1b4m5(OSR C0.01)	79,141	149,139	131,361	273,817	1.884
p8s2b4m5(OSR C0.01)	55,515	89,087	81,341	138,045	1.604
p7s3b4m5(OSR C0.01)	47,568	71,385	62,879	101,689	1.500
p6s5b4m5(OSR C0.01)	32,767	44,751	37,154	60,505	1.365
p5s5b4m5(OSR C0.01)	31,073	42,063	28,481	56,727	1.353
p7s3b4m5(OSR C0.05)	28,003	89,596	44,140	595,569	3.199
p7s3b4m4(OSR C0.1)	27,516	80,842	41,921	520,773	2.938
p7s3b4m5(TSR C0.01)	32,902	70,284	41,567	133,833	2.136

Table 4.10 Average molecular weights of polyurethane homo-polymer separated from polyurethane-starch blends in psb2m3 (TSR C0.01) and psb4m5 (TSR C0.01) series

Samples	$M_n$	$M_w$	$M_p$	$M_z$	$M_w/M_n$
p1b2m3(TSR C0.01)	127,793	261,373	198,603	485,182	2.04
p9s1b2m3(TSR C0.01)	156,323	309,230	288,286	521,531	1.97
p8s2b2m3(TSR C0.01)	86,814	189,282	161,319	381,571	2.18
p7s3b2m3(TSR C0.01)	52,328	102,230	59,687	184,494	1.93
p6s4b2m3(TSR C0.01)	39,400	76,292	56,066	134,677	1.93
p5s5b2m3(TSR C0.01)	30,644	63,115	44,882	121,199	2.06
p1b4m5(TSR C0.01)	132,259	273,067	267,338	495,872	2.06
p9s1b4m5(TSR C0.01)	81,713	176,605	140,181	3,660,941	2.16
p8s2b4m5(TSR C0.01)	90,842	181,466	152,925	354,077	1.99
p7s3b4m5(TSR C0.01)	32,902	70,284	41,567	133,833	2.13
p6s5b4m5(TSR C0.01)	51,545	110,436	86,783	225,575	2.14
p5s5b4m5(TSR C0.01)	37,949	82,658	74,680	10,786	2.17

Table 4.11 Average molecular weights of polyurethane homo-polymers separated from samples polyethylene glycol based polyurethane-starch blends. Influence of the molecular weight of prepolymer

Samples	$M_n$	$M_w$	$M_p$	$M_z$	$M_w/M_n$
p7s3b2m3(OSR C0.01), PEG-2000	8915	11228	14853	13173	1.25
p7s3b2m3(OSR C0.01), PEG-4000	9297	11823	16627	13908	1.27
p7s3b2m3(OSR C0.01), PEG-6000	7452	8996	10605	10394	1.20
p7s3b2m3(OSR C0.01), PEG-10000	insoluble				

### ***4.1.7 Thermogravimetric Analysis***

#### ***4.1.7.1 One-Step Reaction (rapidly cooled)***

The thermal stability of polyurethane for two series of the samples was investigated as a function of the starch content. As shown in Figures 4.30 and 4.31, the starch starts to lose its weight from the temperature of 280 °C whereas the polyurethane-starch blends start to change their weight between 300 and 330 °C. Thermal degradation of the pure starch is easier than those of the blends, psb2m3 and psb4m5 series. The temperature of weight loss was divided into four regions in order to have more detailed information about thermal stability:

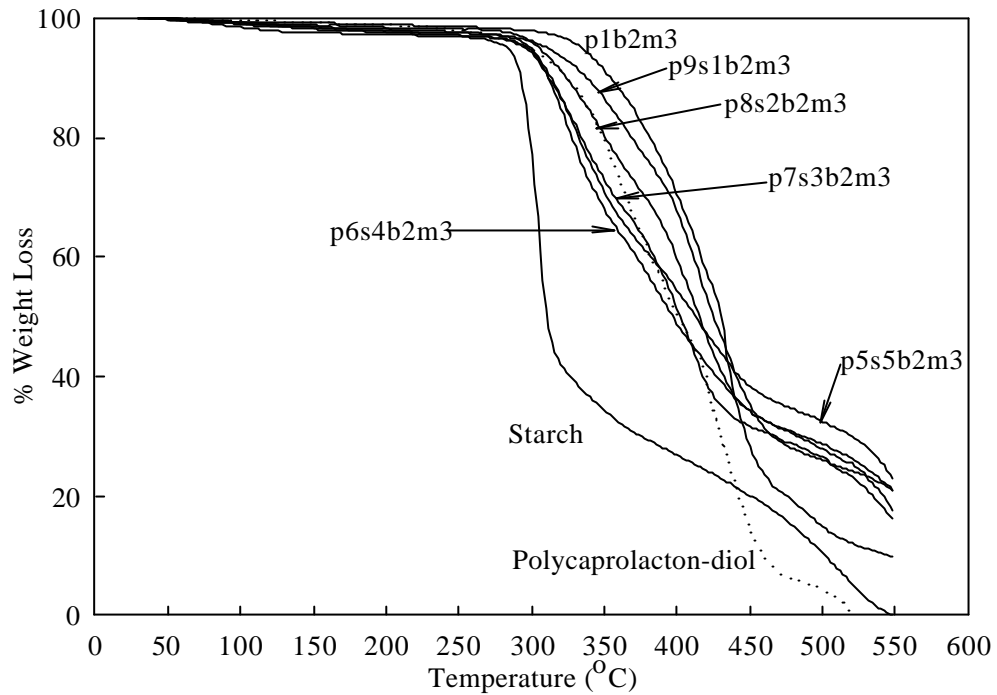
I, < 290 °C ;

II, 290 – 380 °C ;

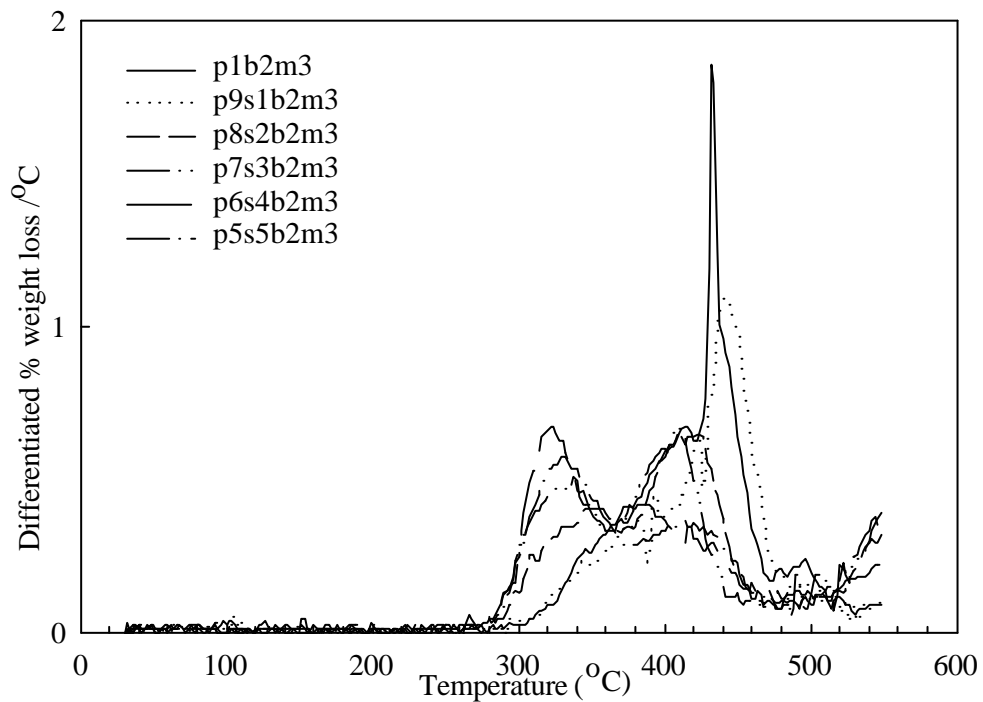
III, 380 – 450 °C and

IV, >450°C.

In region I, the small loss may be due to the drying of the samples. In fact, the weight loss is negligible. In the region II, the weight loss obtained in the order of starch content indicates that psb2m3 series showed higher thermal stability. It was also found that the large decrement of weight loss in the psb2m3 series in this range is caused by starch dehydroxylation. The peak size decreased with the starch content and the peak temperature increased with the starch content. However, this increased thermal stability of the starch, especially at low starch content, may be due to the high grafted crosslinking of the polyurethane with starch. For the psb4m5 series, there is no great difference of the peak size (II) due to the lower starch content compared to the psb2m3 series, but the peak temperature of the dehydroxylation increased with the starch content. The dependence of weight loss in region III showed that the loss of weight for both series were similar with starch contents. Rath et al.<sup>71-73)</sup> studied the thermogravimetric analysis of graft copolymers of polyacrylamide with starch, amylose, and amylopectin. The amylose grafted polyacrylamide maintains a higher thermal stability than amylose, amylopectin grafted polyacrylamide. Results also indicated that starch-grafted-polyacrylamide has a higher weight percent left (19 % at 546 °C), followed by amylose-grafted-polyacrylamide (15 % at 546 °C) and amylopectin-grafted-polyacrylamide (6 % at 546 °C). Therefore, the residual weight after TGA analysis appearing in region IV is mainly caused by the starch.



(a)



(b)

Figure 4.30 Thermogravimetric Analysis (TGA); (a) integral and (b) differential weight loss for psb2m3series (OSR C0.01).

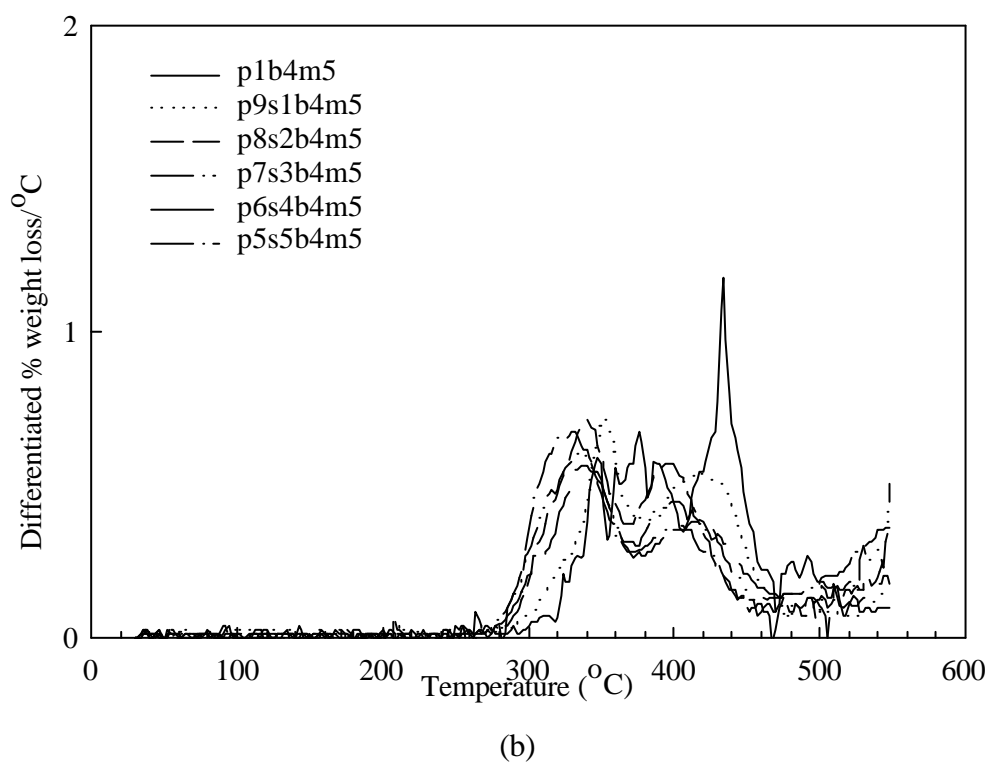
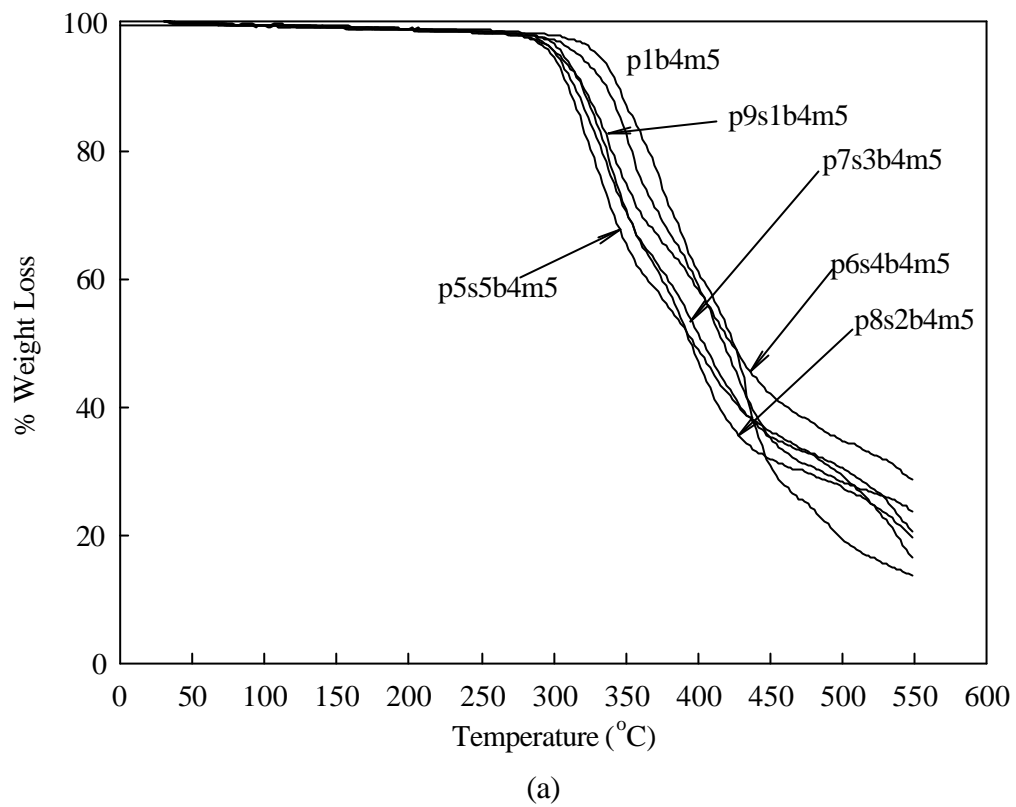


Figure 4.31 Thermogravimetric Analysis (TGA); (a) integral and (b) differential weight loss for psb4m5 series (OSR C0.01).

Table 4.12 indicates the residual weight after the TGA analysis, in which we could not find any significant difference in relation to the reaction conditions such as catalyst concentration and the reaction scheme. However, for the sample containing high concentration of the catalysts, e.g. 0.1 wt.%, the residual weight is slightly high, probably due to the crosslinking in the polyurethane phase.

The catalyst effects on thermal stability of the p7s3b2m3 and p7s3b4m5 samples are also characterized in Figures 4.32 and 4.33. In fact, no difference in the weight loss curves was found despite the variation of the catalyst concentration. However, for the sample with the higher concentration of the catalyst, the region III showed a decreased weight-loss in both series. Due to the higher concentration of the catalyst, starch networking with the polyurethane had occurred, which increased the thermal stability.

#### ***4.1.7.2 Two-Step Reaction***

The different process of the synthesis, i.e. two-step polymerization, also changed the thermal stability of starch-polyurethane blends in the higher temperature range. In Figures 4.34 and 4.35, results are shown for the psb2m3 (TSR C0.01) and psb4m5 (TSR, C0.01) series. The two-step reaction shows clear starch decomposition with increasing temperature. This peak temperature of the decomposition of the starch in the blends decreases with the starch content in the psb4m5 series whereas it is constant in the psb2m3 series. This phenomenon is the opposite to that in the OSR series.

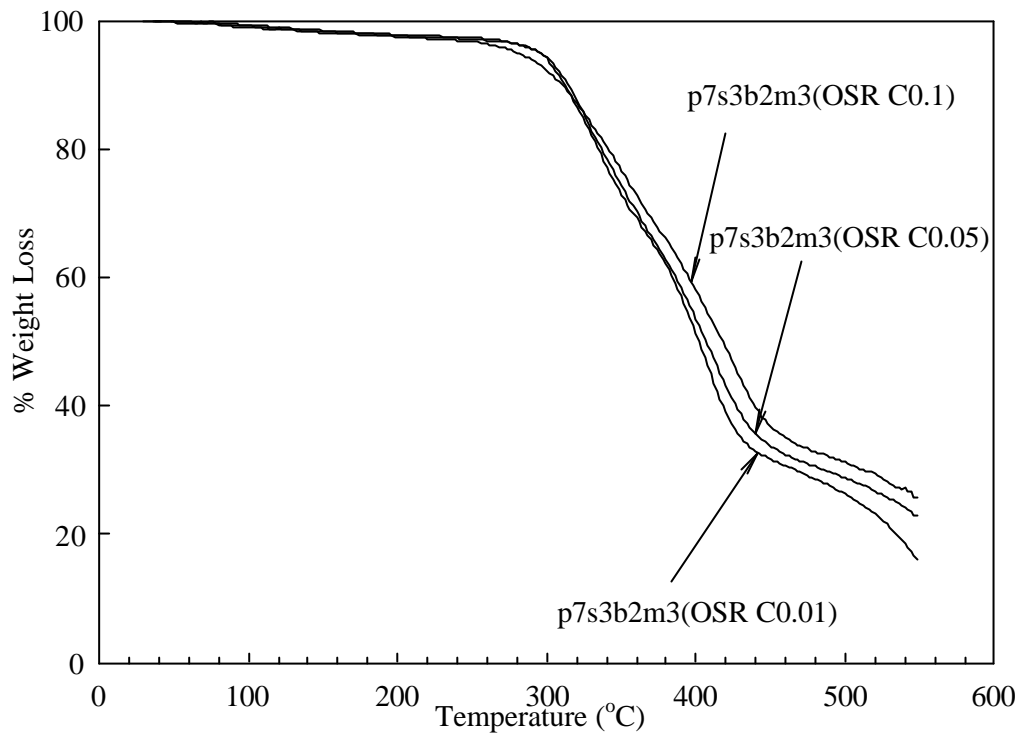
#### ***4.1.7.3 Effect of the Different Molecular Weight of Polyethylene Glycol Prepolymer***

As shown in Figure 4.36, the differential weight losses show one large peak at the position of the starch decomposition although other small peaks between 400 and 540°C were found, except for the sample prepared with PEG-10000. Therefore, we assume that the first peaks include the decomposition of the polyurethane phase. However, the polyurethane phase of the sample prepared with PEG-10000 is thermally more stable probably due to a strong crosslinking between polyurethane chains.

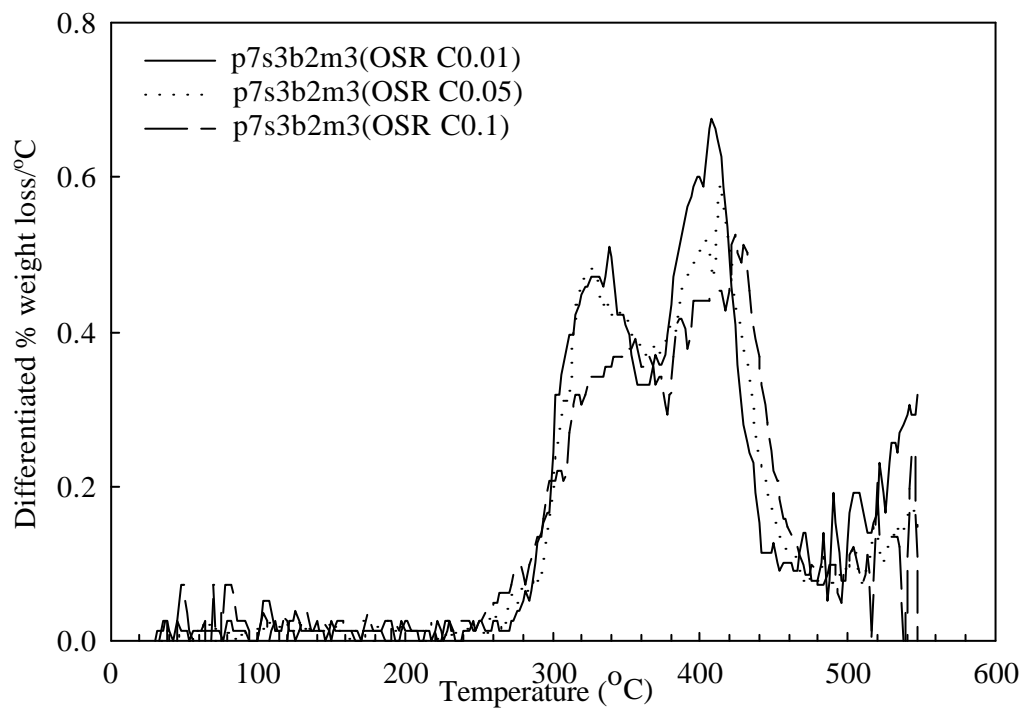


Table 4.12 Residual percentage weight loss in two series of samples

Samples (OSR)	Weight % of residual sample	Samples (TSR)	Weight % of residual sample
p1b2m3(OSR C0.01)	9.70	p1b2m3(TSR C0.01)	-
p9s1b2m3(OSR C0.01)	21.02	p9s1b2m3(TSR C0.01)	20.92
p8s2b2m3(OSR C0.01)	20.93	p8s2b2m3(TSR C0.01)	23.17
p7s3b2m3(OSR C0.01)	16.07	p7s3b2m3(TSR C0.01)	20.46
p6s4b2m3(OSR C0.01)	17.63	p6s4b2m3(TSR C0.01)	18.55
p5s5b2m3(OSR C0.01)	22.93	p5s5b2m3(TSR C0.01)	15.11
p7s3b2m3(OSR C0.05)	22.78	-	
p7s3b2m3(OSR C0.1)	25.58	-	
p1b4m5(OSR C0.01)	13.75	p1b4m5(TSR C0.01)	-
p9s1b4m5(OSR C0.01)	23.79	p9s1b4m5(TSR C0.01)	22.51
p8s2b4m5(OSR C0.01)	19.61	p8s2b4m5(TSR C0.01)	27.31
p7s3b4m5(OSR C0.01)	20.48	p7s3b4m5(TSR C0.01)	23.76
p6s4b4m5(OSR C0.01)	28.59	p6s4b4m5(TSR C0.01)	15.53
p5s5b4m5(OSR C0.01)	16.36	p5s5b4m5(TSR C0.01)	23.65
p7s3b4m5(OSR C0.05)	23.07	-	
p7s3b4m5(OSR C0.1)	31.27	-	

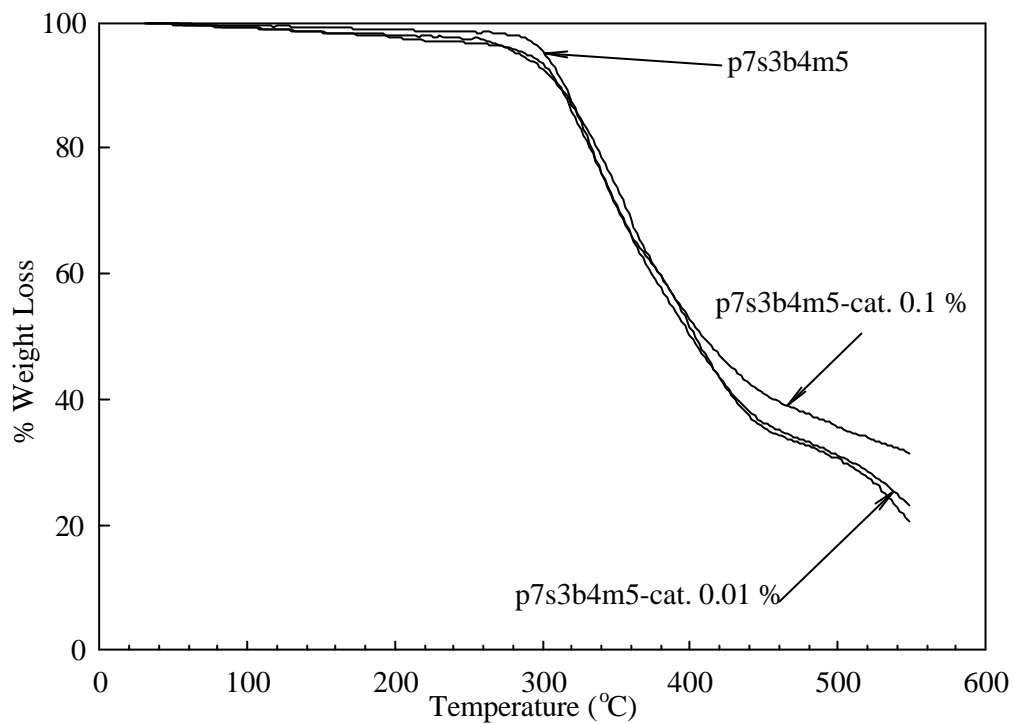


(a)

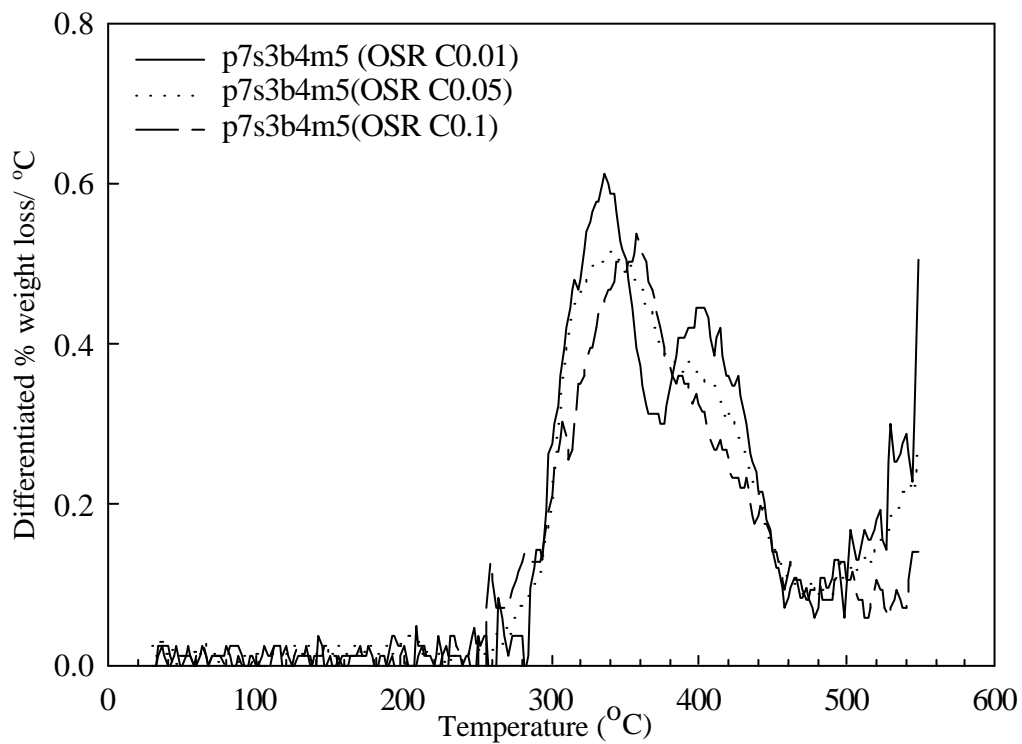


(b)

Figure 4.32 Thermogravimetric Analysis (TGA); (a) integral and (b) differential weight loss for p7s3b2m3 (OSR C0.01) series at different catalyst concentration.

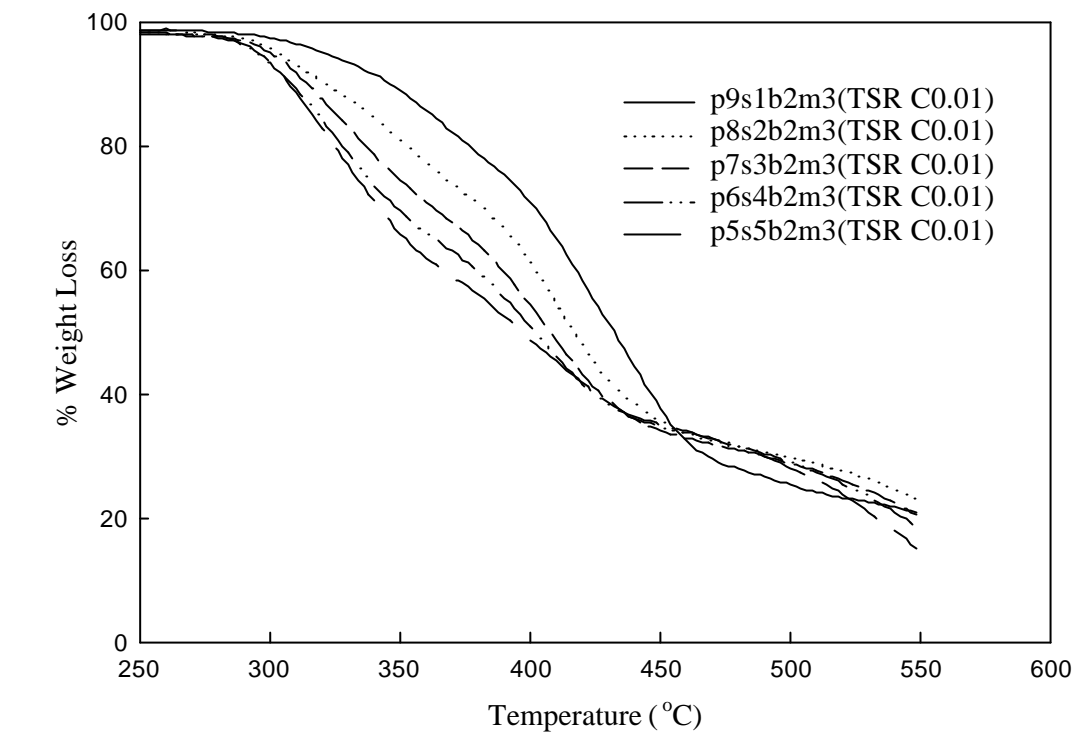


(a)

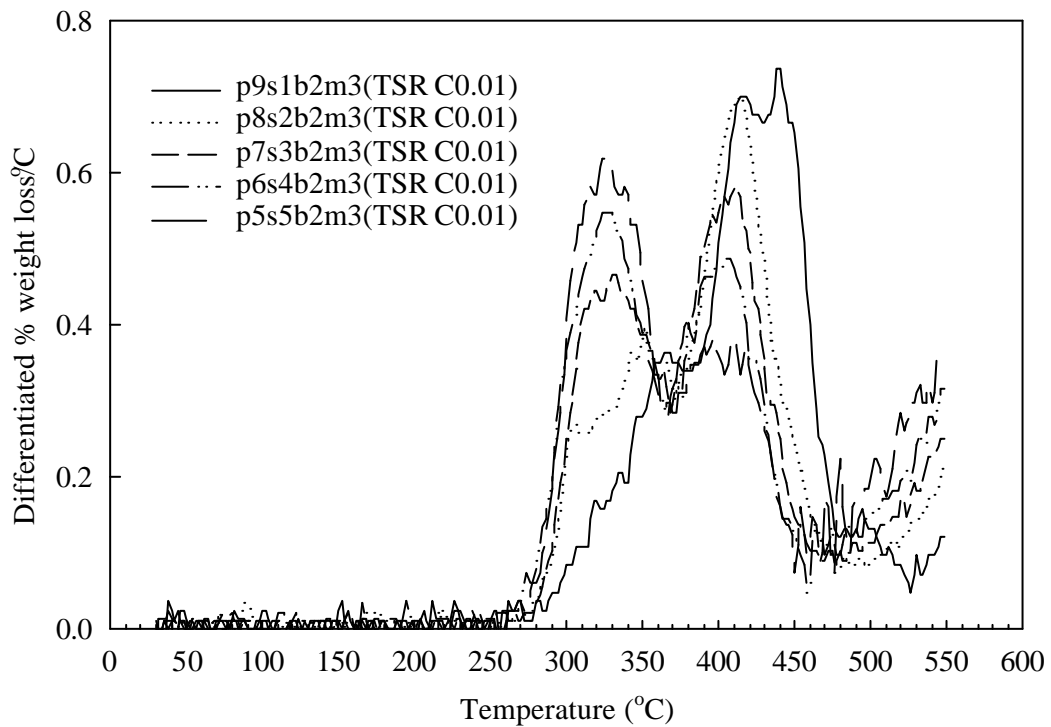


(b)

Figure 4.33 Thermogravimetric Analysis (TGA); (a) integral (b) differential weight loss for p7s3b4m5 (OSR C0.01) at different catalyst concentration.

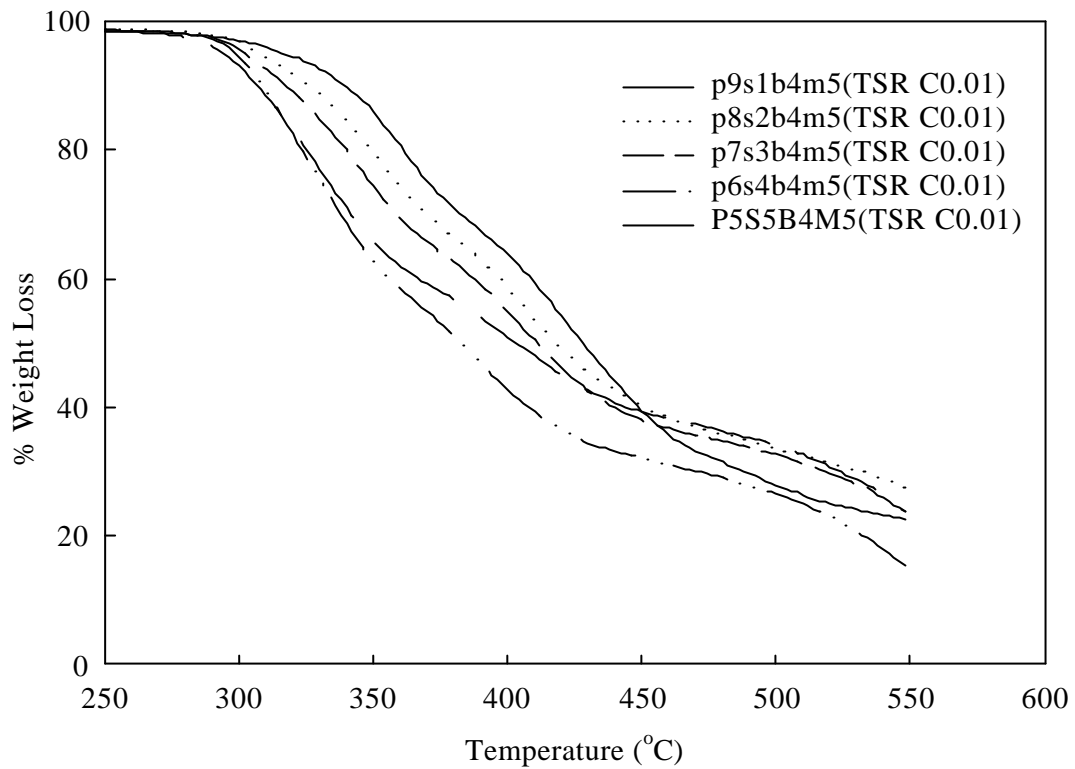


(a)

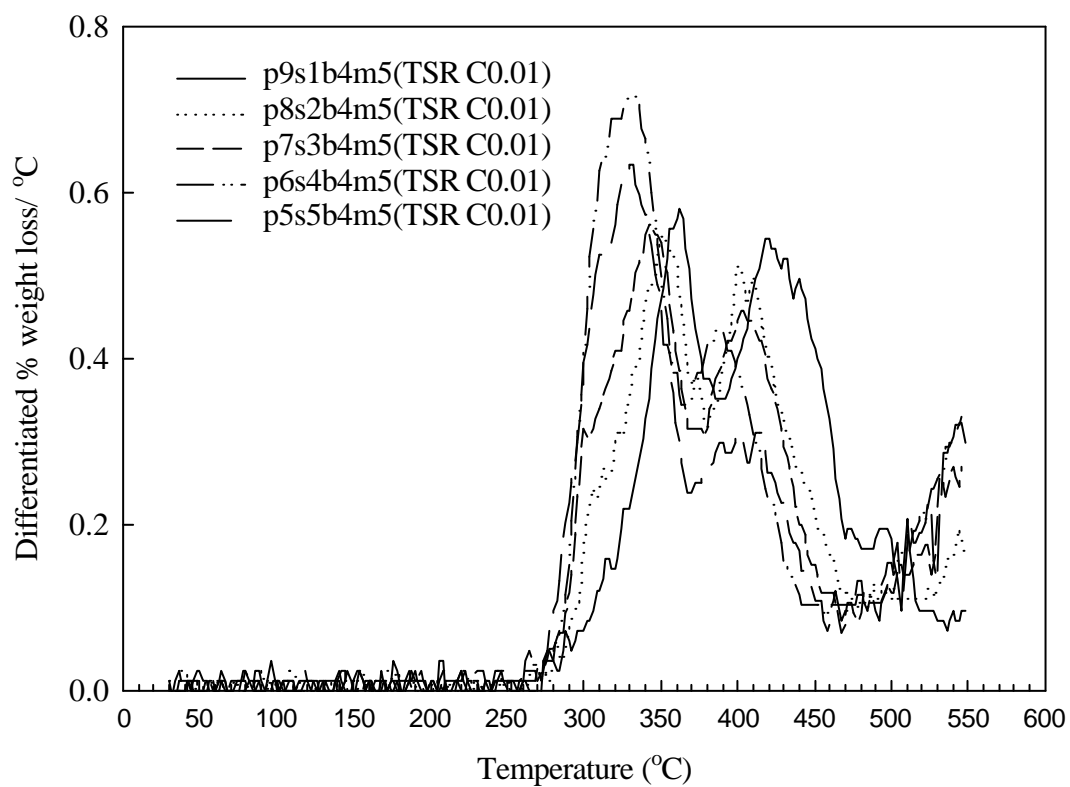


(b)

Figure 4.34 Thermogravimetric Analysis (TGA); (a) integral, (b) differential weight loss for the psb2m3 series (TSR C0.01)

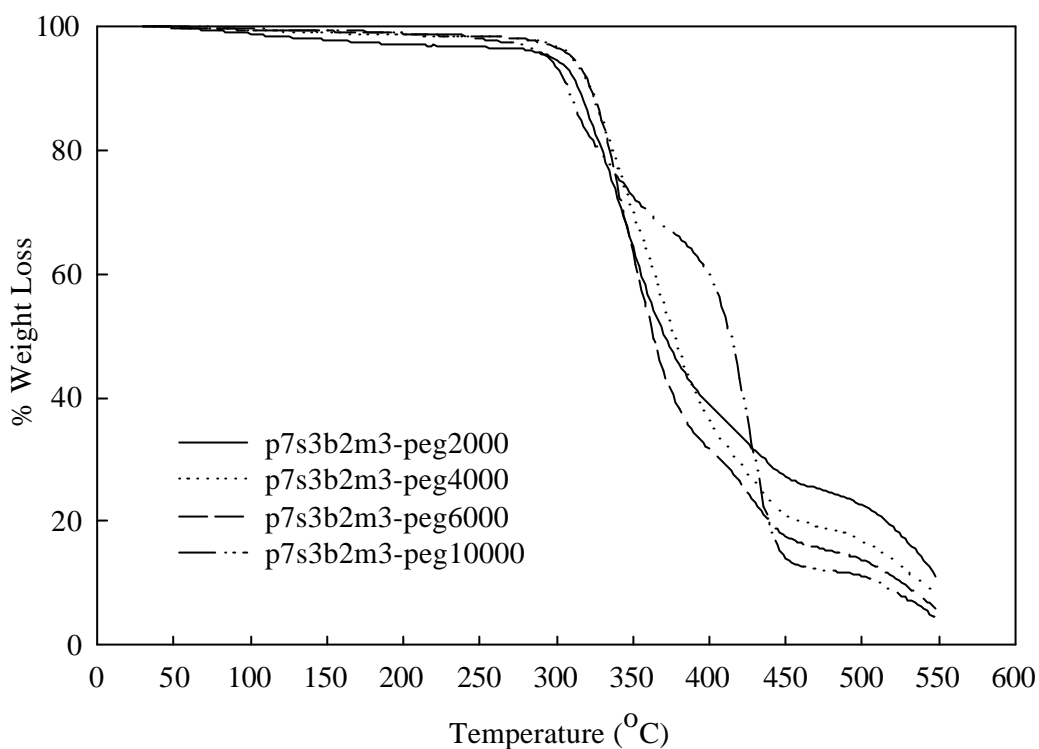


(a)

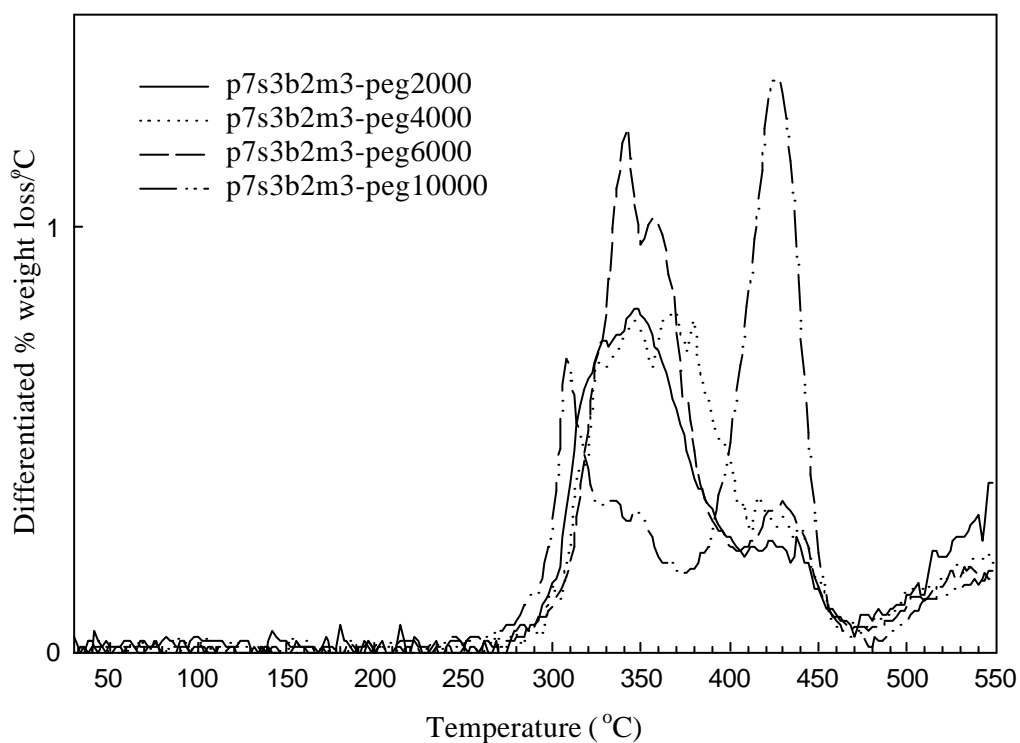


(b)

Figure 4.35 Thermogravimetric Analysis (TGA); (a) integral (b) differential weight loss for the p5b4m5 series (TSR C0.01)



(a)



(b)

Figure 4.36 Thermogravimetric Analysis(TGA); (a) intergral (b) differential weight loss for p7s3b2m3 series (OSR C0.01) prepared with different molecular weight of polyethylene glycol prepolymer

### **4.1.8 Mechanical Properties**

#### **4.1.8.1 One-Step Reaction (rapidly cooled)**

The results for the tensile strength and elongation [%] for two series are presented in Figures 4.37 and 4.38. As shown in the figures, the tensile strength and elongation percent are either improved or not changed for the lower range of starch contents. As shown above, at low starch contents in the psb2m3 series the average molecular weights of homo-polyurethane are similar and the grafted weight increased as shown in Figure 4.23. The slight increase or non-change in the tensile strength and elongation at lower starch contents could be caused by several parameters such as the molecular weight of homo-polyurethane, the percentage of grafting, degree of crosslinking and the development of the hard-segment formation in the polyurethane phase. The heats of fusion appearing in Table 4.2, which were obtained by DSC analysis, could, in principle, also be related to the tensile strength. However, no correlation with these parameters was found.

The mechanical properties have been plotted with swelling uptake as crosslinking parameter in Figures 4.39 and 4.40 and with average molecular weight of extracted homo-polymer polyurethane in Figures 4.41 and 4.42. As shown in Figures 4.37 and 4.38, elongation and strength at break decrease rapidly for starch contents of more than 20 wt.%. These decreases could be influenced by several variables such as (1) degree of grafting, (2) degree and shape of crosslinking, (3) average molecular weight of polyurethane homo-phase, (4) the hardness of the starch granule and an entanglement between the amylose and amylopectin. I suggest correlating the two mechanical properties with starch content, solvent uptake and molecular weight. As shown in the figures, elongation is constant or slightly increased with the decrease of solvent uptake up to 1.5 or 2 and then it rapidly decreases. For the tensile strength, although the data were scattered, at the higher range of the solvent uptake they slightly increased, but they decreased rapidly for the high range of crosslinking (low solvent uptake). Fracturing of the starch granules and/or gapping between two phases, which define the limit of the tensile strength of the samples, may cause the rapid decrease of tensile strength and the elongation in the range of high starch content. As already mentioned, Figure 4.6 also shows the fractured surface of a tensile bar of p5s5b4m5 (~34wt% of starch). Phase separation between starch granules and the polyurethane phase, and division of the starch granules into two parts can be seen on the SEM-micrograph of p5s5b4m5. The hole appearing in the figure is small compared to the mean size of the starch granules,

which indicates that a small area of the starch granule was stripped when the bar was broken.

#### ***4.1.8.2 Two-Step Reaction (rapidly cooled)***

The first step was carried out in an excess of isocyanate (prepolymer(PCL)+MDI) and then as second step the excess of isocyanate was terminated by starch and 1,4 butane diol. The results are presented in Figures 4.43 and 4.44. Generally, the variation tendency of the mechanical properties such as elongation and the tensile strength at break were not much changed at the low range of starch content and decreased rapidly in the higher range of starch content. The phenomena for the variation tendency are similar to the results of the one step reaction. However, for the psb4m5 series, the decrease of the tensile strength is not rapid. This increased tensile strength may be explained by the increased crosslinking in the two-step reaction, especially for the high hard segment samples.

#### ***4.1.8.3 Effect of the Different Molecular Weight of the Polyethylene Glycol Prepolymer***

The mechanical properties of the polyurethane were examined by changing the average molecular weight of the prepolymer. As with the previously used prepolymer, different molecular weights of polycaprolactone diol (PCL) were difficult to obtain commercially, therefore, we used a prepolymer of polyethylene glycol. The ultimate tensile strength and elongation are shown in Figures 4.45 and 4.46.

The mechanical properties increased rapidly at the low molecular weight of the prepolymer whereas they slowly increased at higher range of the molecular weight of prepolymer. In contrast, the mechanical properties of the samples prepared with PCD (polycaprolactone diol) showed low values for the lower molecular weight of prepolymer. The average molecular weights of the homopolymers of the polyethylene glycol are similar, as shown in Table 11. Therefore, the increase of the elongation depends on the molecular weight of the prepolymer, while the strength at break of the sample depends on the crystal concentration of the soft segment of the polyethylene glycol that is a crosslinker of the polymer.



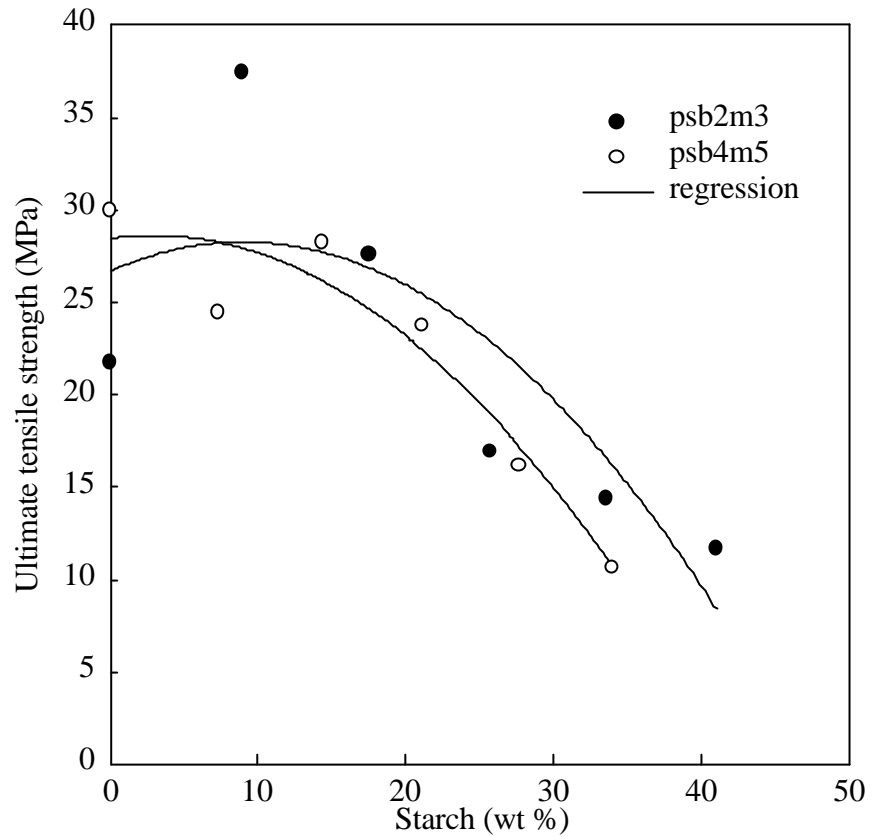


Figure 4.37 Tensile strength as a function of starch contents for psb2m3 and psb4m5 series (OSR C0.01)

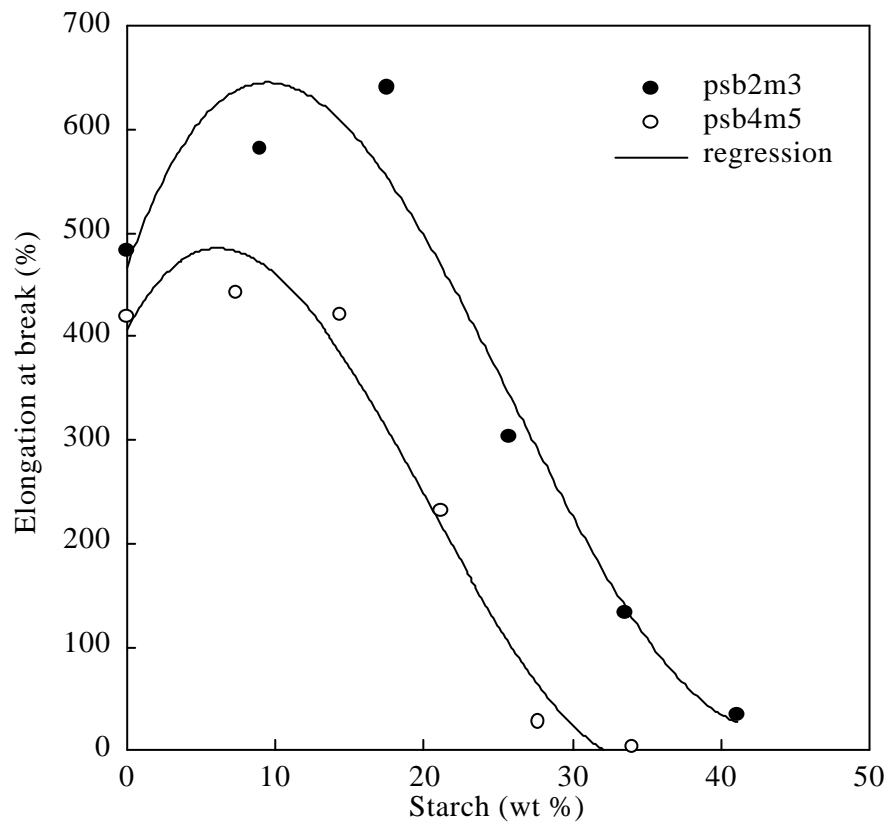


Figure 4.38 Elongation at break as a function of starch contents for psb2m3 and psb4m5 series (OSR C0.01)

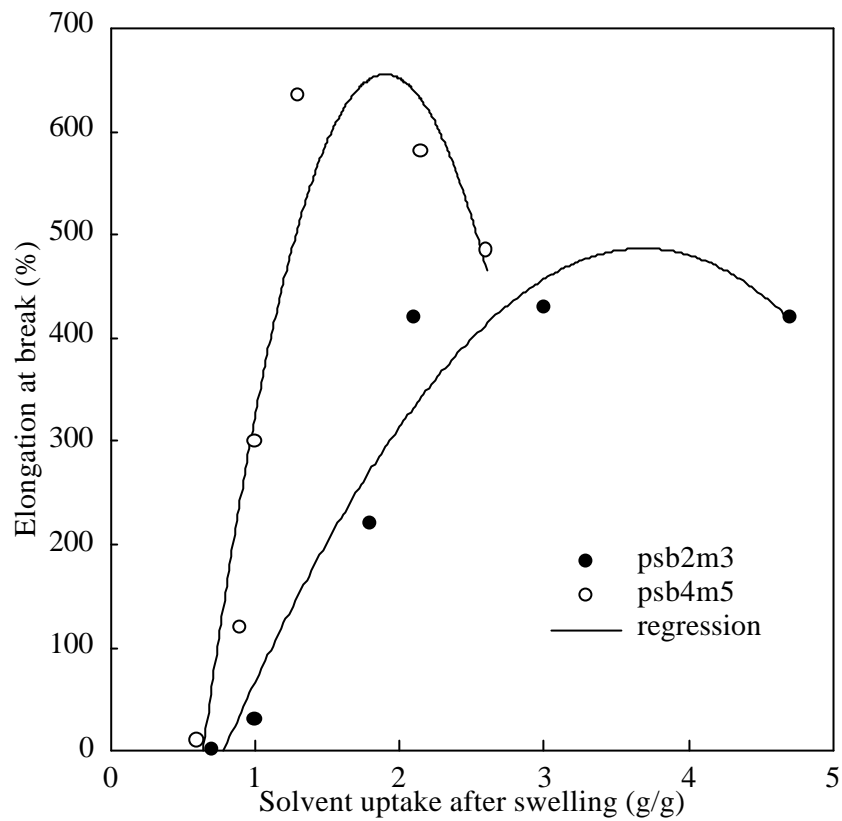


Figure 4.39 Elongations at break as a function of solvent uptake (crosslinking parameter) for two series of samples. Swelling agent: THF for 3 weeks

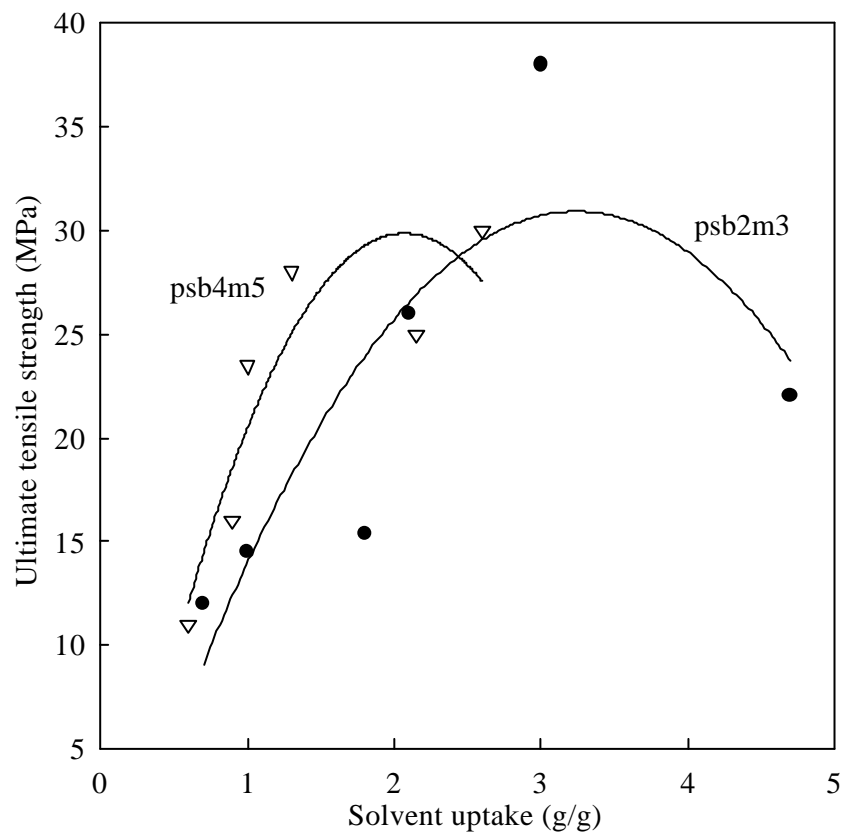


Figure 4.40 Tensile strength as a function of solvent uptake for two series of samples. Swelling solvent: THF for 3 weeks

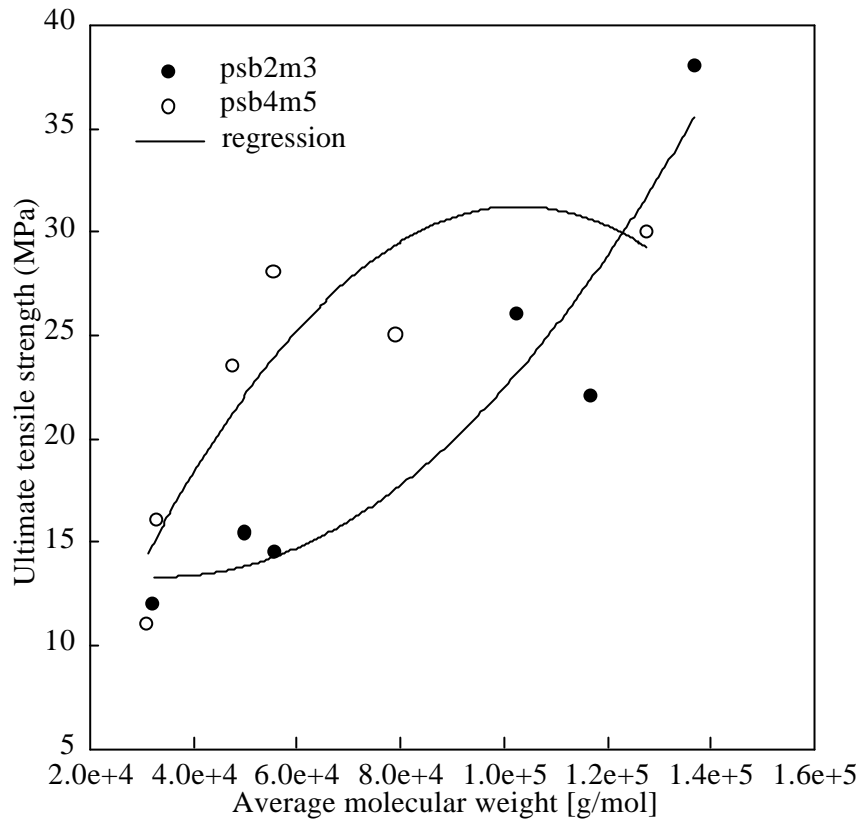


Figure 4.41 Tensile strength as a function of average molecular weight of homo-polymer extracted polyurethane-starch-blends.

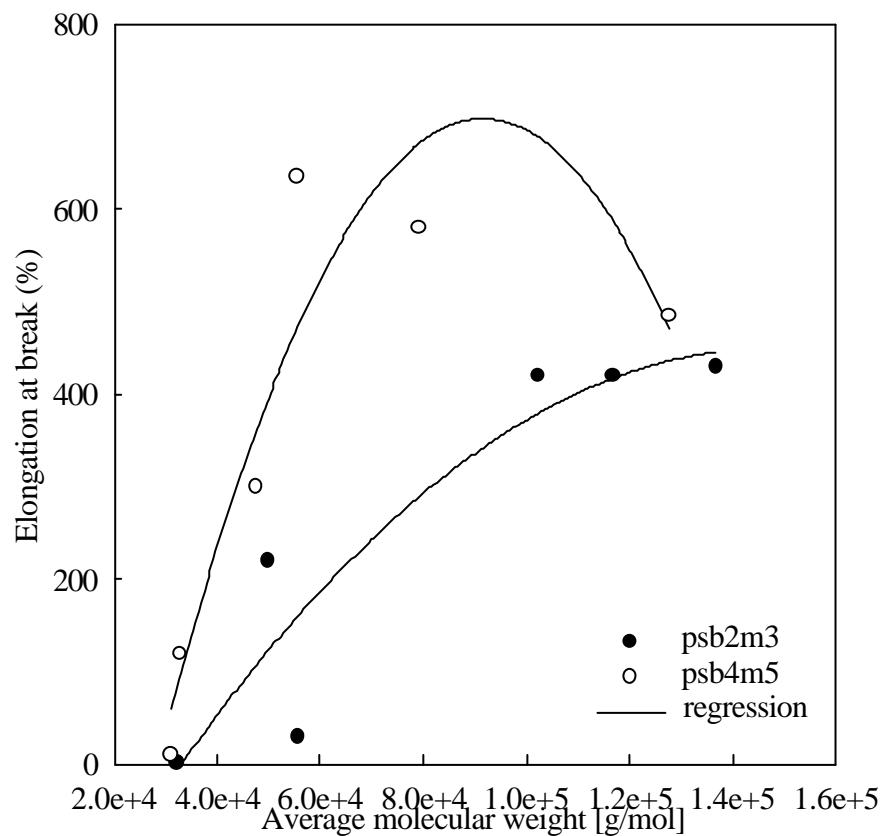


Figure 4.42 Elongations at break as a function of average molecular weight of homo-polymer extracted polyurethane-starch-blends

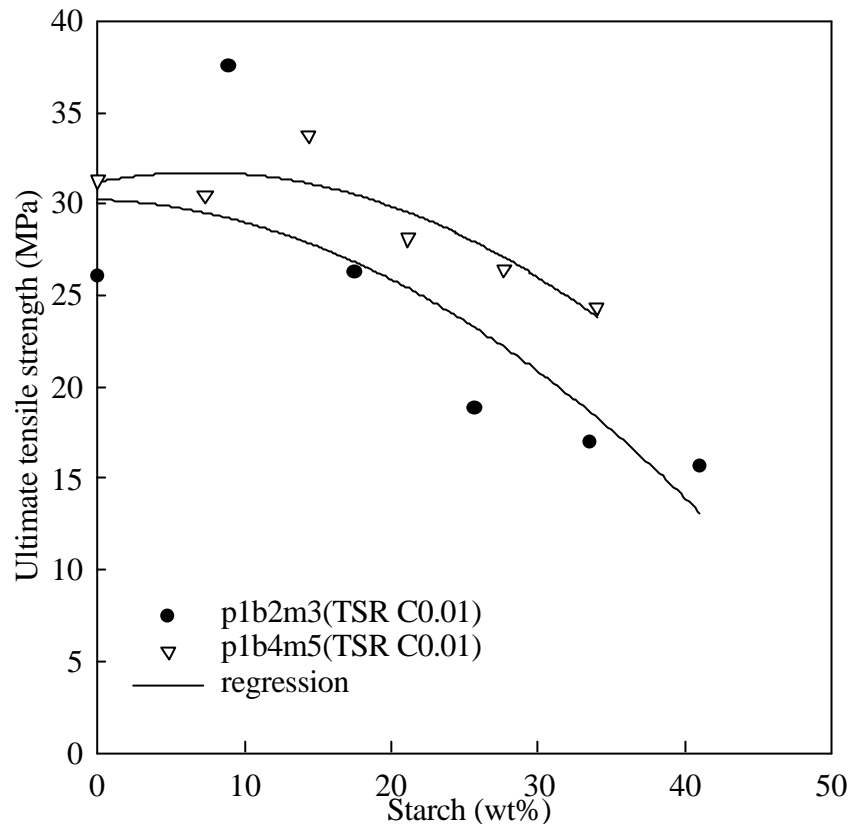


Figure 4.43 Tensile strength as a function of starch content for p1b2m3 and p1b4m5 series (TSR C0.01)

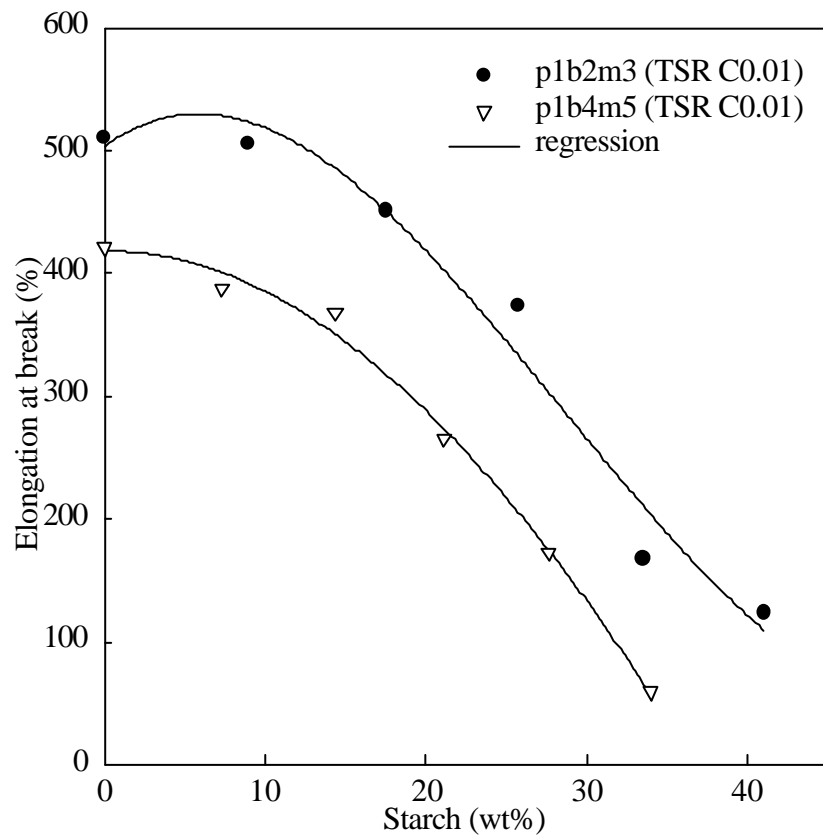


Figure 4.44 Elongation at break as a function of starch content for p1b2m3 and p1b4m5 series (TSR C0.01)

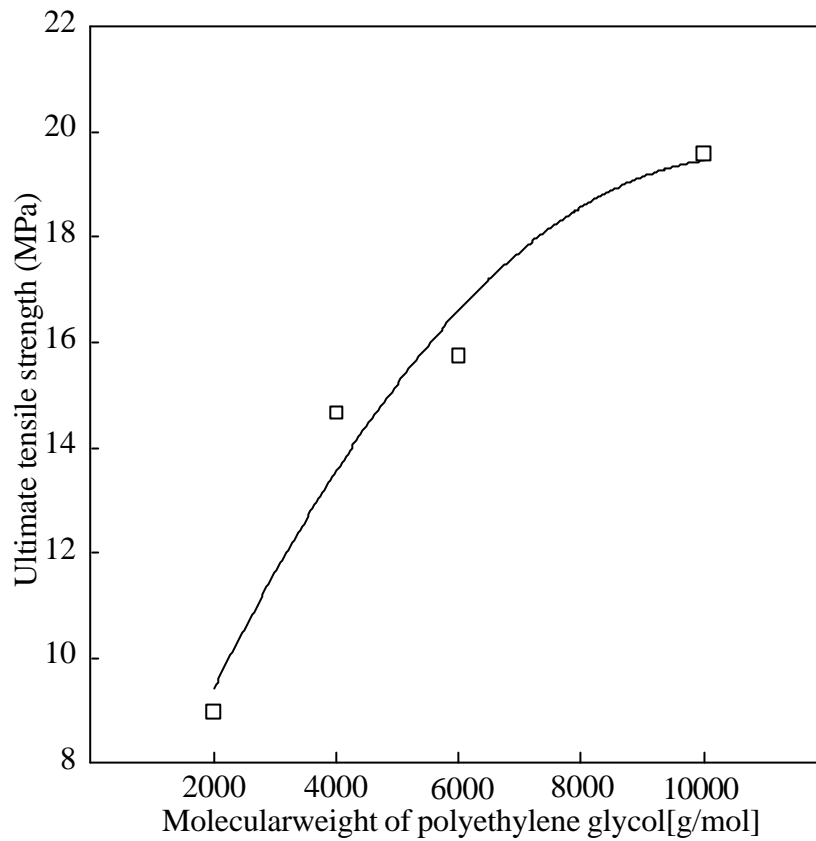


Figure 4.45 Ultimate tensile strength against different molecular weight of polyethylene glycol prepolymer (OSR C0.01)

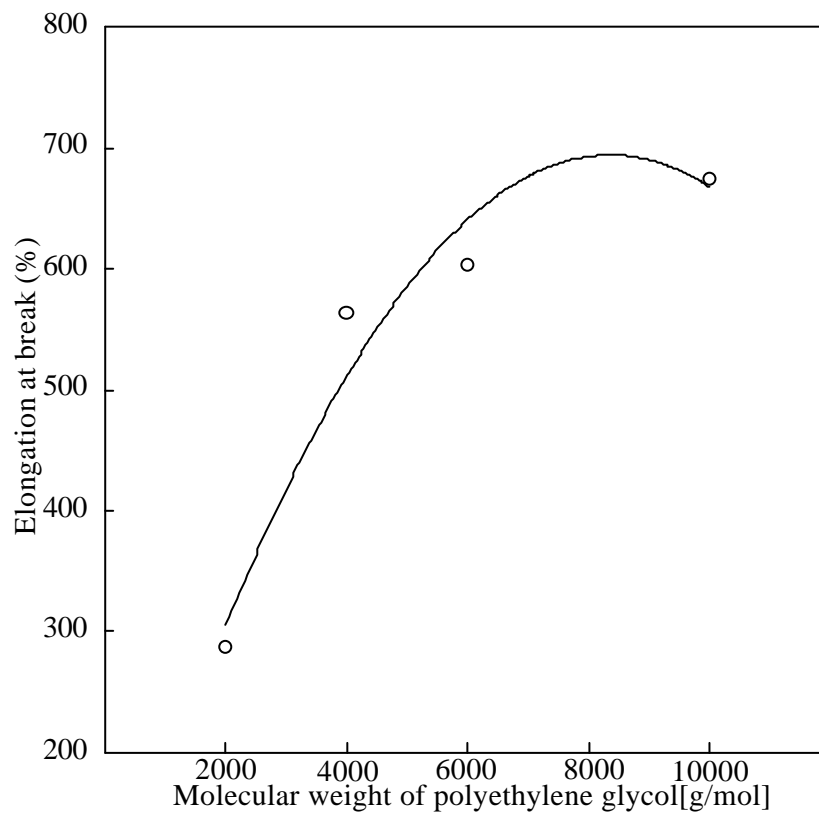


Figure 4.46 Elongation at break against different molecular weight of polyethylene glycol prepolymer (OSR C0.01)

## ***4.2 Rheological Properties***

### ***4.2.1 Viscosity $\zeta^*$***

#### ***4.2.1.1 One Step Reaction***

In Figures 4.47 and 4.48, the complex viscosity  $\zeta^*$  was plotted against angular frequency  $\omega$  for various starch contents for two series of the samples, psb2m3 and psb4m5 to identify the effects of crosslinking between polyurethane chains and/or starch granules.<sup>11)</sup> For the lower range of frequency, we found an increase of viscosity with increasing starch content. For two samples p1b2m3 and p1b4m5, the curves led to a plateau at low frequency, as viscosity  $\zeta^*$  approaches the limit of zero shear viscosity. However, starch addition to the polyurethane phase (p9s1b2m3, ~9wt. % starch) diminished the plateau of the curve resulting in increased viscosity. The average molecular weights of homopolymer separated from the starch were  $M_n=116,930$  for p1b2m3 and  $M_n=136,878$  for p9s1b2m3. This similarity of the average molecular weight indicates that the increase of viscosity at low frequency may have been caused by the crosslinking of starch granules with polyurethane and/or between polyurethane-chains (bulk polymerization possibly induced the crosslinking for the thermoplastic polyurethane at a high temperature.<sup>3)</sup> For the remaining samples, the complex viscosity continues to increase linearly as frequency decreases. This linearity indicates a well-developed three-dimensional network through crosslinking between polyurethane and the starch granules, as already<sup>6)</sup> pointed out in other polymer systems. For samples of higher starch content (p5s5bm) the viscosity decreased compared to p6s4bm. This may be due to a lower grafting level.<sup>63)</sup>

#### ***4.2.1.2 Two Step Reaction***

The viscosities measured for the samples prepared with the two-step reaction scheme are presented in Figures 4.49 and 4.50 for two series, psb2m3 and psb4m5. The presence of a plateau at low frequency, as viscosity  $\zeta^*$  approaches the limit of the zero shear rate, is similar with the results of the one-step reaction. The viscosity increases at the lower range of the frequency which is also the same tendency as the result of the one step reaction.

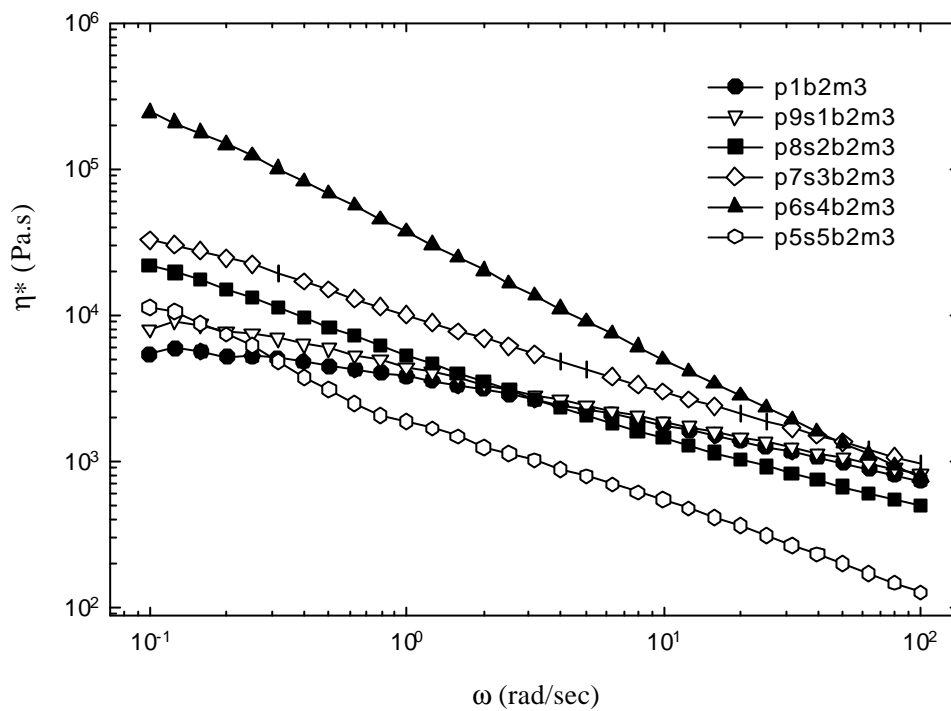


Figure 4.47 Complex viscosities  $\zeta^*$  as a function of frequency  $\dot{\gamma}$  for psb2m3 (OSR) series of samples.

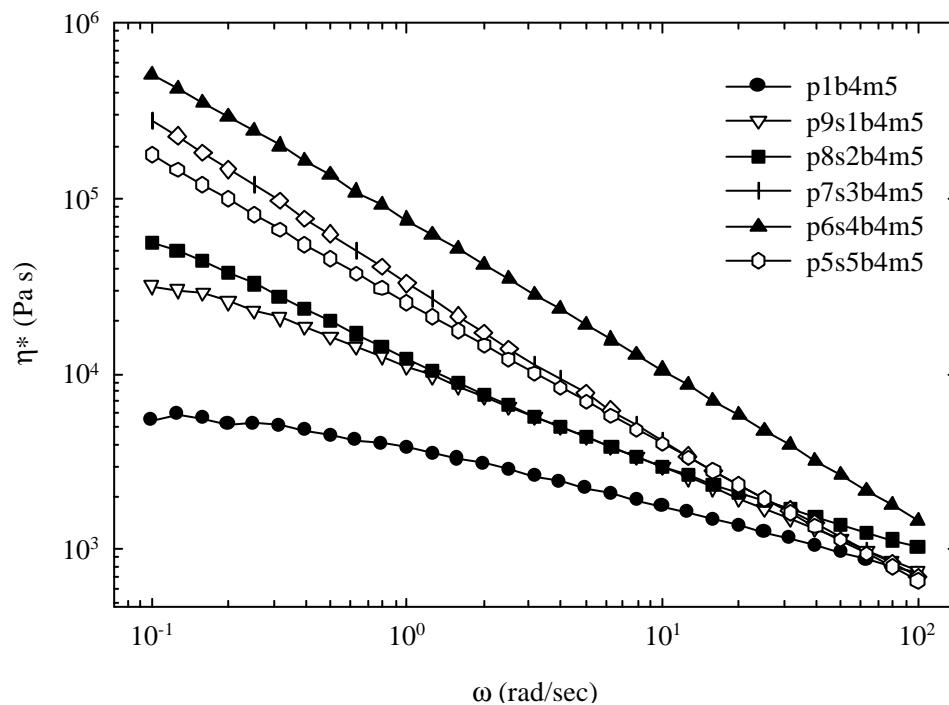


Figure 4.48 Complex viscosities  $\zeta^*$  as a function of frequency  $\dot{\gamma}$  for psb4m5 (OSR C0.01) series of samples.

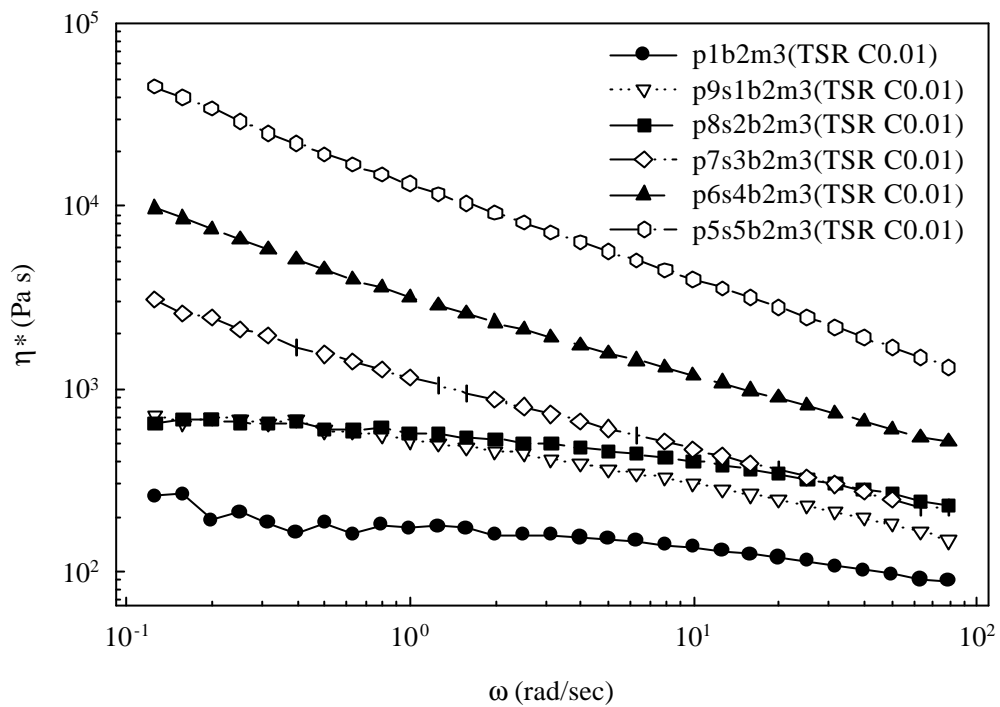


Figure 4.49 Complex viscosities  $\zeta^*$  as a function of frequency  $\dot{\omega}$  for psb2m3 (TSR C0.01) series of samples prepared in the two-step reaction

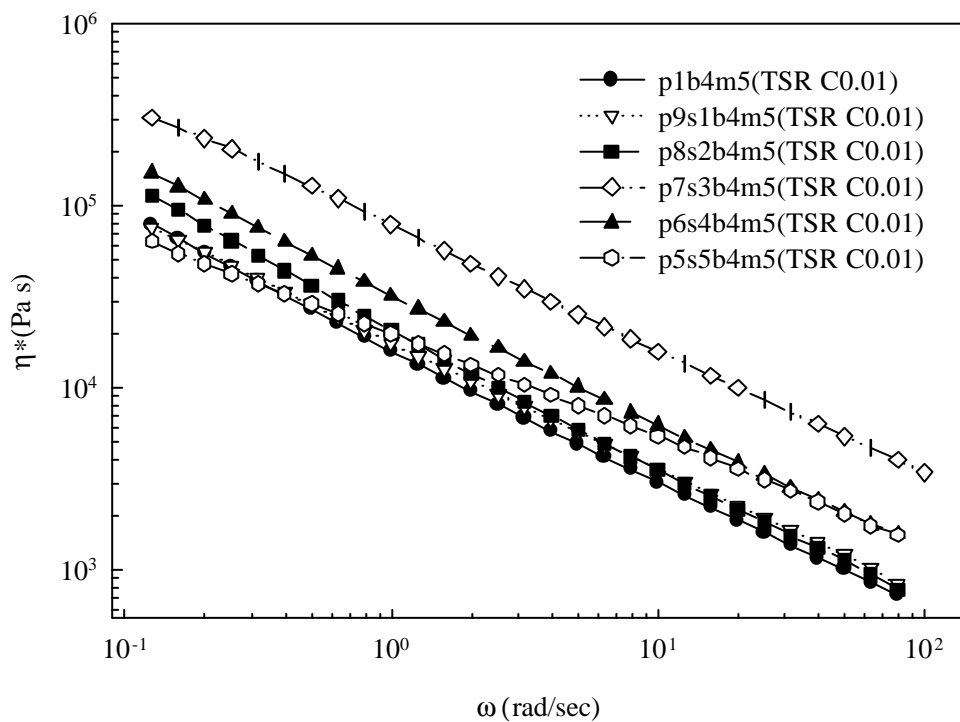


Figure 4.50 Complex viscosities  $\zeta^*$  as a function of frequency  $\dot{\omega}$  for psb4m5 (TSR C0.01) series of samples prepared in the two-step reaction



However, even at the higher range of frequency the viscosity increases, and the slope of the linear correlation does not change with the starch content. The viscosity shows a maximum point of  $\eta'$  in the series of  $\eta''$ .

#### ***4.2.1.3 Viscosities against Starch Contents at Low Frequency $\eta'$***

The viscosities at a frequency of 0.12 are presented in Figures 4.51 and 4.52 for both series prepared by OSR and TSR. The viscosities of  $\eta'$  (OSR) are higher than those of  $\eta'$ (TSR), whereas the viscosities of  $\eta''$  (OSR) are lower than those of the  $\eta''$ (TSR) in the low range of starch content. For the  $\eta'$  series, the low viscosity of the samples prepared by TSR may be related to the low crosslinking, as shown already in the solvent uptake. The comparison of Figure 4.25 to Figure 4.26 indicates that the solvent uptake of  $\eta'$ (OSR) is smaller than that of  $\eta'$ (TSR), which reveals less crosslinking of the latter.

In contrast, for the  $\eta''$  series, initial concentration of isocyanate is already sufficiently high for the two reaction schemes at the second step of starch addition of TSR compared to  $\eta'$  series. However, the reason for the inverse result between  $\eta'$  and  $\eta''$  can not be explained clearly in this moment, and needs to be investigated further.

#### ***4.2.1.4 Effects of the Different Molecular Weight of Polyethylene Glycol Prepolymer***

The viscosities of the samples,  $\eta'$ (PEG) prepared with different molecular weights of prepolymer of polyethylene glycol were measured. The large molecular weight of the prepolymer increases the soft segment concentration as indicated in Table 4.11. It is considered that the increased soft segment concentration may decrease the viscosity. However, as shown in Figure 4.53, the viscosity increased in the range of low frequencies and decreased in the range of high frequencies. The samples prepared with prepolymer of molecular weight 10,000 were not soluble in DMF even at high temperature (80 ~ 90°C) and under strong agitation. This indicates that strong crosslinking occurred in the samples prepared with high molecular weight of prepolymer. Furthermore, as shown in the DSC study, the transition peak of the melting point of soft segments increased with the molecular weight of the prepolymer of polyethylene glycol. This may be another type of crosslinking of the polyurethane system.

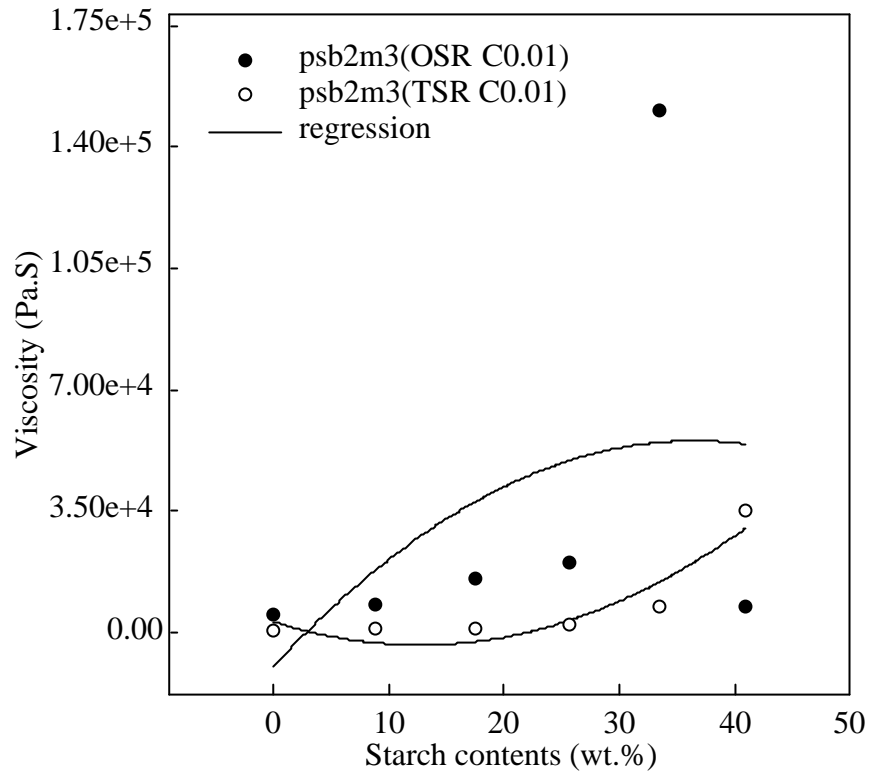


Figure 4.51 Melt viscosities as a function of the starch contents at frequency 0.2, the samples prepared by OSR and TSR for psb2m3 series.

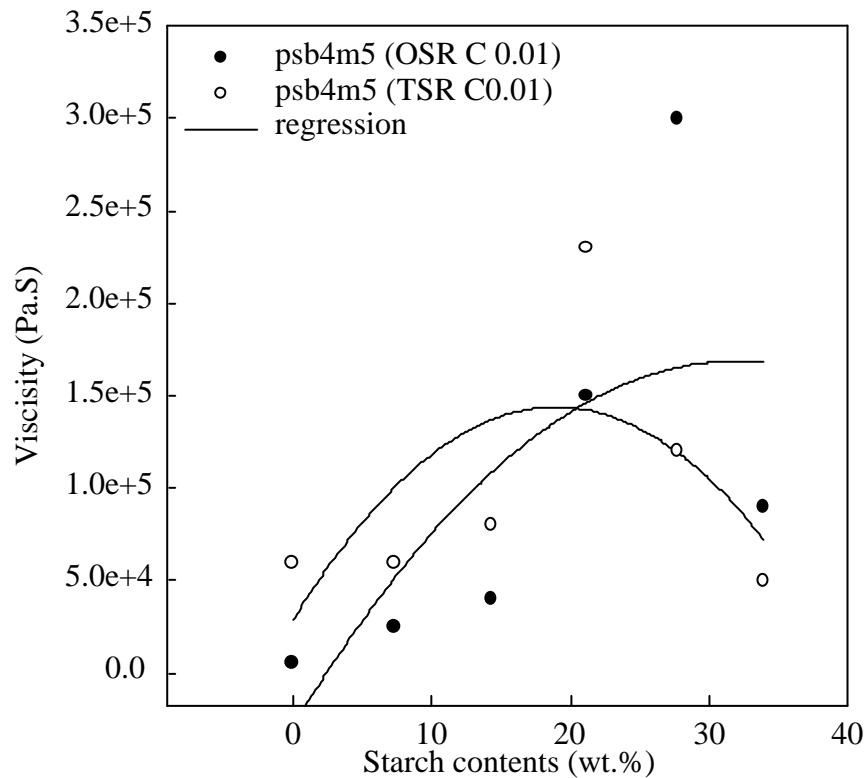


Figure 4.52 Melt viscosities as a function of the starch contents at frequency 0.2, the samples prepared by OSR and TSR for psb4m5

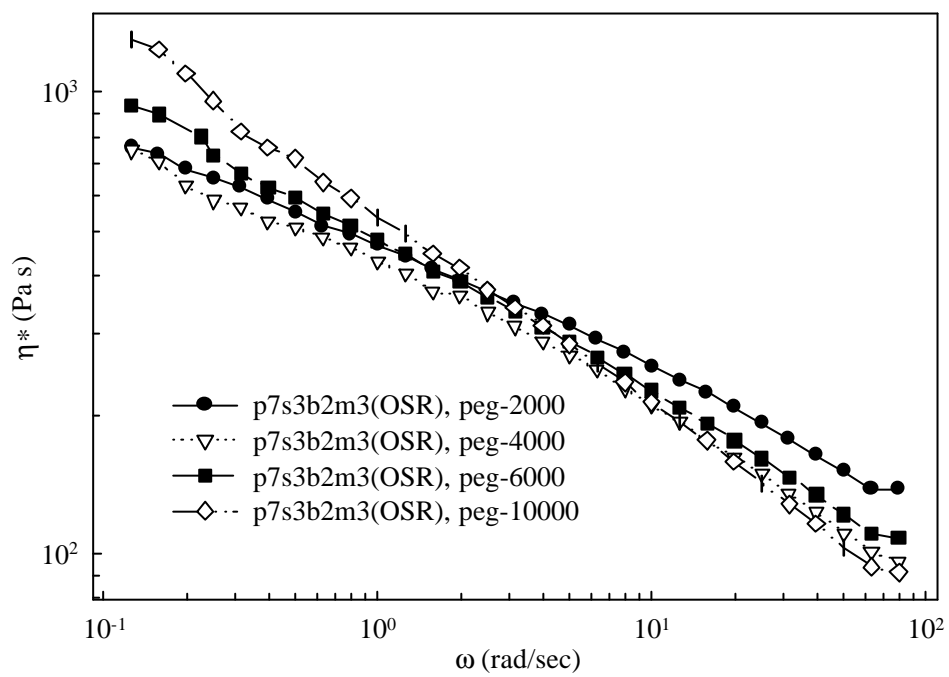


Figure 4.53 Complex viscosity  $\zeta^*$  against frequency  $\dot{\gamma}$  for the samples (p7s3b2m3, (OSR C0.01)) prepared by different molecular weight of polyethylene glycol prepolymer

## **4.2.2 Plots of $\log G'$ against $\log G''$**

### **4.2.2.1 One-Step Reaction**

The correlations between storage modulus  $G'$  and loss modulus  $G''$  were studied to characterize the polymer materials and determine the crosslinking level. In a plot of  $\log G'$  vs  $\log G''$ , the region above the line  $G'=G''$  represents the elastic behavior whereas the region below  $G'=G''$  gives evidence of the viscous behavior. Intersection of  $\log G'$  and  $\log G''$  defines the gel point of the material. The higher crosslinking reveals greater elastic properties. The crosslinking density of polyurethane with starch granules increased with the content of the starch granules and with the grafted percentage of starch.

Correlations are plotted in Figures 4.54 and 4.55. All plotted lines are non linear for the examined range of  $\omega$ . In the higher range of  $G''$  and  $G'$  (higher  $\omega$ ), there are linear parts. For the samples of the psb2m3 series, the plots are on the diagonal line or in its lower region except for p5s5b2m3. This indicates low crosslinking and/or higher molecular weights than those of psb4m5 that is more crosslinked than psb2m3, in other words, it is rather viscous. However, for the psb4m5 series that have higher hard segment concentration than those of the psb2m3, most of the correlation lines are also located in the region above the diagonal line. Due to crosslinking, the polyurethane incorporated with low starch content is located on the line near  $G'' = G'$  <sup>64</sup>.

However, for the samples with a high starch content (p5s5bm), especially for p5s5b2m3,  $G'$  was lowered due to decreased grafting. In our high starch content samples, the plots deviated from the linear lines, which means that the morphology of the polyurethane changed due to gel formation by crosslinking between starch granules and polyurethane chains. This gel formation was also confirmed by unsolving the samples in THF.

### **4.2.2.2 Two-Step Reaction**

For the samples prepared in the two step reaction, as shown in Figure 4.56 and 4.57, we found that the samples of psb2m3(TSR C0.01) are more viscous than psb2m3(OSR C0.01) whereas the samples of psb4m5(TSR C0.01) are more elastic than psb4m5(OSR C0.01).

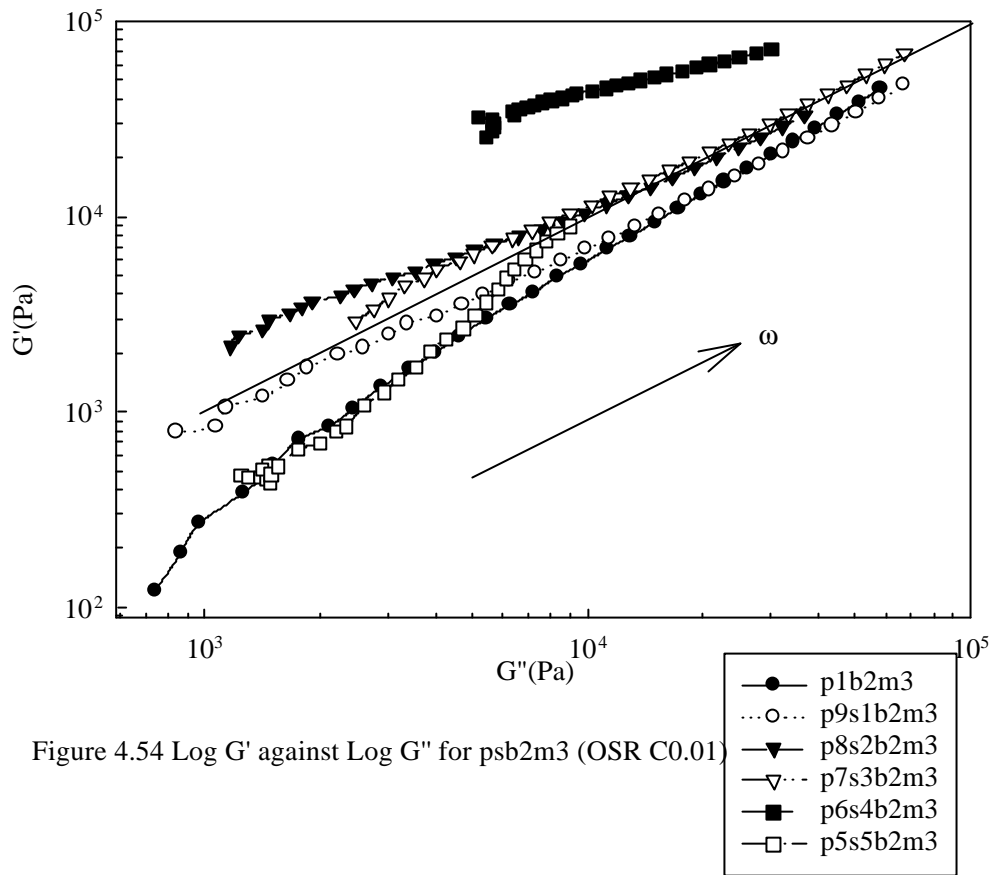


Figure 4.54 Log  $G'$  against Log  $G''$  for psb2m3 (OSR C0.01)

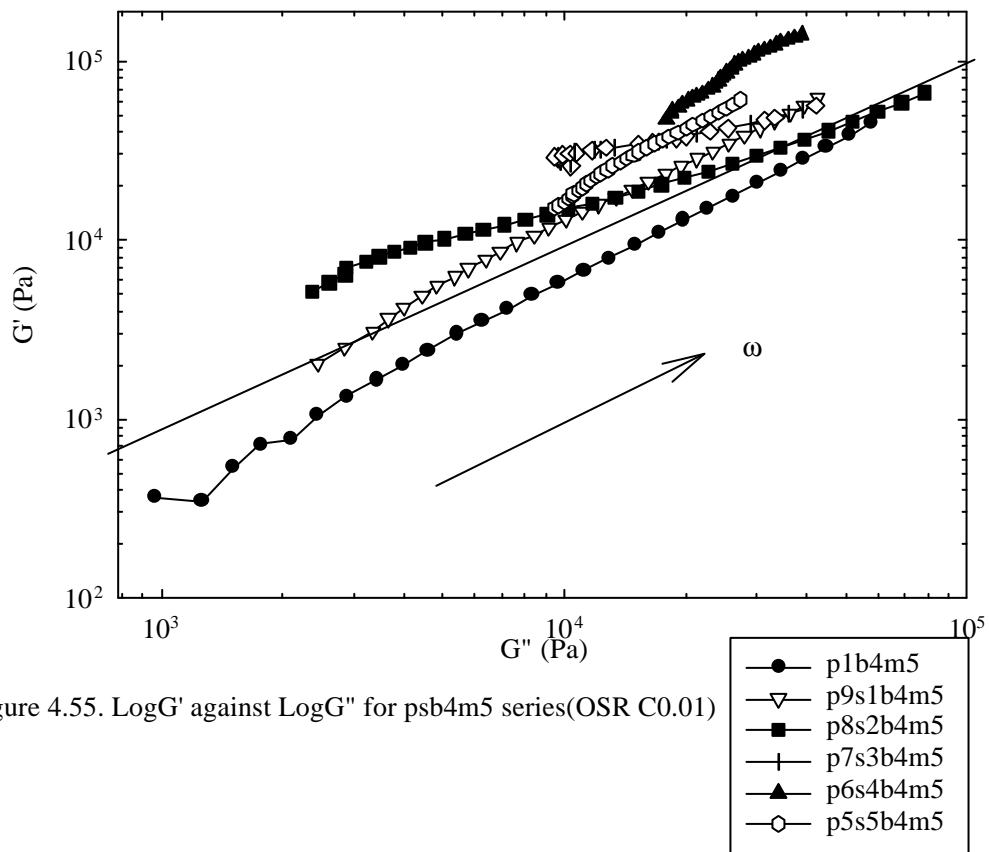


Figure 4.55. Log $G'$  against Log $G''$  for psb4m5 series(OSR C0.01)

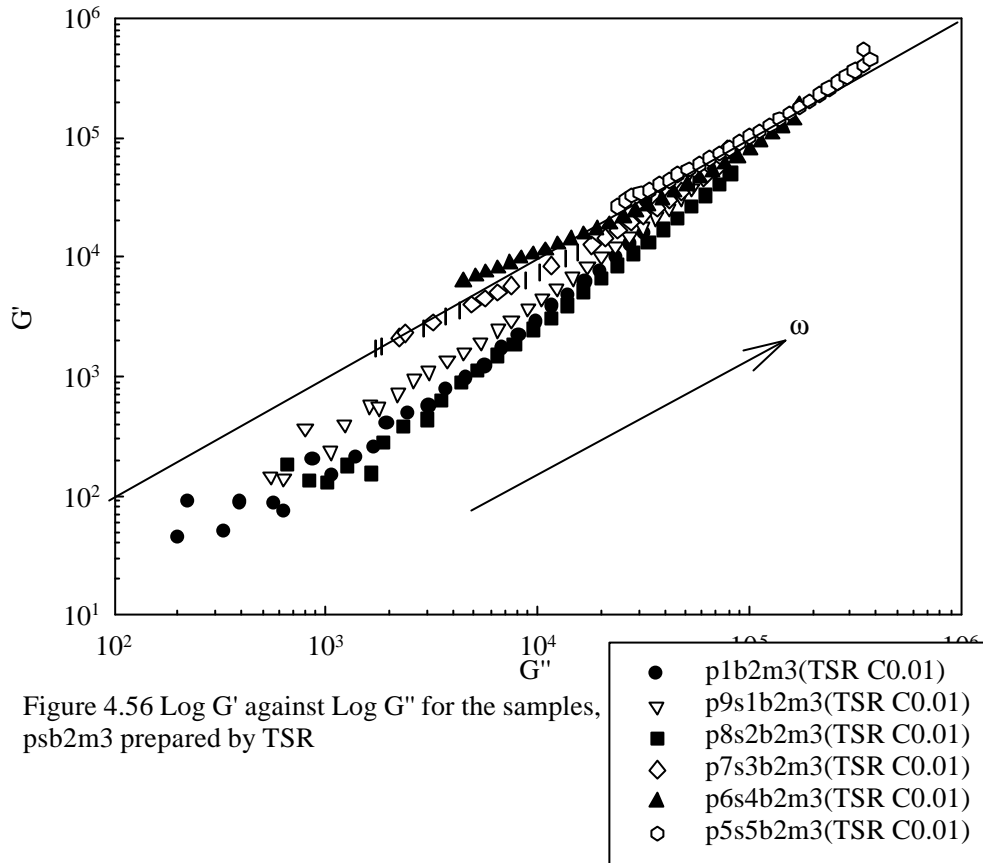


Figure 4.56 Log  $G'$  against Log  $G''$  for the samples, psb2m3 prepared by TSR

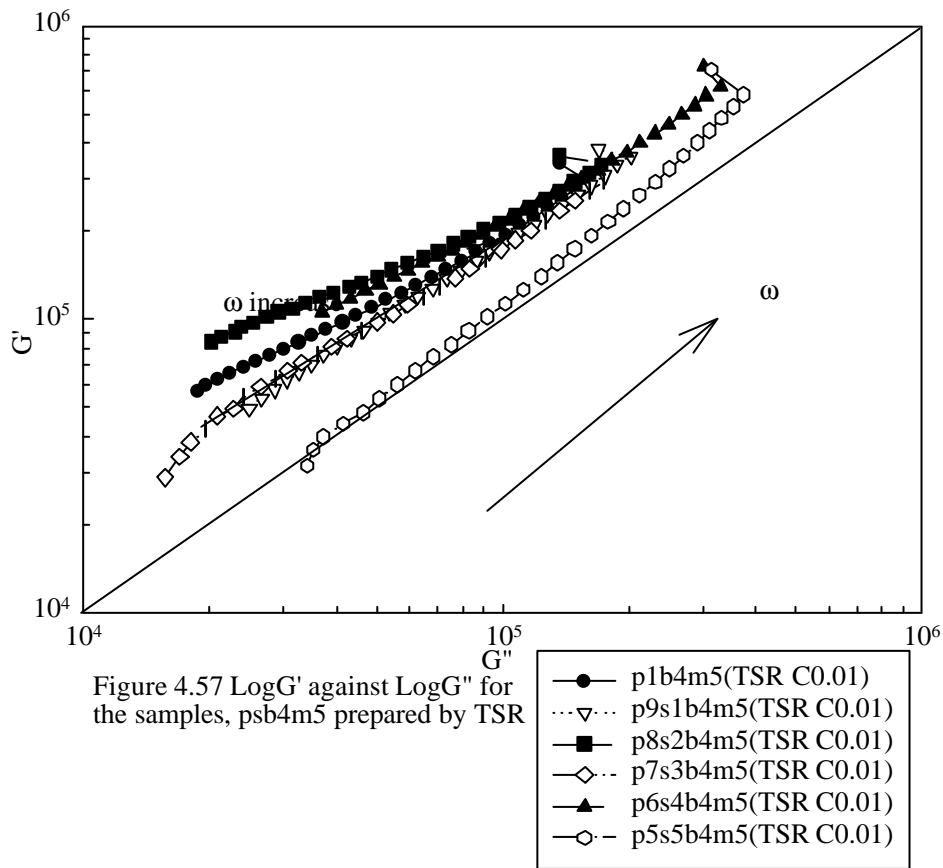
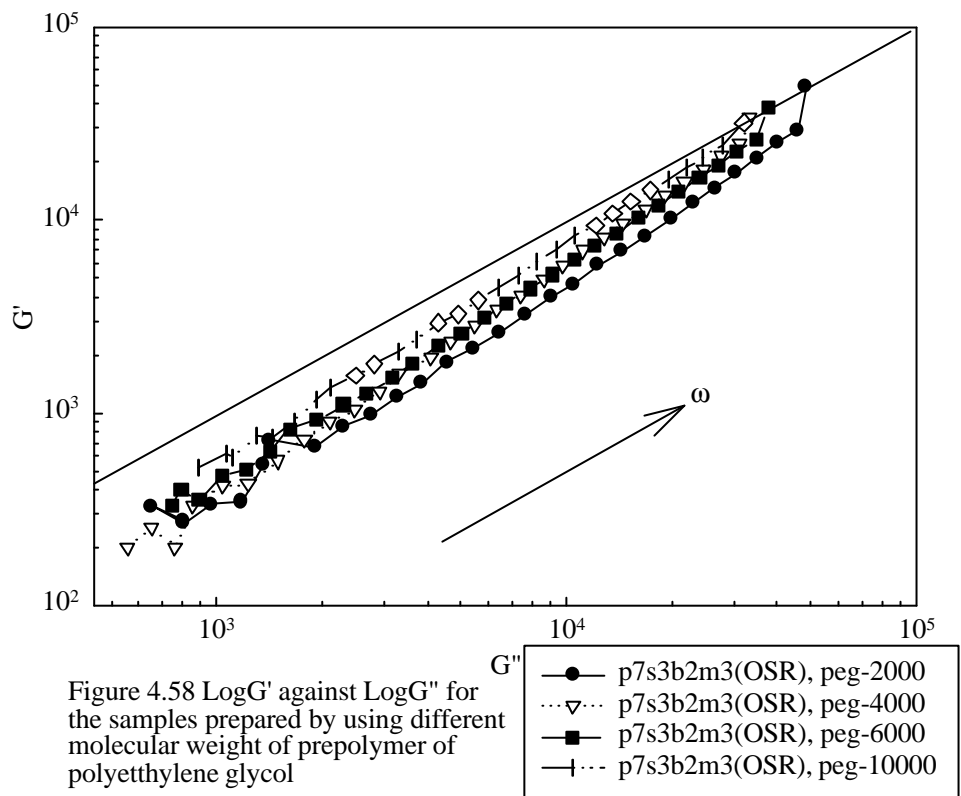


Figure 4.57 Log  $G'$  against Log  $G''$  for the samples, psb4m5 prepared by TSR



#### 4.2.2.3 Effects of the Different Molecular Weight of Polyethylene Glycol Prepolymer

It is interesting to plot  $G'$  against  $G''$ , because it can give the viscoelastic properties for the samples prepared with different molecular weights of prepolymer of the polyethylene glycol. As shown in Figure 4.58, all the samples are located at the range of  $G' < G''$  that indicates viscous behavior. However,  $G'$  decreases with the molecular weight of the prepolymer, despite the similarity of the molecular weights of the prepared polyurethane, as shown in Table 4.11. This result also indicates a higher crosslinking level of the samples prepared with higher molecular weight of the prepolymer. As shown in Figure 4.22 in the DSC study, the crystalline hard segments formed in the polyethylene-glycol-based polyurethane depend on the molecular size of the prepolymer and this crystal of the soft segment is a type of crosslinking which may influence the viscoelastic properties.

#### 4.2.3 Effect of Catalyst Concentrations

The above two sample series were synthesized at 0.01 wt.% catalyst concentration. We increased the concentrations to 0.05 and 0.1 wt.%, respectively. The increased catalyst concentration may increase the polyurethane reaction between the -OH of the starch-surface and -NCO of the polyurethane chain. Crosslinking influenced by catalyst concentration could be also confirmed by the increase of the viscosity and linearity of the plots of  $\zeta^*$  against  $\dot{\gamma}^{\text{6)}$ . These relations are presented in Figures 4.59 and 4.60. The increase in the catalyst concentration increased the viscosity. However, the molecular weight of the samples prepared at high concentration of the catalyst rather decreased as shown in Figure 4.28. Therefore, such an increase of viscosity is caused by the crosslinking of the polyurethane. In fact, increasing the catalyst concentration increased the slope of the plot, which proves crosslinking of the polyurethane. All samples are elastic as shown in Figures 4.61 and 4.62. For a catalyst concentration of 0.05 wt.%,  $G'$  values are maximum, indicating higher crosslinking; but for the 0.1 wt% concentration they are lower than for the 0.01wt%-samples. The curved lines of the plots of  $G'$  against  $G''$  for the two samples (p7s3b2m3(OSR C0.05) and p7s3b4m5(OSR C0.1)) indicate strong micro-heterogeneities,<sup>65), 66)</sup> which possibly formed between the starch granule and the polyurethane phase due to high concentration of the catalyst although the morphological picture of the formed system could not be developed. This complicated heterogeneity could be confirmed by DSC-analysis as shown in Figures 4.18 and 4.19. For the samples synthesized with the concentration of 0.01% of the catalyst, transition II



(attributed to dissociation of long range ordering in the hard micro-phase) appeared, but the increased catalyst concentration made this transition disappear, indicating that the hard micro-phase crystallites could not be formed due to higher crosslinking. However, the morphological change could not be determined. In fact, for the p7s3b4m5 that has a higher hard segment concentration, melting transition at 205°C disappeared due to the increased catalyst concentration.

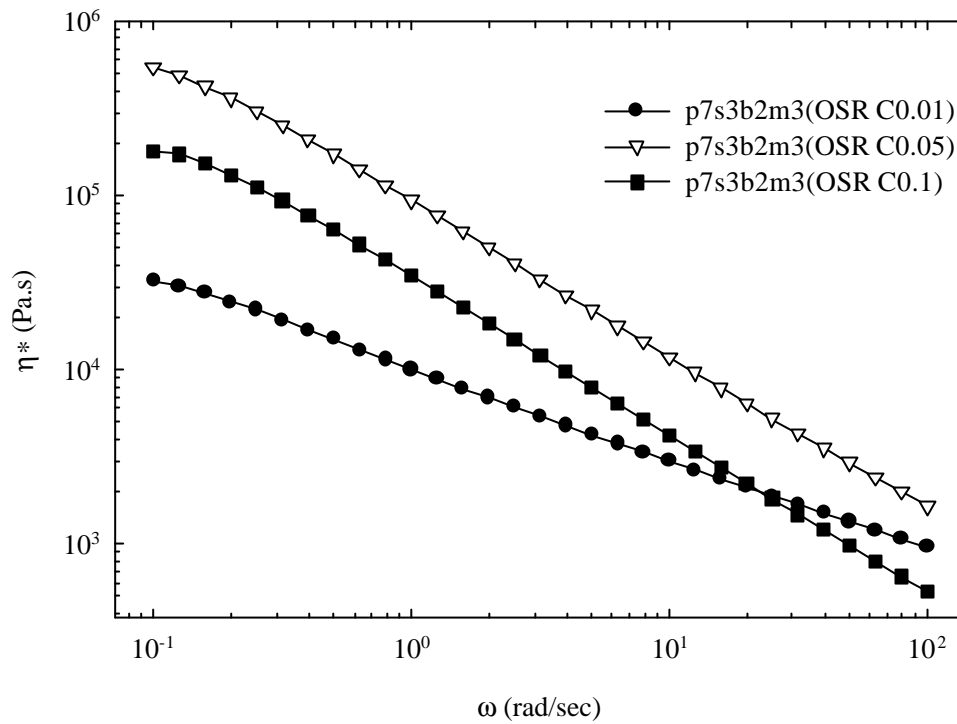


Figure 4.59 Complex viscosity  $\eta^*$  against frequency  $\omega$  for p7s3b2m3 at different catalyst concentration.

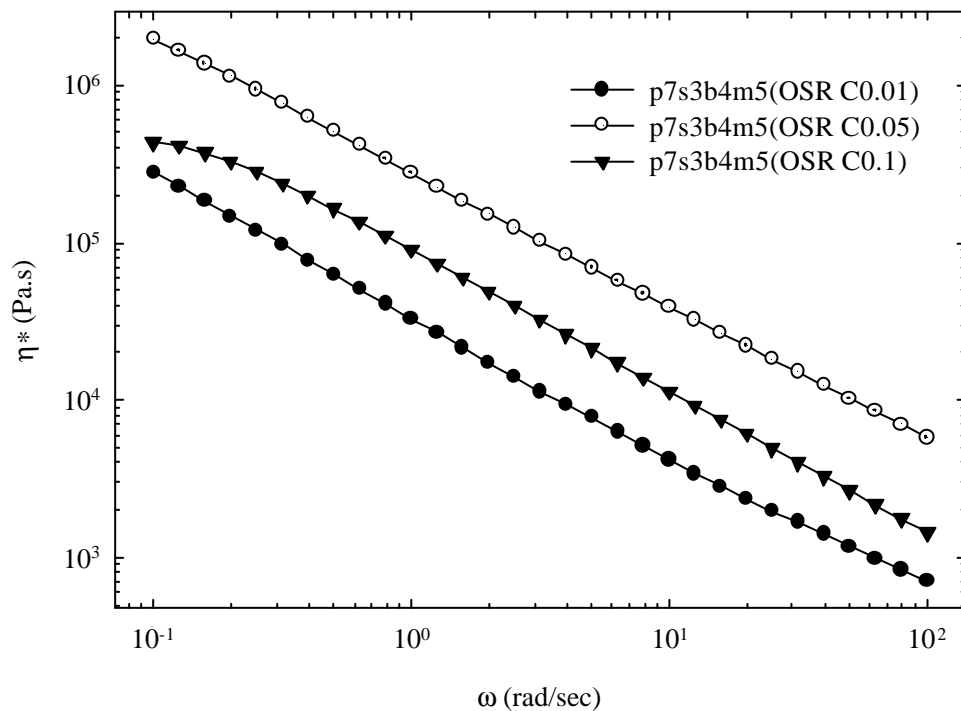
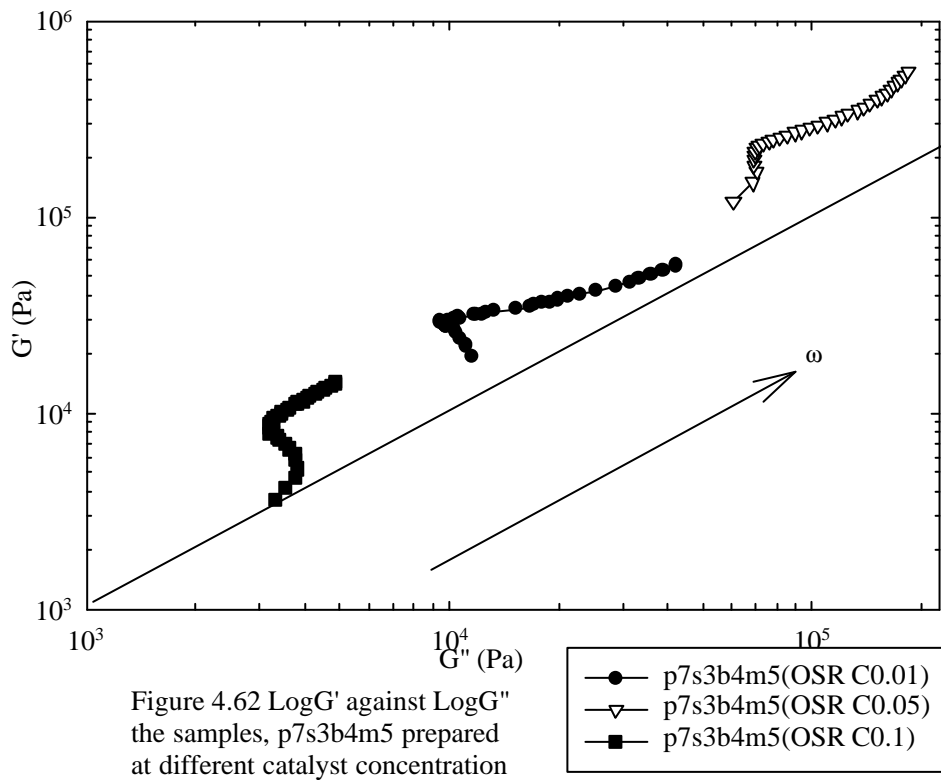
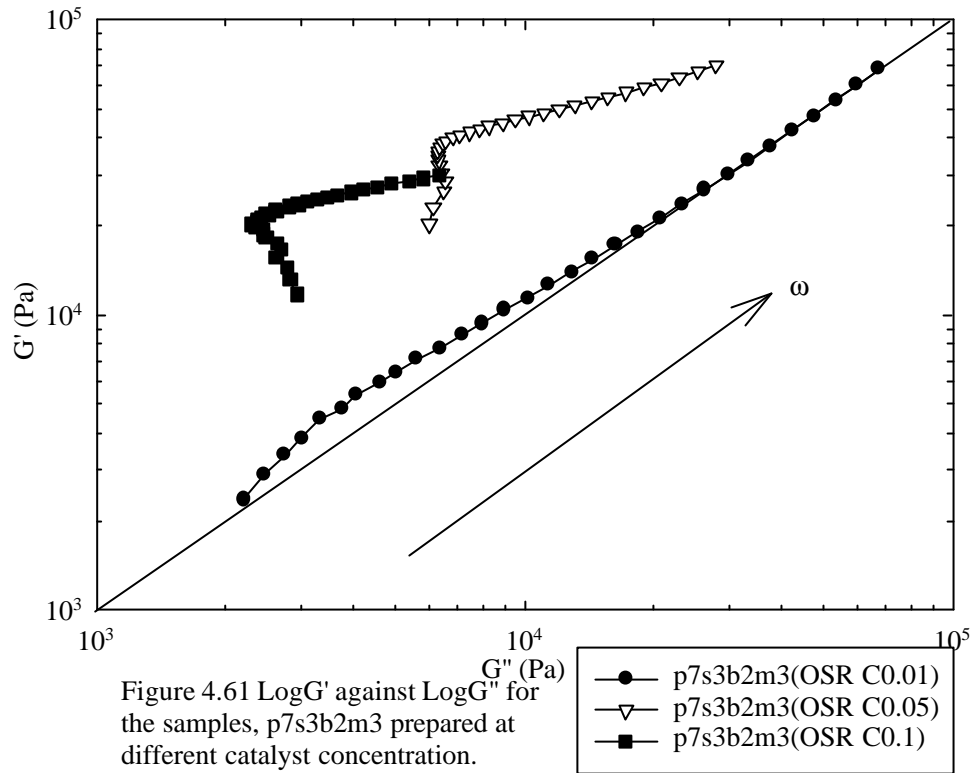


Figure 4.60 Complex viscosity  $\eta^*$  against frequency  $\omega$  for p7s3b4m5 at different catalyst concentration.



## 5. CONCLUSION

Polyurethane was synthesized with a pre-polymer of polycaprolactone diol ( $M_n=2000$ ), MDI, and 1,4 butane diol in the presence of starch granules (polyol) in a bulk phase at  $175^\circ\text{C}$  to understand its applicability for the use of starch as a raw material in a polyurethane system. The starch granules were well dispersed without shape modification of the granule in the continuous polyurethane phase, and there was crosslinking between the starch granules and between the polyurethane chains.

The grafted percentage for the samples, psb2m3(OSR C0.01) was higher than that of the samples, psb4m5 (OSR C0.01) and increased to about 20wt% and then decreased in the range of high starch content due to the homo-polymerization tendency of polyurethane at the higher starch content, which produced phase separation between the two phases. However, the grafted percentage of the samples prepared by two-step reaction were not changed, but the grafted percentage for psb2m3(TSR C0.01) was lower than that of psb4m5(TSR C0.01) in the middle range of starch content.

The average molecular weight of the homo-polymer separated from the samples prepared by two reaction schemes decreased with the starch content due to the diminishing of pre-polymer concentration of polycaprolactone and also probably due to the limited space between starch grains.

The polyurethane-starch blends prepared by the two reaction schemes also showed improved tensile strength and elongation of the samples at the lower starch content up to about 20 wt.%, but these properties decreased rapidly for the higher range of starch content due to phase separation between the starch granule and polyurethane phase because of lowering of the grafting and fracturing of the starch granules. Mechanical properties of the blends were improved as solvent uptake and the average molecular weight of the separated homo-polymer increased.

The thermal stability of the blends decreased as a function of the starch content, whereas that of the starch increased probably due to the grafting phenomena with the polyurethane for the samples prepared by both reaction schemes.

Rheological studies also indicated that the polycaprolactone diol ( $M_w=2000$ ), butane diol and MDI could produce a linear polymer, but the addition of the starch granule that offers enormous hydroxyl groups to the polyurethane reaction system, formed crosslinked network structures. This networking increased with the content of starch granules which produced partial gelation so as to having a gel point with  $G' = G''$  for a

range of starch contents. The increase of catalyst concentration increased the allophanating and biureting of crosslinking, which reduced the crystallinity of the hard segments in the polyurethane phase.

The conclusion obtained from this study is considered that polyurethane-starch blends could be used commercially without loss of mechanical properties up to 20 wt.% of the starch granule in polyurethane.

### ***General Comments on the Study***

It is considered that starch granules incorporated into polyurethane could form a micro-heterogeneous polymer system due to large particle size to be dispersed in the polyurethane phase. Furthermore, the grafting of hydroxyl group (OH) of the surface of the starch granule with isocyanate group (-NCO) could result in a more complicated polymer system; especially this complication may be increased if different grafting percentages are obtained in each synthesis process. Therefore, it was expected that this complication would end in different mechanical and rheological properties, which could not be easily determined with only a few parameters such as average molecular weight and the starch content. Improved studies for the mechanical properties, therefore, have been carried out, hitherto, through reducing this micro-heterogeneity; for example the de-structuring the starch granule to be well dispersed homogeneously in the continuous polymer phase. Another study is to improve the compatibility of the de-structured starch by chemically introducing the compatible component to the starch. However, in fact, there are no distinct improved results in mechanical properties obtained yet. Only the filler effect has been obtained. So then, without such a modification of the starch, directly using the starch granule in the polymer system is advantageous.

Such polymer systems have not been studied yet for chemistry and rheology.

As shown in our results, low content of the starch granule in polyurethane based on the polycaprolactone prepolymer did neither changed the chemistry of the polyurethane formation nor the rheology of the materials very much although crosslinking increased with the starch granule content. If reactive extrusion could be performed, such a crosslinking is good for the mechanical and rheological properties.

With a mind on the reactive extrusion process, the reaction will be carried out in bulk phase at 190°C, which induces crosslinking by biuret and allophanate bonding in the polyurethane polymer phase.

The purpose of this study is to incorporate a starch granule that has a large granule size, with synthetic polyurethane so as to make use of its function as a polymer because the starch granule is a type of polyol that could polymerize with the polyurethane phase by grafting. We used polycaprolactone diol and diisocyanate, which could form a thermoplastic polymer. Therefore, our objective in this study was to overcome the problems using an appropriate synthetic scheme and/or blending formulation. Another reason for this study was to examine the use of starch granules in the plastics market. The use of starch granules without any modification would be economically important. As described already, in the reactive extrusion process, crosslinked three-dimensional networking was preferred in the case of an articles production, because three-dimensional networking occurred in the postcuring step. Furthermore, this polyurethane system is ideal due to bio-degradability of the starch blending.

Scanning electron microscopy (SEM) indicated that the starch granules were dispersed tightly in the polyurethane phase. If complete gelation could have been achieved by crosslinking between starch granules, we thought at the beginning of the study, the melt-rheological and mechanical properties could not be measured. However, it was possible to measure these characteristics without any other problems for most of the samples. Although the samples are located near the gel point, we could imagine that the crosslinking is formed by indirect bridging through allophanate and biuret bonds in the polyurethane phases, which possibly dissociate at high temperature of injection ( $>150^{\circ}\text{C}$ ). We think that these phenomena are rather preferred for the large particle size of the starch granule and partial grafting of the granule surface, which gives easy processing. This condition was satisfied in our study.

Here, we used two synthetic schemes, a one-step reaction and a two-step reaction, without addition of additives such as plasticizers. However, different properties were found chemically and rheologically. According to the processing scheme and the formulation of the reactants, the polyurethane-starch polymer system could be recommended as a new and useful polymer system in the polyurethane field. In order to maintain the mechanical properties, less than about 15~20 wt. % of starch addition is preferred. Thus, according to the processing method and the purpose of the product, many advantages of starch addition can be found.

We also found in this study that starch is an ideal component for the polyurethane in its thermal stability. The two components, polyurethane and starch, are close in their decomposition temperature, and this temperature is sufficiently high,  $260\sim 290^{\circ}\text{C}$  for

two prepolymers; polycaprolactone and polyethylene glycol. Furthermore, these components are ideal for the polymer processing due to grafting of hydroxyl group of the starch granule with the isocyanate of the reactant of the polyurethane. Therefore, we carried out chemical and rheological research on this new micro-heterogeneous polymer system.

### ***Closing Comments***

We have tried to find the grafting position of the isocyanate with glucose units (position 2, 3 and 6) using NMR study. However, the grafted fraction was too small to be detected by both  $C^{13}$ -NMR and  $H^1$ -NMR. We hope that this kind of study will be continued with de-structured starch in the future.

We used a large size of starch granule in this study, but nano-size particles could be further studied in polymer systems in the future.

## 6. REFERENCES

1. P. J. Yoon, C. D. Han, *Macromolecules*, 33, 2171 (2000)
2. J. Blackwell and C.D Lee, *J. of Polym. Sci.*, 21, 2169 (1983)
3. C. Hepburn, *Polyurethane Elastomers*, Elsevier Applied Science (1991)
4. R. J. Zdrahala, R. M. Gerkin, , S. L. Hager and F. E. Critchfield, *J. of Appl. Polym. Sci.*, 24, 2041 (1979)
5. S-T Lim and J-lin Jane, S. Rajagopalan and P. A. Seib, *Biotechnol. Prog.*, 8, 51 (1992)
6. K. J. Kim, K. Kim, *J. Appl. Polym. Sci.*, 48, 981 (1993)
7. V. D. Athawale and S. C. Rathi, *J. of Appl. Polym. Sci.*, 66, 1399 (1997)
8. M. H. Abo-Shosha and N. A. Ibrahim, *Starch/Stärke.*, 44, 296 (1992)
9. A. Bayazeed, M. R. Elzairy and A. Hebeish, *Starch/Stärke.*, 41, 233 (1986)
10. V. B. Pfannemuller, W. N. Emmerling, *Starch/Stärke.*, 35, 298 (1983)
11. K. J. Yoon, M. E. Carr, E. B. Bagley, *J. of App. Polym. Sci.*, 45, 1093 (1992)
12. R. L. Cunningham, M. E. Carr, and E. B. Bagley, *J. Appl. Polym. Sci.*, 44, 1477 (1992)
13. S. Desai, I. M. Thakore, B. D. Sarawade and S. Devi, *Polym. Eng. Sci.*, 40, 1200 (2000)
14. M. Yaz' ddani-Pedram, H. Vega and R. Quijada, *Macromol. Rapid Commun.* 17, 577 (1996)
15. C. G. Seefried, J. V. Koleske, and F. E. Critchfield, *J. Appl. Polym. Sci.*, 19, 2493 (1975)
16. C. G. Seefried, J. V. Koleske, and F. E. Critchfield, *J. Appl. Polym. Sci.*, 19, 2503 (1975)
17. C. G. Seefried, J. V. Koleske, and F. E. Critchfield, *J. Appl. Polym. Sci.*, 19, 3185 (1975)
18. R. W. Seymour, G. M. Estes, and S. L. Cooper, *Macromolecules.*, 3(5), 579 (1970)
19. H. N. Ng, A. E. Allegrezza, R. W. Seymour and S. L. Cooper, *Polymer*, 14, 255 (1973)
20. T. K. Kwei, *J. Appl. Polym. Sci.*, 27, 2891 (1982)
21. C. S. Paik Sung and N. S. Schneider, *Macromolecules*, 10(2), 453 (1997)
22. M. M. Coleman, K. H. Lee, D. J. Skrovanek and P.C. Painter, *Macromolecules*, 19, 2149 (1986)



23. D. S. Huh, S. L. Cooper, *Polym. Eng. Sci.*, 11, 369 (1971)
24. J. Blackwell and K. H. Gardner, *Polymer.*, 20, 13 (1979)
25. H. Domininghaus, "Plastics for Engineers : Material, Properties, Applications", page 706, Hanser, Munich (1993)
26. A. Guilbot, and C. Mercier, "The polysaccharides", vol. 3, page 210, Academic press, (1985)
27. N. St-Pierre., B. D. Favis, B. A. Ramsay, J. A. Ramsay and H. Verhoogt., *Polymer*, 38(3), 647 (1997)
28. M. Bhattacharya, *J. Appl. Manu. Sys.*, Winter, 25 (1996-97)
29. J. A. Radley, "Examination and analysis of starch and starch products' ", page 22, Applied science publishers LTD, London, (1982)
30. F. S. Buhler, E. Schmid, H. -J. Schultze, U. S. Patent (filed Oct. 6, 1992) 5,436,078 (1995)
31. H. Carlsohn and M. Hartmann., *Acta Polymerica*, 33, 640 (1982)
32. W. Xu, W. M. Doane, U. S. Patent (filed Sep. 4, 1997) 5,854,345 (1998)
33. D. Raghavan, *Polym. Plast. Tech. Eng.* 34(1), 41(1995)
34. L. E. Roque, L. N. Zivko, W. Sung, J. L. Jane, R. J. Gelina, *Ind. Eng. Chem. Res.*, 30, 1841 (1991)
35. R. Chandra, R. Rustgi, *Polym. Degrad. Stab.*, 56, 185 (1997)
36. S. Simmons and E. L. Thomas, *J. Appl. Polym. Sci.*, 58, 2259 (1995)
37. M. G. Cascone, G. Polacco, L. Lazzeri, N. Barbani, *J. Appl. Polym. Sci.*, 66, 2089 (1997)
38. M. F. Koenig and S. J. Huang, *Polymer.*, 36, 1877 (1995)
39. L. Averous, L. Moro, P. Dole, C. Fringant, *Polymer.*, 41, 4157 (2000)
40. M. Vikman, S. H. D. Hulleman, M. Van der zee, P. Myllärinen, H. Feil, *J. Appl. Polym. Sci.*, 74, 2594 (1999)
41. D. Bikiaris, J. Aburto, I. Alric, E. Borredon, M. Botev, C. Betchev, C. Panayiotou, *J. Appl. Polym. Sci.*, 71, 1089 (1999)
42. D. R. Paul, S. Newman, "Polymer blends" ., vol 1, 2, Academic press, 1978
43. M. E. Carr, *J. Appl. Polym. Sci.*, 42, 45 (1991)
44. C. E. Brockway, *J. Polym. Sci-Part A.*, 2, 3733 (1964)
45. G. F. Fanta, C. L. Swanson, R. C. Burr, W. M. Doane, *J. Appl. Polym. Sci.*, 28, 3003 (1983)

46. F. Wolf, H. J. Mallon and H. Gerlach, *Starch/Stärke*, 32, 229 (1980)
47. F. H. Otey, B. L. Zagoren, F. L. Bennett, C. L. Mehlretter, *I&EC Prod. Res.*, 4, 225 (1965)
48. F. H. Otey, F. L. Bennett, B. L. Zagoren, C. L. Mehlretter, *I&EC Prod. Res.*, 4, 229 (1965)
49. R. H. Leitheiser, C. N. Impola, and R. J. Reid, F. H. Otey, *I&EC Prod. Res.*, 5, 276 (1966)
50. L. A. Gugliemelli, M. O. Weaver, C. R. Russell, *Polym. Lett.*, 6, 599 (1968)
51. U. R. Vaidya, M. Bhattacharya, *J. Appl. Polym. Sci.*, 52, 617 (1994)
52. U. R. Vaidya, M. Bhattacharya and D. Zhang, *Polymer*, 36, 1179 (1995)
53. M. Bhattacharya, U. R. Vaidya, D. Zhang, R. Narayan, *J. Appl. Polym. Sci.*, 57, 539 (1995)
54. R. Mani, and M. Bhattacharya, *Eur. Polym. J.*, 34, 1477 (1998)
55. R. Mani, and M. Bhattacharya, *Eur. Polym. J.*, 34, 1467 (1998)
56. K. J. Yoon, M. E. Carr, and E. B. Bagley, *J. Appl. Polym. Sci.*, 45, 1093 (1992)
57. T. Seidenstücker, and H. –G. Fritz, *Polym. Degrad. Stab.*, 59, 279 (1998)
58. T. Seidenstücker, and H. –G. Fritz, *Starch / Stärke.*, 51, 93 (1999)
59. S. H. Park, K. Y. Park, K. D. Suh, *J. Polym. Sci.*, : Part B, 36, 447 (1998)
60. T. R. Hesketh, J. W. C. Van Bogart and S. L. Cooper, *Polym. Eng. Sci.*, 20, 190 (1980)
61. R. W. Seymour, S. L. Cooper, *Macromolecules.*, 6, 48 (1973)
62. C. H. M. Jacques, *Polym. Sci. Tech.*, 10, 287 (1977)
63. S. K. Ha and H. C. Broecker, Paper accepted in *Polymer.*, May (2002)
64. H. H. Winter, P. Morganelli and F. Chambon, *Macromolecules.*, 21, 535(1988)
65. H.-K. Chuang and C.D.Han, *J. of Applied Polymer Science.*, 29, 2205(1984)
66. C. H. Han and J.K. Kim, *Polymer.*, 34, 2533(1993)
67. E. Contou, G. Spathis, M. Niaounakis and V. Kefalas, *Colloid & Polymer Science.*, 268, 636 (1990)
68. J. A. Miller, S. B. Lin, K. K. S. Hwang, K. S. Wu, P. E. Gibson, S. L. Cooper, *Macromolecules.*, 18, 32 (1985)
69. V. W. Srichatrapimuk, S. L. Cooper, *J. Macromol. Sci.-Phys.*, B15(2), 267 (1978)
70. K. E. Oliphant, K. E. Russell, W. E. Baker, *Polymer.*, 36, 1597 (1995)

71. S. K. Rath and R. P. Singh, *J. Appl. Polym. Sci.*, 70, 1795 (1998)
72. D. K. Kweon, D. S. Cha, H. J. Park, S. T. Lim, *J. Appl. Polym. Sci.*, 78, 986 (2000)
73. P. Zetterlund, S. Hirose, T. Hatoyama, H. Hatakeyama, A. C. Albertsson, *Polym. Int.*, 42, 120 (1997)